STABLE FREE RADICAL POLYMERIZATION CONDUCTED IN EMULSION POLYMERIZATION SYSTEMS

by

HIDEO MAEHATA

A thesis submitted to the Department of Chemical Engineering

In conformity with the requirements for

The degree of Doctor of Philosophy

Queen's University

Kingston, Ontario, Canada

February 2010

ABSTRACT

Free radical polymerization is the most common polymerization technique that is used for the manufacturing of polymers, due to the ease of the polymerization initiation, wide latitude of the material design for a large variety of monomers, and the excellent process robustness for commercial production. In the 1990's, research activities for the precise control of radical polymerization process resulted in the discovery of 'Living Radical Polymerization'. The discoveries opened the door for the next generation of radical polymerizations. Extensive research has been conducted to understand the mechanisms and kinetics for numerous practical applications, particularly for polymerization in bulk and solution systems. However, despite the interest of industry, the mechanistic understanding in aqueous dispersed systems such as emulsion and miniemulsion polymerization is far behind the aforementioned two systems. There are still major challenges from the production viewpoint. One reason for the poor understanding is the complexity of the heterogeneous system, which includes multiple reaction phases that are accompanied by the segregation and transfer of the reaction species among different phases.

The purpose of this research was to investigate living radical polymerization or "Stable Free Radical Polymerization" (SFRP) in aqueous dispersed systems to obtain better mechanistic understanding of how the heterogeneous nature of the system interacts with the novel living radical chemistry. The theoretical and experimental feasibility of the SFRP emulsion process were studied in this research, in particular, focusing on the compartmentalization effect. Particle size influence on the polymerization kinetics and the polymer livingness was experimentally confirmed, and compared to bulk

polymerization. In addition, a comprehensive mathematical model including all major chemical and physical events was developed to further our mechanistic understanding. Based on the results from the experimental and modeling studies, it was shown that rate reduction in the smaller particles is the primary cause of difficulty in implementing a conventional emulsion process (i.e. ab initio emulsion polymerization). Finally, for overcoming this difficulty, a new approach using a combination of TEMPO with highly hydrophobic 4-stearoyl TEMPO was proposed for a coagulum free ab initio emulsion process.

ACKNOWLEDGEMENTS

I gratefully thank my thesis supervisor Dr. Michael Cunningham for his extraordinary support and guidance. The completion of this thesis would not have been possible without his advice.

I also thank all of the members of the Cunningham team, in particular Catherine Buragina for her support on the livingness analysis in this thesis.

In addition, I have a profound debt to all the members of the Xerox Research Centre of Canada. Their input and encouragement always motivated me to complete this research. I give special thanks to Barkev Keoshkerian, Dr. Peter Kazmaier, and Dr. Hadi Mahabadi for giving me the great opportunity to work with them.

Lastly, I express my extreme gratitude to Fuji Xerox Co.,Ltd for their continued support and financial assistance.

TABLE OF CONTENTS

LIST OF SCHEMES

LIST OF TABLES

LIST OF FIGURES

NOMENCLATURE

a_p surface area per polymer particle [m^2]

CA chain transfer agent

d_p diameter of polymer particle [m]

$DI^{\bullet}$ dimer radical by the Diels-Alder reaction

D_n dead polymer having chain length n

D_{n+m} dead polymer having chain length (n+m)

D_p diffusion coefficient of monomer radical in polymer particle [m^2/s]

D_w diffusion coefficient of monomer radical in water [m^2/s]

F probability for an entering radical to be captured in side particle

j number of free nitroxide molecule

K_0 rate coefficient for overall desorption of monomer radical [1/s]

k_0 overall mass transfer coefficient [m/s]

k_{act} rate coefficient of activation reaction [1/s]

k_{adp} rate coefficient of alkoxyamine disproportionation [1/s]

k'_{adp} adjusted rate coefficient of alkoxyamine disproportionation [1/s]

k_{deact} rate coefficient of deactivation reaction [L/(mol s)]

k_{dim} rate coefficient for dimerization of styrene by autopolymerization

k_{disp} rate coefficient for disproportionation reaction [1/s]

$k_{disp.1}$ rate coefficient of disproportionation reaction which competes with deactivation reaction [L/(mol s)l]

$k_{disp.2}$ rate coefficient of disproportionation reaction which competes with activation reaction [1/s]

k_{ep} mass transfer coefficient for radical entry into particle [1/s]

k_f rate coefficient for radical exit from particle [1/s]

k_i' rate coefficient to react with a styrene molecule with Diels-Alder dimer

K_L equilibrium constant of reversible activation and deactivation reaction

k_L film mass transfer coefficient for inner diffusion film adjacent to interface between polymer and water phase [m/s]

k_{mf} rate coefficient for chain transfer of radical to monomer [L/(mol s)]

k_p rate coefficient of propagation reaction [L/(mol s)]

k_t rate coefficient of termination reaction [L/(mol s)]

k_{ith} rate coefficient of thermal initiation of monomer (autopolymerization) [L^2/(mol ^{2}s)]

k_w film mass transfer coefficient for outer diffusion film adjacent to interface between polymer particle and water phase [m/s]

m_i partition coefficient for radical between polymer particle and water phase

m_d partition coefficient of species (monomer or nitroxide) between organic phase and water phase

M monomer molecule

M_{tn} / ligand transition metal complex for atom transfer reaction, without the halide

n number of radicals

$N_{i,j}$ fraction of particles containing i active radicals and j molecules of free nitroxide

N_i^j fraction of particles containing i active radicals and j molecules of free nitroxide

N_n fraction of particles, which contain n radicals in particle

N_{n+1} fraction of particles, which contain (n+1) radicals in particle

N_{n-1} fraction of particles, which contain (n-1) radicals in particle

N_T total number of particles

N_p total number of particles

$P^{\cdot}$ polymer radicals

P_x-T oligoradical initiator capped by nitroxide

r rate of radical generation [mol/(L s)]

R_I rate of additional radical generation in SFRP [mol/(L s)]

R_i -T polymer molecule of chain length i capped by a nitroxide radical

$R_{i+1}^{\cdot}$ polymer radical of chain length i+1

$R_i^{\cdot}$ polymer radical of chain length i

$R_j^{\cdot}$ polymer radical of chain length j

R_p rate of polymerization [mol/(L s)]

R-T initiator radical capped by nitroxide

P_n-T propagating dormant chain capped by nitroxide

TH hydroxylamine molecule

t polymerization time [s]

$T^{\cdot}$ free nitroxide radical

v_p particle volume

x monomer conversion

X-Mt_{n+1} / ligand transition metal complex for atom transfer reaction, with the halide

XR_i alkyl halide of chain length i

[M] monomer concentration [mol/L]

$[M]_0$ monomer concentration (t = 0) [mol/L]

$[M]_p$ monomer concentration in particle [mol/ L : organic phase]

$[M]_w$ monomer concentration in water [mol/L : water phase]

$[M^{\bullet}]_w$ monomeric radical concentration in water [mol/L :water phase]

$[P_x\text{-}T]_0$ concentration of oligoradical initiator capped by nitroxide [mol/L]

$[P\text{-}T]_w$ dormant chain concentration having chain length 1 in water phase [mol/L :water phase]

$[P_n\text{-}T]_p$ dormant chain concentration in particle [mol/L :organic phase]

$[P_n\text{-}T]_{w\to p}$ dormant chain concentration entering from water phase into particle [mol/L:organic phase]

$[R_i\text{-}T]$ concentration of polymer molecules of chain length i capped by a nitroxide radical [mol/L]

$[R_i^{\cdot}]$ concentration of polymer radicals of chain length I [mol/L]

$[R\text{-}T]_0$ concentration of initiator radicals capped by nitroxide [mol/L]

$[R^{\bullet}]_w$ radical concentration in water [mol/L: water phase]

$[T]_0$ initial concentration of free nitroxide [mol/L]

$[T^{\cdot}]$ concentration of nitroxide radical [mol/L]

$[T^{\bullet}]_w$ nitroxide radical concentration in water [mol/L: water phase]

$[TH]_p$ concentration of hydroxamine in particle [mol/L : organic phase]

$[R^{\bullet}]_{Exit}$ exit radical concentration from particle into water phase [mol/L: organic phase]

$[R^{\bullet}]_{Entry}$ entry radical concentration from water phase into particle [mol/L: organic phase]

$\bar{n}$ average number of radicals per particle

$\bar{n}_t$ average number of free nitroxides per particle

ρ_a rate of radical entry to particle [1/s]

ρ_w rate of radical generation in water phase [mol/ L :water phase]

μ_0 the zeroth order moment of dormant chains

δ the ratio of the water side to overall diffusion resistance

λ equilibrium partition coefficient of radicals between particle and water phases

CHAPTER 1

INTRODUCTION

1.1 Classification of Living Radical Polymerization

Living radical polymerizations can be classified as having the chain growth controlled either by reversible termination or reversible transfer.[1), 2)] Reversible termination mechanisms, such as nitroxide mediated polymerization (Stable Free Radical Polymerization (SFRP: Scheme 1.1) [3)] and Atom Transfer Radical Polymerization (ATRP: scheme 1.2) [4)] use a controlling agent that reacts reversibly with a propagating polymeric radical to yield a dormant chain. The main feature of SFRP is the reversible 'activation –deactivation' reaction between a stable radical $T^{\cdot}$ and a propagating radical $R_i^{\cdot}$ The reaction produces the dormant species R_i-T, which can reversibly activate. Typical examples of $T^{\cdot}$ are nitroxides such as 2,2,6,6-tetramethyl piperadine-1-oxy (TEMPO).

In ATRP, XR_i is activated by a catalyst (transition metal complex Mt^n / ligand). In typical examples, X is a halogen atom such as Br or Cl, and Mt^n is the transition metal species Cu (I). In addition, the choice of the ligand is also very important in this system. 2,2'-Bipyridine is a commonly used ligand for this purpose.

Scheme 1.1

Reversible Termination

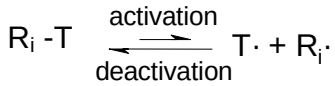

Propagation

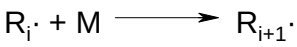

Scheme 1.2

Reversible Termination

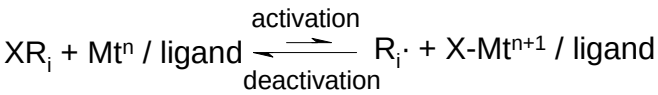

Propagation

In SFRP and ATRP, the equilibrium is shifted strongly toward the dormant species during polymerization, so that the active (propagating) radical concentration is lower than in conventional radical polymerization. Because propagation is first order with respect to radical concentration, while irreversible biradical termination is second order, the lower radical concentration results in a significantly reduced termination rate that preserves the living character of the propagating chains.

Reversible transfer mechanisms, for instance Reversible Addition Fragmentation Transfer (RAFT) [5] employ a chain transfer agent CA that reacts with a propagating radical, and exchanges the radicals between R_i· and R_j· (Scheme 1.3). Benzyl and cyanoisopropyl for R_j· and phenyl and methyl for Z are typical examples used in RAFT agents.

Scheme 1.3

Reversible Addition and Fragmentation

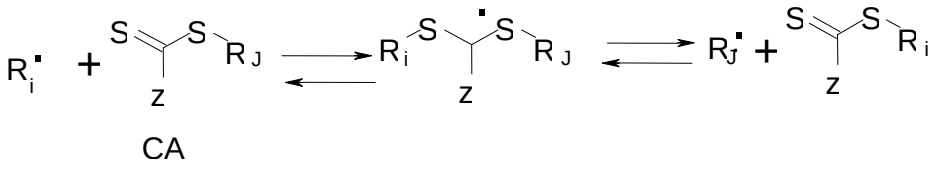

Propagation

The reversible reaction is between a dormant chain and an active radical, in which an end group originating from the transfer agent is exchanged between the two chains. In this case, the radical concentration before and after the exchange reaction is not changed, unlike that of the reversible termination process, and the equilibrium state is shifted toward the dormant species and the intermediate radical species.

1.2 Stable Free Radical Polymerization in Bulk Systems

1.2.1 Polymerization Mechanism and Kinetics

After the first report of successful polymerization for high molecular weight polystyrene in SFRP [3], numerous efforts have being conducted to understand the polymerization mechanism and the kinetics in bulk. As described in Section 1-1, the basic concept in SFRP is to control the net radical concentration by reversible activation and deactivation (Scheme 1.4)

Scheme 1.4

$$R_i\text{-}T \underset{k_{deact}}{\overset{k_{act}}{\rightleftharpoons}} T\cdot + R_i\cdot \qquad K_L = \frac{k_{act}}{k_{deact}}$$

Ideally, when the characteristic time for the deactivation reaction is fast compared to that of termination and propagation, nitroxide can trap most of the active radicals to form dormant species. In this situation, the overall radical concentration largely depends on the equilibrium constant K_L of this reversible reaction. Typical value of the equilibrium constant for TEMPO styrene system is 2.1×10^{-11} mol/l [6], which causes the equilibrium to shift strongly toward the dormant species. In this reversible mechanism, the free nitroxide plays a key role in controlling the polymerization kinetics. The influence of the free nitroxide level was first studied in early works conducted by Veregin et al.. [7),8)] First of all, they assumed that the biradical termination was not important (i.e., the rate of termination is negligibly small and the polymerization kinetics are only governed by propagation and reversible activation-deactivation reactions). Based on this concept, they proposed the following rate equation,

$$R_p = kp[M]\,[R_i - T]\left(\frac{K_L}{[T^\bullet]}\right) \qquad \textbf{(1-1)}$$

where $[M]$ is the monomer concentration, k_p is the rate constant of propagation, [R_i-T] is the concentration of the dormant species, and [$T^\bullet$] is the concentration of the free nitroxide. In this equation, what is unique to a nitroxide-mediated polymerization is that the rate of the polymerization is not only proportional to k_p and the monomer concentration but also the dormant species and the equilibrium constant K_L. In addition, it is in inverse proportion to the free nitroxide concentration. In their analysis, the excess free nitroxide is treated as a constant during the polymerization since termination, which causes two free nitroxides to be released in every biradical termination reaction, was neglected.

On the other hand, several computer simulations have provided more insight on living radical polymerization, especially on the importance of the biradical termination reaction. Fischer et al. presented an intensive kinetic analysis of reversibly terminated living radical polymerization (SFRP, ATRP) .[9), 10)] In this development, they initially assumed an ideal initiation by the homolysis of a stoichiometric initiator [R -T]$_0$. In addition, the stable radical is treated as a "persistent" radical, which does not self-terminate. The initiating and propagating radicals are defined as "transient" radicals, which can be terminated in the usual biradical reaction.

In this ideal situation, once the initiation by the homolysis of [R -T]$_0$ commences, both the transient radical and the persistent radical concentrations gradually increase with

polymerization time. By about 10^{-4} sec, the biradical termination rate among the transient radicals becomes significant, so that their concentration begins to decrease. However, the persistent radical concentration keeps increasing since every termination releases two free persistent radicals. This has been deemed the "Persistent Radical Effect".

The time variations of $[R_i^{\bullet}]$ and $[T^{\bullet}]$ can be calculated and follow the following power law (1-2, 1-3, 1-4).

$$[R_i^{\bullet}] = \left(\frac{r}{3 k_{deact} \; k_t} \right)^{\frac{1}{3}} t^{-\frac{1}{3}} = \left(\frac{K_L [R - T]_0}{3 k_t} \right)^{\frac{1}{3}} t^{-\frac{1}{3}} \qquad \textbf{(1-2)}$$

$$[T^{\bullet}] = \left(\frac{3 k_t r^2}{k_{deact}^2} \right)^{\frac{1}{3}} t^{\frac{1}{3}} = (3 K_L^2 k_t [R - T]_0^2)^{\frac{1}{3}} t^{\frac{1}{3}} \qquad \textbf{(1-3)}$$

$$\therefore \; k_{deac} \; [R_i^{\bullet}][T^{\bullet}] = k_{act} \; [R - T]_0 \qquad \textbf{(1-4)}$$

In this case, equation 1-4 is the equilibrium relation for the reversible dissociation with the actual time-dependent concentration of [R_i-T] replaced by its initial value, and this relation can be transformed into the following Equation 1-5.

$$[R_i^{\bullet}] = K_L \frac{[R - T]_0}{[T^{\bullet}]} \qquad \textbf{(1-5)}$$

The equation (1-5) is the same relation that is shown by Veregin et al., except for the time-dependent relationships.

From these relations, the rate of polymerization and the conversion can be derived as shown in equations 1-6 and 1-7.

$$R_p = k_p[M]\left(\frac{K_L[P-T]_0}{3k_t}\right)^{\frac{1}{3}} t^{\frac{-1}{3}} \qquad \textbf{(1-6)}$$

$$\ln\frac{[M]_0}{[M]} = \frac{3}{2}k_p\left(\frac{K_L[P-T]_0}{3k_t}\right)^{\frac{1}{3}} t^{\frac{2}{3}} \qquad \textbf{(1-7)}$$

In the above equations, it is clearly shown that the active radical concentration continuously decreases with the polymerization time, and consequently the polymerization rate also decreases from the early stages of polymerization. Therefore, in order to maintain a reasonable rate, it is essential to keep the radical concentration higher than its natural value. For this purpose, Fischer et al. suggested that additional radical sources, such as conventional initiator and autopolymerization, are important. In particular, their simulation results showed that autopolymerization of styrene could lead to a quasi-steady state which preserves the constant level of both the radical and the free nitroxide concentrations.

Heating styrene to temperatures over 100 ºC causes the thermal initiation of the monomer. At elevated temperatures, Mayo demonstrated that styrene forms a dimer through a Diels-Alder reaction (Scheme 1.5). In this reaction, k_{dim} is the rate coefficient

for dimerization and its value has been estimated to be 3×10^{-8} $M^{-1}\cdot s^{-1}$ at 120 ºC. [11] The Diels-Alder dimer can further react with another styrene molecule to form a dimer radical and a monomer radical with the rate coefficient k_i' of 5×10^{-8} $M^{-1}\cdot s^{-1}$ (120 ºC).

Scheme 1.5

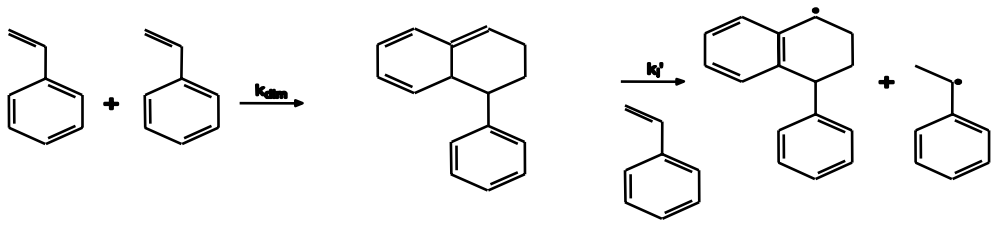

Fukuda et al. discovered this situation more precisely in their kinetic treatment.[12),13),14),15)] Transient radicals are generated not only by the dissociation of [R_i-T] but also by the additional radical sources such as conventional initiator and autopolymerization. In this situation, generation of [$R_i^\bullet$] and [$T^\bullet$] can be expressed by the following equations.

$$\frac{d[R_i^\bullet]}{dt} = R_I + k_{act}([R-T]_0 - [T^\bullet]) - k_{deac}[R_i^\bullet][T^\bullet] - k_t[R_i^\bullet]^2 \qquad \textbf{(1-8)}$$

$$\frac{d[T^\bullet]}{dt} = k_{act}([R-T]_0 - [T^\bullet]) - k_{deac}[R_i^\bullet][T^\bullet] \qquad \textbf{(1-9)}$$

where R_I is the rate of the additional radical generation. When the steady state condition is achieved, [$R_i^\bullet$] and [$T^\bullet$] can be written as follows.

$$\left[R_i^{\bullet}\right] = \left(\frac{R_I}{k_t}\right)^{\frac{1}{2}} \qquad \textbf{(1-10)}$$

$$\left[T^{\bullet}\right] = K_L\left[R-T\right]_0\left(\frac{k_t}{R_I}\right)^{\frac{1}{2}} \qquad \textbf{(1-11)}$$

Overall, the polymerization rate and the polymerization index (conversion) in the steady state can be calculated by equations 1-12 and 1-13.

$$R_p = k_p[M]\left[\frac{R_I}{k_t}\right]^{\frac{1}{2}} \qquad \textbf{(1-12)}$$

$$\ln\frac{[M]_0}{[M]} = k_p\left(\frac{R_I}{k_t}\right)^{\frac{1}{2}} t \qquad \textbf{(1-13)}$$

If R_I is too large to maintain the steady state conditions, the system will lose its living characteristics and behave like a conventional system. The importance of the additional radical generation is that the rate of polymerization is independent of the concentration of R-T. The rate can be controlled only by the additional radical generation. In addition, the conversion rate can be expected to be markedly enhanced, in comparison to the absence of any additional initiation. In connection with this, Souaille et al.[16] explored further details on this rate enhancement effect. In this study, they pointed out that $[R_i^{\bullet}]$ must not exceed 10^{-8} M to keep living characteristics. The rate of the additional initiation must be

small compared to the dissociation of [R_i-T], i.e. $R_I << k_{act}[R\text{-}T]_0$. In their simulations, a ratio $R_I / k_{act}[R\text{-}T]_0 = 0.01$ showed a ~ x 10 rate enhancement.

1.2.2 Free Nitroxide Control and Rate Enhancement

In SFRP, the termination reaction causes a continuous decrease of the active radical concentration and accumulation of free nitroxide, so that the rate of polymerization also continuously decreases from the early stages of polymerization. In fact, unrealistically low polymerization rates are often observed, and the polymerization eventually levels off around 60 ~80% conversion due to a large amount of free nitroxide. In order to solve this issue, minimizing termination is crucial. At the same time, it is also important to reduce the free nitroxide accumulation. An additional radical source is one of the countermeasures for this purpose. Moreover it is known that some acid addition can markedly enhance the rate of the polymerization due to consumption of the excess nitroxide.

Georges et al.[17] found that addition of camphorsulfonic acid (CSA) resulted in significant rate enhancement with conversions reaching 92% in 5.5 hrs, compared to the case without CSA, 85% for 70 hrs. Veregin et al.[18] investigated the mechanism of this rate enhancement by ESR studies. In their studies, they observed that the concentration of free nitroxide decreased remarkably due to direct consumption of free nitroxide by CSA. It is worth noticing that significant reduction of styrene autopolymerization was also reported by Buzanokowski et al.[19] with the addition of acid. Acetic anhydride was also reported as a rate enhancement additive by Malmston. et al.[20], and they proposed that

acetic acid enhanced the rate of polymerization either by promoting the activation reaction or by free nitroxide consumption.

Keoshkerian et al.[21] first attempted to apply this concept to acrylate monomer. In SFRP, the polymerization rate of the acrylate monomer is very slow and the conversion usually levels off around 5%. Because of the faster deactivation constant of acrylate monomer, it seems to be more sensitive to excess nitroxide. In addition, negligible thermal initiation causes more free nitroxide accumulation than for styrene. In this system, addition of glucose as a reduction agent for free nitroxide was shown to give remarkable rate enhancement and higher final conversion (60% for 5 hrs). Free nitroxide consumption was confirmed by their ESR studies.

1.2.3 Alkoxyamine disproportionation

In the early studies of SFRP, it had been recognized that biradical termination was the major factor causing the formation of dead polymer chain. Because of that, it had been also considered that polydispersity was broadened. However, it was found that alkoxyamine disproportionation produced more dead polymer chains than biradical termination (Li et al. [22], Gresza et al.[23]).

The disproportionation of alkoxyamine involves β-hydrogen abstraction by nitroxide from a propagating radical chain end, resulting in formation of terminally unsaturated polymer and hydroxylamine. Two pathways are being proposed for the β-hydrogen abstraction (scheme 1.6), either by usual disproportionation between dissociated radicals (path 1, Moffat et al.[24], Souaille et al.[25]) or direct fragmentation (chain cleavage) of alkoxyamine followed by a radical cage reaction (path 2, Li et al.[22],

Gresza et al.[23], Ohno et al.[26]). In these reactions, Path 1 competes with the deactivation reaction, and path 2 competes with the activation reaction.

Scheme 1.6

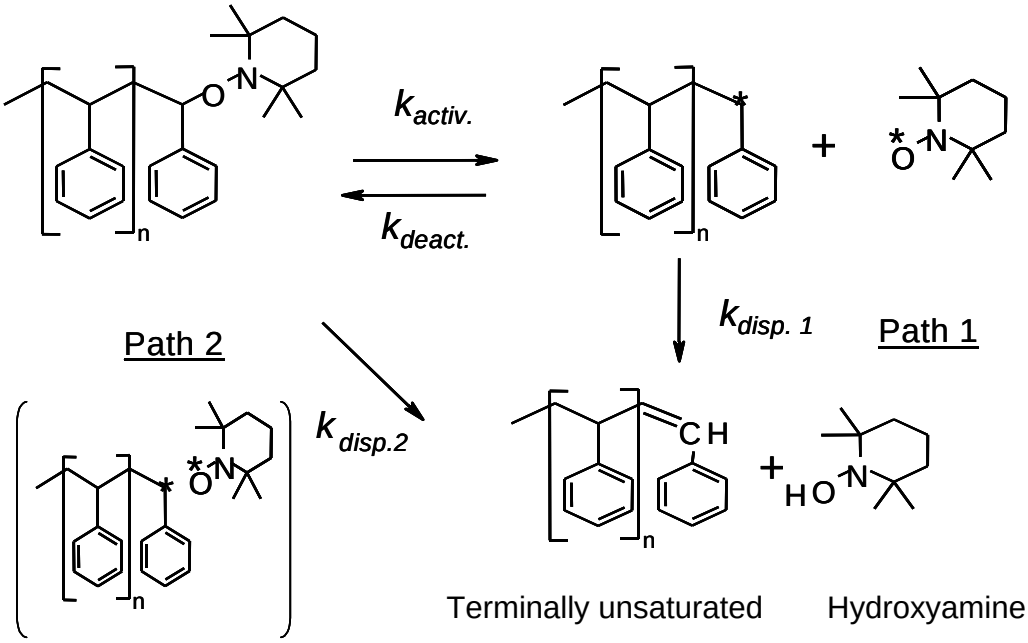

It is worth noting that the hydroxylamine from disproportionation is believed to undergo further disproportionation with another polymer radical in the presence of oxygen (hydroxylamine disproportionation), yielding a dead chain and regenerating free nitroxide (Le et al.[22], Gridnev et al.[27]). But the existence of oxygen is less likely in typical radical polymerizations, and therefore, it is believed to play a minor role. No further supporting results to show the importance of hydroxylamine disproportionation in SFRP have been reported.

Several discussions have been reported regarding how the alkoxyamine disproportionation impacts the overall kinetics and degree of final polymer livingness. Greszta et al.[23] proposed that the rate of disproportionation was in proportion to alkoxyamine concentration (i.e. path 2), and estimated the rate constant $k_{disp.2} = 1x\ 10^{-5}\ s^{-1}$ at 120 ^{o}C. By using this rate constant, they simulated how the overall kinetics were influenced, and how the degree of livingness was affected by the disproportionation reaction (styrene system). As a result, it was suggested that the disproportionation had a minor effect in terms of the rate of polymerization, but final livingness was impacted significantly. After 80% conversion, ~50 % of chains lost the livingness, and ~99% of the dead chains were produced by disproportionation. In this case, thinking of the fraction of the disproportionation reaction, which competes with activation reaction in path 2 (i.e. $F_2 = k_{disp.2}/ (k_{disp.2}+k_{act.})$), approximately 1.25% of the dormant chains could be disproportionated ($k_{act.}$ = 8.0 x10-4 S^{-1} [23]), and therefore the minor influence on the rate is not surprising, but the impact on the final livingness was unexpectedly high.

On the other hand, in path 1 there is no report on the rate constant $k_{disp.1}$ so far. But Souaille et al.[25] estimated that the disproportionation fraction F_1, competing with deactivation (i.e. $F_1 = k_{disp.1}/ (k_{disp.1}+k_{deactiv.})$), was 0.22 ~ 6.9% ($M_n$ = ~10000, k_p = 2000 ~ 20000 $M^{-1}S^{-1}$). In their simulation, while the time evolution of conversion was almost identical regardless of the F_1 value in the early stages, it leveled off at lower conversion with larger F_1 values (e.g. 93% for F_1 = 1%, 81% for F_1= 2%, 59% for F_1= 5%). In terms of the degree of final livingness, a similar result was observed compared to that in path 2, provided by Greszta et al.. In path 1, ~50% of polymer chains also lost livingness after ~ 81% conversion (F_1 = 2 %), and most of the dead chains (~98%) arose from

disproportionation. Souaille et al. also pointed out kinetic similarities in both pathways such as the time evolution of the degree of polymerization and polydispersity when the fraction F was the same, and therefore distinguishing between the two pathways is kinetically difficult.

1.3 Emulsion and Miniemulsion Polymerization

1.3.1 Classic Kinetics in Emulsion Polymerization

Emulsion polymerization[28), 29)] involves a free radical reaction to yield polymer particles in the 50-500 nm range, starting from a monomer dispersed in an aqueous phase. The free radical source is generally derived from water-soluble thermally degradable initiator. In order to achieve heterogeneous colloidal stability, anionic and/or nonionic surfactants are added to the aqueous phase, over the CMC of the surfactant. The dispersed system is composed of monomer droplet with diameter ~1 – 25 μm and micelles with diameters less than 10 nm.

In emulsion polymerization, three intervals are usually observed. Initially polymerization is started in the water phase after decomposition of initiator upon heating. The generated radicals propagate with the small amount of monomer dissolved in water phase and form aqueous oligoradicals. After adding a few monomer units, the oligoradicals become sufficient hydrophobic to enter the micelles. The particle nucleation continues until all micelles have either been nucleated or have been adsorbed onto the growing particles. During this particle nucleation period, the rate of polymerization gradually increases with the number of the particles nucleated (Interval I). Particle

nucleation from monomer droplets is negligible in emulsion polymerization. Most of the oligoradicals are captured by the micelles or particles. Monomer droplets function as "monomer reservoirs", with monomer diffusing through the water phase to the particles to maintain equilibrium swelling of the particles. By this monomer diffusion from the droplets, the rate of polymerization is kept constant once all particles are nucleated (Interval II). The constant rate is continued until the monomer droplets are depleted, and then it gradually decreases with monomer consumption in the particles (Interval III).

The first mechanistic studies of emulsion polymerization were done by Harkins[30], and Smith and Ewart.[31] In their studies, the most important conclusion is that the polymerization locus is mainly in the polymer particles (or micelles in the beginning stage), and the propagating radicals are segregated from each other in the particles. Therefore the radical concentration in each particle is crucial. Based on this concept, they proposed that the overall polymerization rate can be expressed by the product of the total particle number N_p and the average number of radicals per particle $\bar{n}$ (1-18).

$$R_p = k_p[M]_p \bar{n} N_p / N_a$$

$$\bar{n} = \sum_{n=0}^{\infty} nN_n / N_p \qquad \textbf{(1-18)}$$

where $[M]_p$ is the monomer concentration in the particles, and N_n is the fraction of the particles which include n radicals in the particle. In this case, $\bar{n}$ can be calculated by considering the overall radical balance, which includes radical entry, exit, and termination in the particles (1-19).

$$\frac{dN_n}{dt} = \left(\frac{\rho_A}{N_p}\right)N_{n-1} + k_e a_p\left(\frac{n+1}{v_p}\right)N_{n+1}$$
$$+ k_{tp}\left[\frac{(n+2)(n+1)}{v_p}\right]N_{n+2} - \left(\frac{\rho_A}{N_p}\right)N_n - k_e a_p\left(\frac{n}{v_p}\right)N_n - k_{tp}\left[\frac{n(n-1)}{v_p}\right]N_n \qquad \textbf{(1-19)}$$

where a_p and v_p are the particle surface area and particle volume respectively, ρ_A is the rate of the radical entry to the particles, k_e is the rate constant of radical exit from the particles, and k_{tp} is the rate constant of radical termination in the particles. The solution of the above equation was provided through the quasi-steady state approximation[32] (1-20).

$$\bar{n} = \frac{a}{4}\frac{I_m(a)}{I_{m-1}(a)}$$
$$a = \sqrt{8\alpha}, \alpha = \rho_A v_p / k_t N_p, m = k_f v_p / k_t, k_f = \frac{k_e a_p}{v_p} \qquad \textbf{(1-20)}$$

Im: Modified Bessel Function

Nomura et al.[33] proposed the following limiting solution, assumed that the radical termination in water phase is zero (1-21).

$$\bar{n} = \frac{1}{2}\left\{\left[\left(\alpha' + \frac{\alpha'}{m}\right)^2 + 2\left(\alpha' + \frac{\alpha'}{m}\right)\right]^{\frac{1}{2}} - \left(\alpha' + \frac{\alpha'}{m}\right)\right\} + \left(\frac{1}{4} + \frac{\alpha'}{2}\right)^{\frac{1}{2}} - \frac{1}{2}$$
$$\alpha' = \left(\rho_w v_p / k_{tp} N_p\right) \qquad m = k_f v_p / k_t \qquad \textbf{(1-21)}$$

where ρ_w is the rate constant of radical generation in water phase, and N_P is the total number of particles.

A distinguishing feature of conventional emulsion polymerizations is "compartmentalization" of propagating radicals, which profoundly affects both the reaction rate and molecular weight. When polymerizations are conducted in dispersed aqueous systems in which the particle size is relatively larger than 1 um, their kinetics are very similar to bulk reactions ($\bar{n} \geq 1$). However as the particle size decreases below approximately 1 um, $\bar{n}$ becomes sufficiently small to change the kinetics. Specifically the termination reaction between two growing chains becomes less likely. Typically $\bar{n}$ in emulsion polymerization (styrene, 100nm –200 nm size range) is 0.5, which implies most particles contain one or zero radicals. As a result of compartmentalization, the reaction rate and the final molecular weight are much increased compared to bulk polymerization due to the reduced termination probability. The particle size is also an important in influencing the kinetics as it impacts the radical concentration in the particles.

1.3.2 Kinetic Features in Miniemulsion Polymerization

Miniemulsion polymerization and emulsion polymerization have much similarity as heterogeneous polymerization systems.[34),35)] The major difference between the two systems is that the monomer droplets are the significant locus of the particle nucleation in miniemulsion polymerization, but negligible droplet nucleation occurs in emulsion polymerization. In miniemulsion polymerization, the initial droplet size is reduced typically to the 100 nm –500 nm range by the homogenization process, unlike emulsion polymerization. The key to achieving a stable droplet emulsion in the above size range is

to use a mixed stabilizer system comprising an ionic emulsifier and a cosurfactant (costabilizer) such as long chain alkane and fatty alcohol to prevent the diffusion degradation of the monomer droplets caused by Ostwald ripening. Since the particle is nucleated from the droplets whose size range is similar to that of emulsion polymerization, the aforementioned Smith –Ewart theory can be applied to explain polymerization kinetics in miniemulsion after particle nucleation. It is, however, known that the following differences, due to the droplet nucleation in miniemulsion, should be considered:

(i) depending on costabilizer, the particle nucleation is unusually long due to low efficiency of the radical entry to the particles. The typical example is case when cetyl alcohol is used as a costabilizer. In addition, the number of particles nucleated is also formulation dependent.

(ii) miniemulsion polymerization does not exhibit the characteristic Interval II, constant rate region of a conventional emulsion polymerization. In the miniemulsion process, when Interval I ends, the polymerization rate starts to decrease due to the depletion of the monomer concentration in the particles, although it may increase later if the gel effect occurs.

1.4 SFRP in Emulsion and Miniemulsion Systems

1.4.1 Overview of Current Research

With increasing understanding of SFRP in the bulk process, its application to the heterogeneous system, such as emulsion and miniemulsion, has been of much interest. However, due to the complex nature of the heterogeneous system, there is still a large gap in its understanding compared to the bulk process. Partitioning of species, their mass transfer among phases, and initiation and particle nucleation have made the process much more complicated in terms of mechanistic understanding.

Initial efforts in emulsion polymerization were reported by Bon et al..[36] Seeded styrene emulsion polymerization (50 wt% seed particles to final polymer) was initiated by an alkoxyamine (1-tert-butoxy-2-phenyl-2-(1-oxy-2,2,6,6-tetramethylpiperidinyl)ethane) at 125 ^{o}C. Near complete conversion (~99%) was achieved but at a low rate (36 hrs). As polymerization progressed, the molecular weight distribution became broader. This broadening was attributed to heterogeneity arising from partitioning and compartmentalization. In addition, an enhanced Diels-Alder reaction (autopolymerization) was suspected to be another possibility. Reported polydispersities were 1.41 – 1.54 compared to 1.39 in the corresponding bulk polymerization. The polydispersity in emulsion polymerization included the seed polymer, therefore the difference compared to bulk polymerization seems to be insignificant.

Cao et al.[37] studied the partitioning influence by using differently substituted TEMPO derivatives of varying water solubility at 120 ^{o}C. Significant differences were observed for different nitroxides. Very low water solubility of the nitroxide resulted in an

uncontrolled polymerization, while too high water solubility resulted in slow aqueous phase initiation that hindered the polymerization rate. While they reported some successful emulsion polymerizations using 4-acetoxy TEMPO (81% conversion in 12hrs with Mn =18K and ~1.3 polydispersity), complete particle size distribution was not reported. In addition, latex stability was very poor (storage stability was only for a few days).

Regarding the latex stability during emulsion polymerization, Marestin et al.[38] reported that emulsion polymerization usually showed bi-modal or broad particle size distribution from submicron to micron range and/or large amounts of coagulum. In addition, they also reported that addition of hexadecanol improved latex stability (hexadecanol is often used in miniemulsion polymerization as a co-stabilizer). The best result was obtained with the combination of hexadecanol, 4-amino-TEMPO and SDS (sodium dodecyl sulfate). It achieved 69 % conversion in 36 hrs with Mn = 6.0K, and polydispersity = 1.7. However the final particle size distribution was still broad from submicron to micron range (weight average diameter 540nm) and it could be stored only for a few days without settling

The reason for this colloidal instability is not yet clear, but droplet polymerization, for instance arising from autopolymerization, has been proposed to be one of the possibilities. If it is true, it could not explain instability in the seeding polymerization process used by Bon et al. as they did not have droplets present. But it was also reported that this instability in emulsion polymerization was observed even at 90 ºC (SG1; N-tert-butyl-N- (1-diethylphosphono-2, 2-dimethylpropyl) nitroxide, styrene), where the

autopolymerization was negligible (Lansalot et.al.[39]). Therefore the observed instability cannot be explained only by droplet autopolymerization.

More successful results were reported using the miniemulsion process. Macleod et al.[40] and Prodpran et al.[41] reported stable latex polymerization in miniemulsion polymerization using a bicomponent initiating system. Macleod produced stable polystyrene latex, using TEMPO, hexadecane, water-soluble initiator (potassium persulfate: KPS), and anionic surfactant (sodium dodecylbenzene sulfonate: SDBS) at 135 ^{o}C ([TEMPO] / [KPS] = 2.9 yielded Mn =14000, and 1.1 polydispersity). The ratio, [TEMPO] / [KPS] = 2.9, was relatively higher than the typical ratio ~ 1.3 used in bulk, suggesting some loss of nitroxide into the water phase by partitioning. In addition, they described that the rate of polymerization was faster than the typical rate reported in the bulk system. While the final conversion leveled off, it reached 87% in 6 hrs without any additives for rate enhancement (e.g. CSA).

On the contrary, Prodpran et al. reported a conflicting result that miniemulsion polymerization was slower than bulk. They conducted polymerizations at 125 ^{o}C, using TEMPO, oil-soluble initiator (benzoyl peroxide: BPO, [TEMPO] / [BPO] = 1.25), and anionic surfactant (disulfonate alkyl diphenyl oxide sodium salt: Dowfax 8390). 90% conversion was reached in 12 hrs compared to 2.5 hrs for the bulk system. Polydispersities were ~ 1.6 in both systems. Diffusion of some active species into the water phase was postulated.

Smith et al.[42] conducted a more systematic kinetic study at 135 ^{o}C. Their purpose was to clarify the effect on partitioning of nitroxides in miniemulsion polymerization. ,

They used TEMPO and 4-hydroxy TEMPO terminated alkoxyamine for initiation (unimolecular initiator). In this case, most of the alkoxyamine would be located in monomer droplets at first, but after dissociation, the nitroxides will be partitioned between the organic phase and the water phase depending on their water solubilities (4-hydroxy TEMPO > TEMPO). Significant difference was observed in the final conversion compared to bulk polymerization. The miniemulsions leveled off ~ 65 % for both TEMPO and 4-hydroxy TEMPO after 6 hrs, while the bulk system reached ~90% after 8 hrs. Interestingly, regardless of the water solubility of the nitroxide, or polymerization system (either miniemulsion or bulk), the conversion – molecular weight profile was almost identical. Polydispersity was slight better in miniemulsion polymerization. Molecular weight mainly depended on initial alkoxyamine concentration. For example, in the case of [alkoxyamine] = 0.020 M for ~60% conversion, the molecular weight was 20K ~ 27K in both system. The polydispersity was 1.28 ~ 1.38 (~60% conversion) for miniemulsion, and 1.49 ~1.62 (~90% conversion) for bulk.

Regarding the polymerization rate, bulk polymerization showed slightly higher rate than in miniemulsion judging from the slope of time –conversion curves (approximately x1.5 times faster in bulk). Moreover, it was found that the water solubility difference between TEMPO and 4-hydroxy TEMPO did not affect the rate of polymerization in miniemulsion. Their conversion – time profiles was also almost identical. This result suggests a very important aspect of partitioning of nitroxide in heterogeneous system. The respective partition coefficients between styrene and water are 2.2 M/M for 4-hydroxy-TEMPO and 98.8 M/M for TEMPO[43)], where M/M is moles of nitroxide in styrene per moles of nitroxide in water at 135 ^{o}C. Hence most TEMPO

resides in the organic phase, but 4-hydroxy TEMPO is considerably more water soluble, and one would expect much greater differences in their polymerization behaviors.

Ma et al.[44] considered theoretical explanations for this phenomenon in their mechanistic modeling studies. In their simulations, the partition coefficient changed the equilibrium concentration of nitroxide but not the time required to reach phase equilibrium. The time required for the phase equilibrium was within 1.5×10^{-5} s for both TEMPO and 4-hydroxy TEMPO, and it was fast enough to maintain phase equilibrium during polymerization (i.e. interfacial mass transfer is faster than the characteristic time of deactivation reaction by nitroxides). In this rapid phase equilibrium, styrene autopolymerization in droplets played a key role. When the autopolymerization occurred in droplets, free nitroxide in droplets was consumed by deactivation reactions. At the same time, phase transfer of the nitroxide from the water phase to droplets quickly occurred to maintain phase equilibrium. The net effect was that the partition coefficient was not very significant in influencing the kinetics.

Various research studies have been conducted in emulsion and miniemulsion systems. The miniemulsion process has achieved considerably more success than the emulsion process. The miniemulsion process is believed not to have issues related to particle nucleation or monomer transport from droplets to particles through the aqueous phase. Partitioning of nitroxide and compartmentalization remain as a potential concern for both systems. Moreover, strong interactions of these factors are also suggested. Further systematic studies are required to understand how these factors influence and interact for the emulsion and miniemulsion processes respectively.

1.4.2 Compartmentalization Effect in Miniemulsion

In the bulk SFRP process, biradical termination, alkoxyamine disproportionation and accumulation of the free nitroxide are keys to understanding the process. Hence it is important to know how these factors are affected by operating in a heterogeneous system. Of particular interest is how compartmentalization influences the kinetics in emulsion and miniemulsion systems.

Butte et al.[45] first reported on the effect of compartmentalization in SFRP miniemulsions. In this study, they considered both active radicals and nitroxide molecules to be compartmentalized and assumed those species did not exit from particles (i.e. no transfer among particles). Their model incorporated radical generation via both the oil soluble initiator [P_x-T] (P_x: low molecular polystyrene unit) and styrene autopolymerization. Accordingly the following modified Smith – Ewart equation was obtained.

$$\frac{dN_{i,j}}{dt} = -(k_a \mu_0 N_a V_p + \frac{k_{deact}}{N_a V_p} ij + \frac{k_t}{2 N_a V_p} i(i-1) + k_{th}[M]^3 N_a V_p) N_{i,j} + k_{act} \mu_0 N_a V_p N_{i-1,j-1} + \frac{k_{deact}}{N_a V_p}(i+1)(j+1) N_{i+1,j+1} + \frac{k_t}{2 N_a V_p}(i+1)(i+2) N_{i+2,j} + k_{th}[M]^3 N_a V_p N_{i-2,j} \quad \textbf{(1-22)}$$

where $N_{i,j}$ is the fraction of particles containing i active chains and j molecules of free nitroxide ($\sum N_{i,j} = 1$), μ_0 is the zeroth order moment of the dormant chains, k_{th} is the rate constant of the thermal initiation of the monomer, and N_a and V_p are the Avogadro

number and the particle volume respectively. They simulated the polymerization as a function of particle size in the range of 20nm – 100 nm. In this simulation, the important conclusions relating to compartmentalization are that;

i) smaller particle size (i.e. higher degree of compartmentalization) causes significant rate reduction of the polymerization. For this reason, Butte et al. pointed out the remarkable increase of the N_0 particle number. Because of the compartmentalization of the active radicals, most of the particles are in states $N_{0,j}$, $N_{1,j}$, and $N_{2,j}$. In this condition, the probability P_1 that an activation instead of a deactivation takes place in $N_{1,j}$ particles (i.e. the transition to $N_{2,j+1}$ instead of $N_{0,j-1}$) is given by the ratio of the corresponding reaction rates as follows (1-23).

$$P_1 = \frac{1}{(1 + jK_L / \mu_0 N_a^2 V_p^2)} \qquad \textbf{(1-23)}$$

Therefore, if segregation of the dormant chains is enhanced by smaller particle size or degree of polymerization, the probability of having $N_{2,j+1}$ particles is increased. The probability P_2, that a radical undergoes bimolecular termination instead of deactivation in the particle is given by 1-24 (limiting expression, assuming that $k_d \approx k_t$ since both reactions involve recombination between two radicals). This relation suggests that the higher degree of compartmentalization

causes larger probability of the biradical termination instead of a deactivation reaction in miniemulsion.

$$P_2 \approx \frac{1}{(1+2j)} \qquad \textbf{(1-24)}$$

Overall, when j is decreased by a higher degree of compartmentalization, the concentration of particles in the N_2 state is enhanced, consequently resulting in an increase of the number of N_o particles.

ii) from the probability P_2, it is seen that the beneficial effect of thermal initiation for rate enhancement, which is expected in the bulk system, is reduced by compartmentalization since thermal initiation always generates two radicals at the same time.

iii) because of the reduction of the average number of the active radicals per particle (particles exist more in the N_0 state), the overall number of dead polymer chains is remarkably decreased by compartmentalization (i.e. narrower polydispersity).

Charleux et al.[46] also reported simulation results in miniemulsion system at 90 ºC (N-tert-butyl-N- (1-diethylphosphono-2, 2-dimethylpropyl) nitroxide (SG1) - styrene system). The major differences from Butte et al. were that they did not consider the compartmentalization of nitroxide, and they did not consider thermal initiation. Only radical segregation was incorporated in their model, meaning nitroxide can quickly

exchange between particles via diffusion through the aqueous phase. Therefore the nitroxide concentration was assumed equal in all particles, and the evolution of the free nitroxide followed the equation (1-3), which was derived by Fischer et al.. Since the polymerization temperature was at 90 ºC, thermal initiation of styrene monomer was neglected. Accordingly the rate of generation of particles having i radicals (Smith-Ewart equation) can be written as follows.

$$\frac{dN_{i,}}{dt} = N_a V_p k_{activ}[P_x - T](N_{i-1} - N_i) + k_{deact}[T^\bullet]((i+1)N_{i+1} - iN_i) + \frac{k_t}{N_a V_p}((i+2)(i+1)N_{i+2} - i(i-1)N_i) \quad \textbf{(1-25)}$$

A distinguishing feature of their model is the treatment for termination rate. Charleux et al. concluded that the termination rate in SFRP miniemulsion and consequent nitroxide accumulation are different from that of the bulk process. Their conclusions regarding termination rate in SFRP and the corresponding free nitroxide concentration are;

i) termination rate in $\bar{n}$ <1 (i.e. zero one system) is slower than that of the case $\bar{n} \geq 1$ (i.e. pseudo-bulk system). It means that compartmentalization of the active radicals causes less radical termination. The termination rate for each case is expressed as follows.

1) $\bar{n} \geq 1$

$$R_t \approx \frac{2k_t}{(N_a V_p)^2}(\sum iN_i)^2 = 2k_t[P^\bullet]^2 \qquad \textbf{(1-26)}$$

2) $\bar{n} < 1$

$$R_t \approx 2k_t[P^\bullet]^2(1-\rho_t)$$

$$\rho_t = \frac{k_t/(N_a V_p)}{k_t/(N_a V_p) + k_{deact}[T^\bullet]} \qquad \textbf{(1-27)}$$

ii) because of the different termination rate in a zero one system, the accumulation of free nitroxide is also reduced, compared with that of the bulk system. The evolution of $[T^\bullet]$ between two systems has the following relationship.

1) $\bar{n} \geq 1$

$$[T^\bullet]_{n\geq 1} = \sqrt{[T^\bullet]_0^2 - B\ln(1-x)} \qquad \textbf{(1-28)}$$

2) $\bar{n} < 1$

$$[T^\bullet]_{n<1} = -A + \sqrt{(A+[T^\bullet]_0)^2 - B\ln(1-x)} \qquad \textbf{(1-29)}$$

$$A = \frac{k_t}{N_a V_p k_{deact}} \qquad B = \frac{4K_L[P_x - T]_0 k_t}{k_p}$$

$$\therefore \quad [T^\bullet]_{n\geq 1} = [T^\bullet]_{n<1}^2 + 2A([T^\bullet]_{n<1} - [T]_0) \qquad \textbf{(1-30)}$$

iii) equations (1-27) and (1-29), i.e. $\bar{n}$ <1, can apply when the particle volume is small enough to satisfy the following (1-31). In this case, the typical particle diameter calculated by V_p in their system is around 100 nm.

$$V_p \leq \frac{1}{N_a \sqrt{2k_t / k_a [P_x - T]_0}} \qquad \textbf{(1-31)}$$

Interestingly, the simulation results on the effects of particle size on polymerization rate are quite different from Butte's conclusions. The smaller particles size (i.e. higher degree of compartmentalization of the active radicals) showed faster polymerization rate but the molecular weight distribution became broader (i.e. compartmentalization can enhance the rate of polymerization but at the expense of less livingness). The reason for this different conclusion is the different treatment of the termination reaction and consequent accumulation rate of the free nitroxide. Butte et al. assumed the termination rate was the same as that of the bulk system, and two radicals were quickly terminated in particles with less nitroxide. The terminated radicals result in two free nitroxides, which never exit from the particles. This situation is likely to cause more N_0 particles (i.e. the active radical concentration in particles becomes lower due to compartmentalization).

While the above two models suggest the importance of the compartmentalization effect in the SFRP miniemulsion system, treatment of the nitroxide compartmentalization remains an issue. In addition, the above models do not treat any radical exit / re-entry in the particle, which is often observed in the conventional emulsion polymerization due to

radical transfer to monomer. Finally, partitioning of nitroxide into the water phase is also important in influencing aqueous phase reactions, which in turn influences radical re-entry.

Compartmentalization is the most important phenomena in emulsion and miniemulsion polymerizations, and it significantly impacts the fundamental kinetics and final polymer characteristics in those processes. Therefore, in order to better understand heterogeneous living radical polymerization, greater understanding of compartmentalization, and specifically how compartmentalization affects the overall SFRP kinetics and consequent polymer livingness, is a crucial research subject.

1.5 Research Objectives

Intensive research studies during the last ten years have remarkably increased our mechanistic understanding of SFRP in homogeneous systems. In addition, some important phenomena in heterogeneous systems were also reported such as the partitioning of nitroxide and its phase transfer. However many uncertainties remain. In particular, the potential use of a conventional emulsion process has never clarified in terms of whether or not an emulsion process in SFRP is theoretically possible. For this purpose, one of the keys is to consider how the compartmentalization behaves under SFRP chemistry. Charleux et al.[46] and Butte et al.[45] reported their mathematical considerations in miniemulsion systems, but completely opposite conclusions were reached. No experimental confirmation of compartmentalization has yet been reported.

Compartmentalization in conventional emulsion polymerization enables the process by ensuring particles grow faster than droplets, so that there is transfer of monomer from droplets to particles. If the compartmentalization effect is not preserved in SFRP, the conventional emulsion process is theoretically impossible. Moreover, even in a miniemulsion process, compartmentalization is very important in terms of prediction of the final livingness. In a bulk system, the termination reaction cannot be avoided in SFRP, and how to minimize it is a crucial matter with keeping a reasonable rate of polymerization in SFRP. For example, more nitroxide can in fact provide less termination due to lower radical concentration during polymerization (i.e. more dormant chains), but it also remarkably decreases the rate of polymerization. Therefore, some balance between the final livingness and the rate of polymerization is currently required. If compartmentalization is preserved in a heterogeneous system, it is expected to result in less termination without sacrificing the rate of polymerization, and it could become a major process advantage in SFRP heterogeneous systems.

The primary objective of this research is to study the theoretical and experimental feasibility of emulsion polymerization in SFRP, in particular, focusing on the compartmentalization effect in heterogeneous polymerization. The final goal for this research is to construct a comprehensive kinetic model including the compartmentalization effect for SFRP heterogeneous systems. In this model construction, the phase partitioning and phase transfer model for nitroxide developed by the Queen's group (Ma et al.[43]) will be adapted for accurately calculating mass transfer of nitroxide

among particles. Through this model construction, the following subjects will be examined:

1) How radical and nitroxide segregation in particles (i.e. polymerization locus) can be preserved under SFRP chemistry; clarification of the number of radicals per particles activated (n bar) in different particle sizes (10 nm: micelle size– 1000 nm: droplet size) and its change during polymerization are the keys. The competition between radical exit and propagation in particles must be incorporated. Experimentally observed values of n bar will also be used in the model development.
2) To what extent the termination and alkoxyamine disproportionation reactions occur as a function of the particle size, and its comparison with the bulk system. Quantitative analysis of the degree of livingness will be also provided to support the model predictions.

3) The feasibility of a conventional SFRP emulsion process. In this discussion, not only the process potential for conventional emulsion polymerization but also the opportunities for an optimized miniemulsion system will be considered in terms of the compartmentalization effect, compared with bulk systems. This optimization works will clearly show which process is advantaged in SFRP. Those conclusions are expected to provide significant contributions for industry application of the SFRP technology.

1.6 References

1. Matyjiaszawski, K., Controlled Radical Polymerization, ACS, 1998
2. Cunningham, MK., Prog.Polym.Sci. 27,1039, 2002
3. Georges, MK., Veregine, RPN., Kazmaier, PM., Hamer, GK., Macromolecules, 26,2987,1993
4. Wang , J-S., Matyjaszewski, K.,. J.Am Chem Soc., 117,5614,1995
5. Chiefari, J., Chong,YK., Ercole, F., Krstina, J., Jeffrey, J., Le, TPT., Mayadunne, RTA., Meijs, GF., Moad, CL., Moad, G., Rizzardo, E., Thang, SH., Macromolecules, 31,5559,1998
6. Fukuda,T., Terauchi,.T., Goto,A.,Ohno,.K.,Tsuji,Y.,Miyamoto,B., Macromolecules, 29, 6393, 1996
7. Veregin, RPN., Georges,.MK., Hamer,GK., Kazmaier,PM,. Macromolecules,28, 4391,1995
8. Veregin, RPN., Odell, PG., Michalak, LM., Georges, MK., Macromolecules, 29, 2746, 1996
9. Fischer, H, Macromolecules, 30,5666, 1997
10. Fischer, H., Chem.Rev.101,3581, 2001
11. Grezsta, D., Matyjiaszewski, K., Macromolecules, 29, 7661, 1996
12. Fukuda,T., Goto, A., Macromolecules, 29, 6393, 1996
13. Goto, A., Fukuda, T., Macromolecules, 30,4272, 1997
14. Fukuda, T., Goto, A., Ohno, K., Macromol. Rapid Commun. 21, 151, 2000
15. Fukuda, T., Goto, A., ACS Symp.Ser., 27,768, 2000
16. Souaille, M., Fischer, H., Macromolecules, 35, 248, 2002

17. Georges, MK., Veregin, RPN., Kazmaier, PM., Hamer, GK., Saban, M., Macromolecules, 27, 7228, 1994

18. Veregin, RPN., Odell, PG., Michalak, LM., Georges, MK., Macromolecules, 29, 4161, 1996

19. Buzanowski, WG., Graham, JD, Priddy, DB., Shero, E., Polymer,33, 3055, 1992

20. Malmstrom, E., Miller, RD., Hawker, CJ., Tetrahedron, 53, 15225, 1997

21. Keoshkerian, B., Georges, MK., Quinlun, M., Veregin, RPN., Goodbrand, B., Macromolecular, 31, 7559, 1998

22. Li, I., Howell, BA., Matyjaszewski, K., Shigemoto, T., Smith, PB., Priddy, DB., Macromolecules, 28, 6692, 1995

23. Greszta, D., Matyjaszewski, K., Macromolecules, 29, 7661, 1996

24. Moffat, K., Hamer, GK., Georges, MK., Macromolecules, 32, 1004, 1999

25. Souaille, M., Fischer, H., Macromolecules, 34, 2830, 2001

26. Ohno, K., Tsujii, Y., Fukuda, T., Macromolecules, 30, 2503, 1997

27. Gridnev, AA., Macromolecules, 30, 9651, 1997

28. Lovell, PA, El-Aasser, MS., Emulsion polymerization and emulsion polymers, Wiley, New York, 1997

29. Gilbert, RG., Emulsion Polymerization : a mechanistic approach, Academic Press, London, 1995

30. Harkins, WD., J. Am. Chem. Soc., 69, 1428, 1947

31. Smith,WV., Ewart, RH., J. Chem. Phys., 16, 592, 1948

32. Gilbert, RG., Emulsion Polymerization : a mechanistic approach, p 107, Academic Press, London, 1995

33. Nomura, M., Fujita, K., Macromol. Chem. Suppl., 10/11, 25, 1985

34. El-Aasser, MS., Preprints: Advanced in emulsion polymerization and latex technology, 26th. Annual short course, vol. 3, Lehigh University, 1995

35. Asua, JM., Prog. Polym. Sci. 27, 1283, 2002

36. Bon, SAF., Bosveld, M., Klumperman, B., German, AL., Macromolecules, 30, 324, 1997

37. Cao,J., He, J., Li, C., Yang, Y., Polymer Journal, 33, 75, 2001

38. Marestin, C., Noel, C., Guyot, A., Claverie, J., Macromolecules, 31, 4041, 1998

39. Lansalot, M., Farcet, C., Charleux, B., Varion, JP., Pirri, R., Tordo, P., Controlled Living Radical Polymerization, ACS , p138, 2000

40. MacLeod, P., Barber, R., Odell, P., Keoshkerian, B., Georges, MK., Macromol. Symp. 155, 31, 2000

41. Prodpran, T., Dimonie, VL., Sudol, ED., El-Aasser, MS., Macromol. Symp. 155,1,2000

42. Smith, J, M. Dissertation, Queen's University, Kingston, Canada, 2001

43. Ma, JW., Cunningham, MF., McAuley, KB., Keoshkerian, B., Georges, MK., Journal of Polymer Science A: Polymer Chemistry, 39,1081,2001

44. Ma, JW., Cunningham, MF., McAuley, KB., Keoshkerian, B., Georges, MK., Chemical Engineering Science, 58,1177,2003

45. Butte, A., Storti, G., Morbidelli, M., DECHEMA Monographs, vol. 134, 497, 1998

46. Charleux, B., Macromolecules, 33, 5358, 2000

CHAPTER 2

Compartmentalization in TEMPO-Mediated Styrene Miniemulsion Polymerization

2.1 Chapter Overview

Research on SFRP heterogeneous systems has been conducted in miniemulsion and in a conventional emulsion process. More successful results were reported in miniemulsion, but not in a conventional SFRP emulsion polymerization. The potential feasibility of a conventional SFRP emulsion process has never been previously clarified in terms of whether or not it is theoretically possible. For this purpose, one of the keys is to consider how SFRP chemistry influences compartmentalization.

In this chapter, we describe our experimental studies on the particle size influence in TEMPO-mediated styrene miniemulsion polymerization, compared with a corresponding bulk system. Conversion, molecular weight distribution and the chain livingness were considered to assess the effects on the particles size.

Finally, the potential feasibility of a conventional emulsion polymerization was discussed based on the results.

The material presented in this chapter has been published in Macromolecules (2007, 40, 7126), and appears in manuscript form.

2.2 Abstract

TEMPO-mediated styrene miniemulsion polymerizations were conducted at varying particle sizes (50nm, 90nm, and 180nm) to study possible effects of compartmentalization. Polymerizations were initiated using a TEMPO-terminated polystyrene macroinitiator that also acted as costabilizer for the miniemulsion. A bulk polymerization was conducted as a control. Conversion, molecular weight distribution, and the chain livingness were measured to assess the effect of particle size. Decreasing particle size resulted in lower rates of polymerization; after 6 hrs of polymerization, conversions were 59% for 180 nm particles and 43% for 50 nm particles. More importantly, large differences in the polymer chain livingness were observed with molecular weight; decreasing particle size resulted in higher Mn at a specified conversion, signifying lower concentrations in smaller particles.

2.3 Introduction

Advances in living/controlled radical polymerization have created a myriad of opportunities for new materials development, offering the promise of facile control of polymer microstructure and morphology. A significant fraction of all commercial polymers made by free radical processes are made using aqueous dispersions such as emulsion polymerizations. There has consequently been extensive interest in adapting living/controlled radical polymerization (LRP/CRP) techniques to aqueous dispersions [1, 2, 3]. While the fundamental kinetic features of emulsion-based polymerizations such as conventional emulsion polymerization (macroemulsion) and miniemulsion polymerization have been elucidated, basic questions remain about the nature of

emulsion-based CRP. Perhaps the most significant for CRP systems based on reversible termination mechanisms (Atom Transfer Radical Polymerization (ATRP) and Nitroxide-Mediated Polymerization (NMP)) is the question of whether compartmentalization (radical segregation) is relevant.

Compartmentalization is responsible for high reaction rates and high molecular weights in conventional emulsion polymerization. Segregating propagating radicals in small reaction volumes leads to reduce occurrence of mutual termination. While it is accepted that compartmentalization does occur in reversible transfer CRP systems (e.g. RAFT, MADIX) [4, 5, 6], it has been generally believed, based on theoretical considerations [7] and experimental studies [8, 9, 10, 11] that in reversible termination systems (ATRP, NMP), compartmentalization effects do not exist. A limited number of theoretical mathematical modeling studies have suggested they may occur at sufficiently small particle size [12, 13, 14] but as yet there has been no experimental data published that provides evidence of the existence of compartmentalization in nitroxide-mediated emulsion-based polymerizations.

Charleux [12] presented a theoretical framework by adapting the Smith-Ewart approach for propagating radical segregation in considering the SG1-mediated polymerization of styrene in a dispersed medium, and concluded compartmentalization effects would occur. Butte et al. [13] extended Charleux's approach by accounting for segregation of the nitroxide (TEMPO) in addition to the propagating radicals (Charleux considered segregation of only propagating radicals). Zetterlund and Okubo [14] have recently extended Butte's model and provided extensive discussion.

Charleux, Butte and Okubo all predicted that compartmentalization effects should be evident for NMP systems, although the nature of their predictions sometimes

conflicted. All agreed smaller particles should have higher livingness than larger particles, but while Charleux predicted smaller particle sizes would yield faster polymerizations, Butte and Okubo predicted the opposite. Despite the importance of such a fundamental question, the issue of whether compartmentalization effects exist in emulsion-based NMP remains unresolved. What is currently lacking is a careful experimental study suitable for comparison with conflicting theoretical predictions and that able to shed light on the questions posed by previous studies.

To probe the issue of potential compartmentalization in NMP emulsion-based systems, we have conducted TEMPO-mediated styrene miniemulsion polymerizations in which the particle diameter was varied from approximately 50 to 180 nm (volume average diameter). We avoided using hexadecane as a costabilizer to avoid its possible effects on the polymerization and to better mimic a true emulsion polymerization environment. Conversion, molecular weight distribution and polymer livingness were quantified. In addition, a bulk polymerization was run as control experiment representing a non-heterogeneous environment in which compartmentalization, and radical exit/entry effects are not factors. We present clear evidence that particle size effects in TEMPO-mediated polymerizations do exist, influencing both the rate of polymerization and the polymer chain livingness.

.

2.4 Experimental

2.4.1 Polymerizations

(a) Preparation of TEMPO-Terminated Oligomers of Polystyrene (TTOPS). 2.44g (0.0100 mol) Vazo 88 (1,1-azobis(cyclohexane carbonitrile)(DuPont) and 2.96 g (0.0189 mol) TEMPO (Aldrich) were used as received, and were dissolved in 600 ml (5.192 mol) distilled styrene (Aldrich). Styrene was washed three times with an equal volume of 2 wt% NaOH solution to remove inhibitor. This was repeated using distilled water, followed by drying over $CaCl_2$ and vacuum distillation. The mixture was polymerized at 135 °C for 2 hours, giving TTOPS with conversion of 15.7%; Mn=3931 g/mole; PDI=1.15.

(b) Miniemulsion polymerizations were run using TTOPS (prepared as described above) as both macroinitiator and costabilizer. One batch of TTOPS was used for all experiments to minimize variability. No hexadecane was used in these polymerizations. The aqueous phase was prepared by dissolving Dowfax 8390 (5mM – 46mM) in DIW (150g). The organic phase (40g), which consists of the TTOPS-styrene mixture, was mixed into the aqueous phase. The mixture was homogenized using a Microfluidizer 110S (Microfluidics International Corporation) (3 cycles at 300 kPa inlet pressure). The miniemulsion was purged with nitrogen, and then polymerized at 135 ^{o}C for 6 hours. Samples were collected over the course of reaction. Initial droplet size was controlled by varying the surfactant concentration, as reported by El-Aasser et al.. [9, 15] The conditions for each formulation are summarized in Table 2-1.

(c) SFRP Bulk Polymerization at 135 °C. 60 mL of the TTOPS-styrene mixture prepared in part (a) was purged with nitrogen and then heated at 135 °C for 6 hours in a round-bottom flask. Samples were collected over the course of reaction.

Table 2-1 Summary of experiments [1)]

Expt ID	[DOWFAX 8390] mM	Conv. (%)	Mn (g/mol)	PDI	Dw (nm)	Dw/Dn
E1 (Bulk)	N/A	86.5	20656	1.14	N/A	N/A
E2 (180 nm)	4.6	58.6	17778	1.16	184.7	1.13
E3 (90 nm)	23.0	49.9	16524	1.17	92.3	1.11
E4 (50 nm)	46.0	43.3	18077	1.15	54.5	1.17

1) Conversion (conv.), number average molecular weight (Mn), polydispersity (PDI), and weight - and number –average diameter (Dw, Dn) are based on final values. Temperature =135 oC for all experiments.

2.4.2 Characterization

All samples were analyzed for monomer conversion (gravimetry), molecular weight distribution and particle size. The "livingness" of selected samples was analyzed using method of Scott et al. [16], employing joint RI and Fluorescence GPC detectors as described below.

2.4.3 Particle Size Measurements

Particle size distributions were measured using a Malvern Mastersizer 2000 equipped with a Hydro 2000S optical unit. Styrene saturated water was used as the dispersant to minimize the diffusion of styrene from the particles.

2.4.4 Gel Permeation Chromatography (GPC)

Molecular weight distributions were measured using a Waters 2960 Separation Module with a Waters 410 Differential Refractometer (DRI) (480 nm). Five Waters Styragel columns (100, 500, 10^3, 10^4 Å) were maintained at 40^{o}C. Flow rate of the eluent (tetrahydrofuran, THF) was 1.0 ml/min. Polystyrene standards were used for calibration. Data were collected and processed using Waters Millenium software.

2.4.5 Livingness Measurements

Polymer samples were precipitated from solution using methanol and filtered to isolate the precipitate. The polymer was dissolved in chlorobenzene (0.012 M), mixed with N-TEMPO (50 equiv.), degassed with three freeze-thaw cycles, and heated at 123^{o}C for 154 min. under nitrogen. N-TEMPO [4-(1-Naphthoyloxy)-2,2,6,6-tetramethylpiperidine-1-oxyl] was prepared following Jones et al.. [17] The reaction mixture was added drop-wise into methanol to precipitate the polymer, which was again dissolved in THF. Following re-precipitation from methanol, the polymer was dried. To measure the alkoxyamine concentration, a Waters 474 Scanning Fluorescence Detector (690 nm) was added to the GPC in series after the DRI. The alkoxyamine 4-naphthoyloxy-1-((1'-phenylethyl)oxy)-2,2,6,6-tetramethylpiperidine (N-TEMPO-PhEt),

used as an internal standard, was dissolved in THF to give a concentration of 1.2×10^{-4} M. N-TEMPO-PhEt was synthesized using the procedure reported by Scott et al. .[16] 10 ml of this solution was added to about 5 mg of each polymer sample, which was analyzed with GPC. Chromatograms of polystyrene standards and N-TEMPO-PhEt at different concentrations were collected from both detectors. From the fluorescence detector, the PS chromatograms allowed the area under a sample chromatogram to be corrected for the fluorescence of the PS backbone. The N-TEMPO-PhEt chromatograms allow calculation of the amount of alkoxyamine (NTEMPO-terminated chains) in the polymer sample from the corrected area. Chromatograms from both detectors were aligned, and processed with the same calibration curve using the N-TEMPO-PhEt peak. With this technique, the quantity of NTEMPO-terminated chains in a sample was determined. Degree of livingness (DOL) is defined as the mass fraction of chains terminated with TEMPO. DOL is determined using the living chain distribution obtained from the fluorescence detector, and the total chain distribution obtained from the DRI detector.

2.5 Results

Polymerizations were run at varying surfactant concentrations to yield final particle diameters (volume average) of approximately 50, 90, and 180 nm. A bulk polymerization was also run as a control experiment. Experimental conditions used for each experiment are shown in Table2- 1. The measured degree of livingness of the TTOPS macroinitiator was 98%. DOWFAX 8390 was selected as surfactant as prior experience in our laboratory has shown that its effect on rate in TEMPO-mediated

miniemulsion polymerizations is minimal, unlike SDBS which is capable of significantly enhancing the rate [18, 19].

2.5.1 Effect of Particle Size on Kinetics

Figure2- 1 shows conversion versus time profiles for the three different particle diameter experiments and the bulk polymerization. There is a pronounced trend of decreasing conversion with decreasing particle diameter, with the bulk polymerization exhibiting the highest conversions throughout the experiment. The 6 hour conversions for the 50 nm and 180 nm particles were 43% and 59% respectively, a 37% difference. At 3 hours, the difference in conversion for these two particle sizes was 45% (29% vs 42% conversion). These differences were very reproducible as determined using replicate runs. Experimental error (estimated at <5% of the conversion value) is significantly less than the observed differences between experiments at different particle sizes. Figure 2-2 shows the evolution of the particle size for the three miniemulsion experiments during the polymerization. All experience some increase in diameter; particle with larger initial diameter experienced the largest increase in size. The particle size increase is similar to that seen by El-Aasser [9].

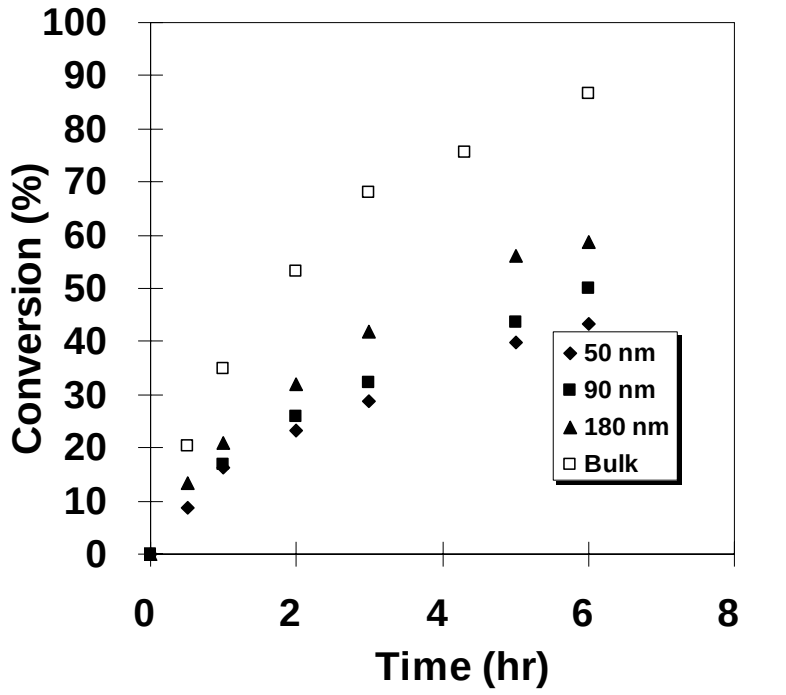

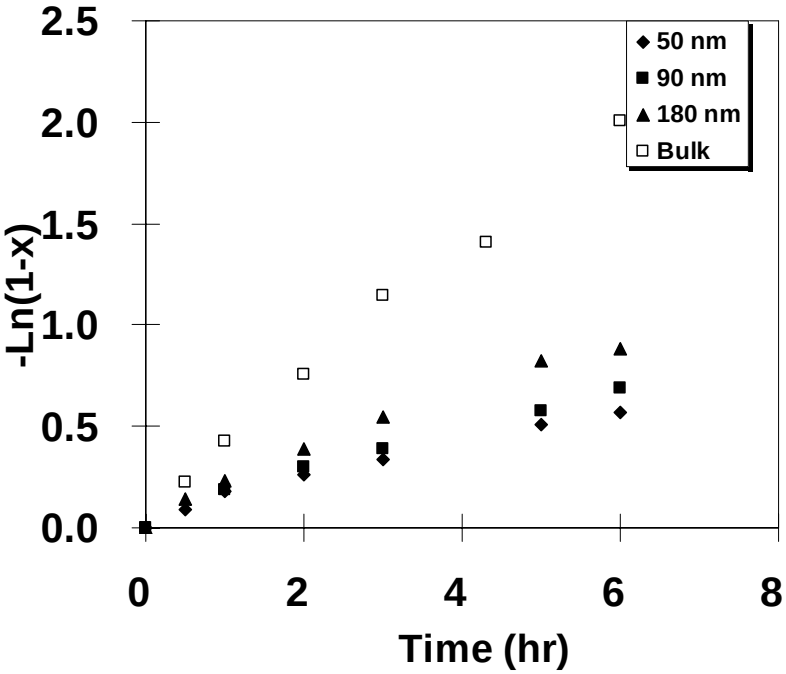

Fig. 2-1 Conversion (1a) and –ln (1-x) (1b) versus time for TEMPO-mediated styrene miniemulsion and bulk polymerizations

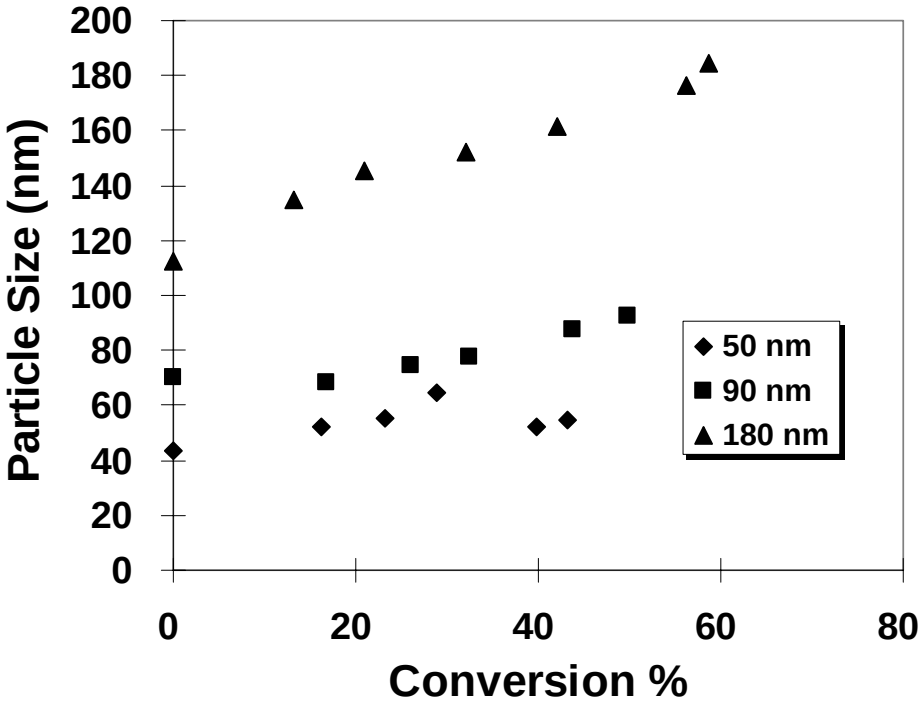

Fig. 2-2. Particle size versus conversion for TEMPO-mediated styrene miniemulsion polymerizations.

2.5.2 Effect of Particle Size on Evolution of Molecular Weight and Polydispersity

Evolution of Mn with conversion and the polydispersities are shown in Figure2-3 for the three miniemulsions and the bulk polymerization. There are not large differences among the different conditions, although there is a consistent trend of smaller particle size polymerizations displaying higher Mn than the larger particle size experiments. This result implies the number of chains was slightly

lower for the smaller particles. Polydispersities exhibit a similar trend for all conditions, decreasing slightly at the outset of polymerization and then gradually increasing as the polymerization progressed to a final value of ~1.15.

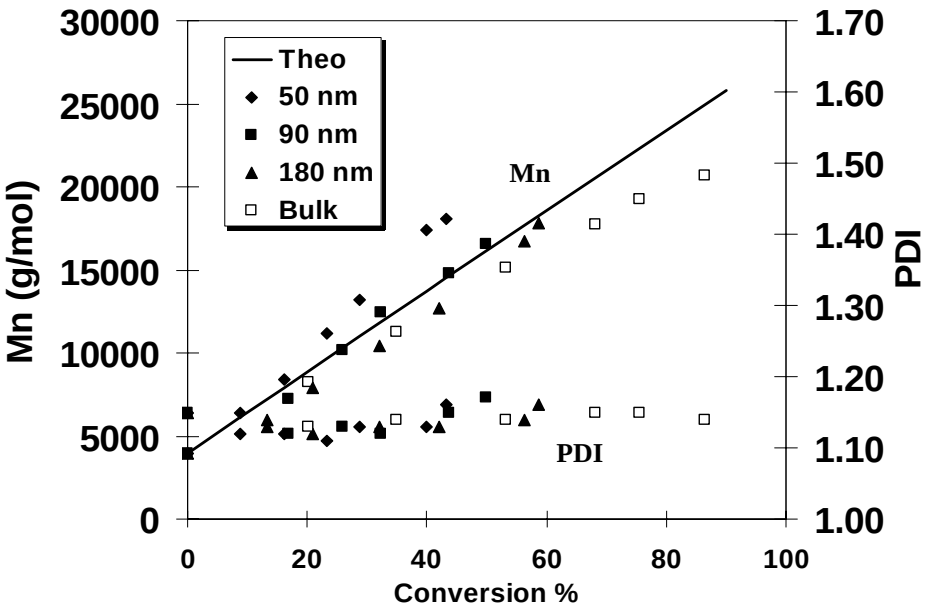

Fig. 2- 3 Mn (3a) and PDI (3b) versus conversion for TEMPO-mediated styrene miniemulsion and bulk polymerizations

2.5.3 Effect of Particle Size on Livingness

The Degree of Livingness (DOL) is shown in Figure 2-4 for all polymerizations. Livingness decreased in the order: 50 nm>90 nm ~bulk>180 nm. The smallest particles (50 nm) displayed noticeably higher livingness at equivalent conversions compared to the other runs. As particle diameter increased, the livingness decreased. Curiously the bulk polymerization exhibited a livingness profile intermediate to the three miniemulsion results, most closely resembling the 90 nm miniemulsion experiment. GPC trace for the 50nm experiment (Fig.2-5) reveals a clean evolution of the molecular weight distribution, with only slight evidence of tailing at lower molecular weights.

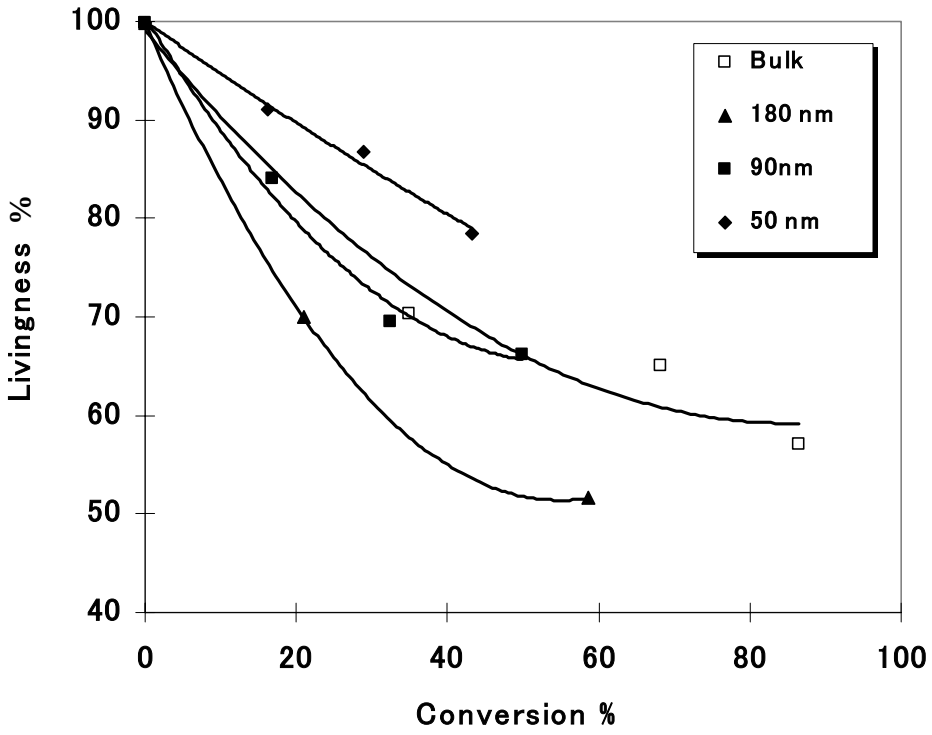

Fig. 2- 4 Degree of livingness (DOL) for TEMPO-mediated styrene miniemulsion and bulk polymerizations

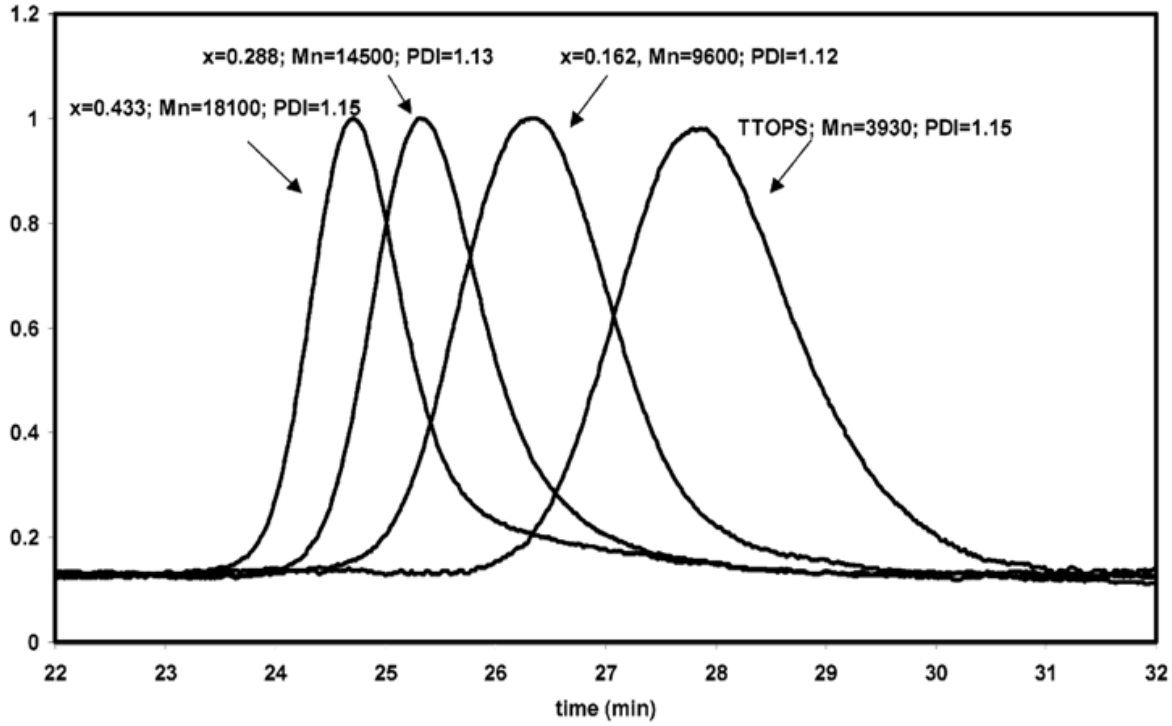

Fig. 2-5 GPC chromatograms for TEMPO-mediated styrene miniemulsion polymerization experiment E4 (50nm particles).

2.6 Discussion

2.6.1 Compartmentalization effect in miniemulsion with SFRP

The data presented above provide, for the first time, experimental evidence that compartmentalization effects do exist in TEMPO-mediated emulsion-based systems. Theoretical predictions based on mathematical modeling studies have predicted the existence of compartmentalization effects but there has not been experimental data published to establish its existence. As particle size is decreased, rate decreases and the livingness of the polymer chains increases. In addition, there is an increase in molecular weight (reduced chain number) in smaller particles at a given conversion. The bulk polymerization behaves distinctly from the miniemulsion runs, with pronounced differences in rate and livingness even, thus dispelling the view that NMP miniemulsions exhibit kinetics that are similar to bulk.

Predictions from the modeling studies of Butte et al. [13] and Zetterlund and Okubo [14] are in qualitative agreement with the experimental data presented in this paper with regards to the effects of particle size on polymerization rate and polymer livingness, and the livingness trends are consistent with Charleux's predictions [12]. (The models did not actually report livingness but rather used the PDI as a measure of livingness. Our experience with living/controlled radical systems is that the PDI is a useful but rather insensitive measure of livingness, which was our motivation for developing the fluorescence-based technique.) Butte concluded that the reduced rate predicted in smaller particles would be caused by geminate recombination of thermally generated radicals, leading to reduced thermal initiation rates and thus a lower overall polymerization rate. Zetterlund and Okubo expanded this discussion, emphasizing the role of enhanced

deactivation of radicals within a small volume that would result in decreasing rates as particle size decreases. The enhanced deactivation is also predicted to result in reduced rates of termination and therefore increased livingness in smaller particles. If geminate recombination of thermal radicals is important and dependent on particle size, there should be an impact on the number of chains. The Mn data (Figure 2-3) is consistent with the postulated fate of thermal radicals, as the number of chains decreases with particle size.

Reduction of rate by geminate termination of thermally generated radicals was also postulated by Pan et al. [11], who provided experimental data showing reduced rates in TEMPO-mediated styrene miniemulsions compared to a bulk polymerization. In TEMPO-mediated styrene miniemulsion polymerization conducted without initiator (i.e. thermal polymerization), the chain number in bulk polymerizations was consistently greater than in miniemulsion. This was attributed to higher thermal initiation efficiencies in bulk compared to miniemulsion. Furthermore they noted the initial polymerization rate was higher in bulk than in miniemulsion, consistent with our observations.

There are features of our data that are not consistent with existing theoretical models. First is that the observed bulk polymerization rate was significantly faster than the miniemulsion system, which is different from a typical heterogeneous emulsion system exhibiting compartmentalization effects due to radical segregation. (In conventional emulsion polymerization, compartmentalization leads to an increase in rate [20].) The Butte, Zetterlund and Charleux models all predict there is an upper limit (~100 nm for Butte and Zetterlund, ~500 nm for Charleux) to the particle size for which compartmentalization effects will be apparent, and that large particles would behave

similarly to bulk polymerization. In addition, the models did not explicitly predict the observed dependence of molecular weight on particle size, although this observed effect is a logical consequence of geminate combination of thermal radicals and is also consistent with Pan's data [11].

Causes for this disagreement in the bulk polymerization behavior between data and model predictions may include the role of radical exit, which is not accounted for in the models. Exit of monomeric radicals resulting from transfer to monomer or of thermally generated radicals could decrease the rate in an emulsion-based system relative to the bulk polymerization. While the fate of exited radicals may often be to re-enter particles (depending on the experimental conditions) [20], with NMP the fate of exited radicals could be much different. The presence of finite amounts of TEMPO in the aqueous phase will likely result in rapid deactivation of the exited radical. Ma [21] measured the TEMPO partition coefficient for a styrene-water system; at the reaction temperatures used in this study, ~2-3% of the free TEMPO in the system will reside in the aqueous phase. Based on an estimate of [TEMPO]~10^{-5} M in the particle phase once a pseudo-stationary state is established, and a 4:1 ratio of aqueous phase: organic phase, [TEMPO] in the aqueous phase will be ~10^{-7} M. Moreover, because of rapid diffusion between the aqueous and organic phases [22], this value will remain approximately constant during polymerization. If we approximate the rate coefficient for radical exit for styrene as ~10^{-2} s^{-1} [23] and the particle number is 10^{17} particles/L aqueous phase, the total radical exit rate is ~10^{15} $(L.s)^{-1}$. [TEMPO] ~10^{-7} M corresponds to ~$6x10^{16}$ molecules TEMPO per L of aqueous phase. These calculations indicate a large excess (~60x) of TEMPO will

be present during the polymerization in the aqueous phase, provided diffusion of TEMPO between phases is rapid.

Once an exited radical is deactivated, its probability of adding monomer units and re-entering another particle will be considerably reduced compared to conventional (mini) emulsion polymerization because of the lower polymerization rate in the aqueous phase (low aqueous phase styrene concentration, coupled with an equilibrium favoring dormant chains, results in low aqueous phase polymerization rates [24]). The outcome is a reduction in the average propagating radical concentration within the particles, and consequently a lower rate. Consider the characteristic times for dormant chain activation (λ_a), deactivation of active radicals (λ_d), and propagation (λ_p) in the aqueous phase (values for the rate parameters[24], and values for TEMPO partition coefficient and aqueous styrene concentration[21] are taken from previous studies in our laboratory):

$$\lambda_a = 1/k_a \approx 1/3.99\text{e-}3\ s^{-1} \approx 251\ s$$

$$\lambda_d = 1/(k_d\,[TEMPO]_{aq}) \approx 1/(8\text{e}7\ M^{-1}s^{-1} \times 10^{-7}\ M) \approx 1.25\text{e-}1\ s$$

$$\lambda_p = 1/(k_p\,[styrene]_{aq}) \approx 1/(2936\ M^{-1}s^{-1} \times 0.0167\ M) \approx 2.04\text{e-}2\ s$$

A chain is activated approximately every 4 minutes. The ratio of characteristic times for deactivation to propagation is 6.13. In contrast, for the particle phase, assuming a mean styrene concentration of 5 M:

$$\lambda_d = 1/(k_d\,[TEMPO]_{org}) \approx 1/(8\text{e}7\ M^{-1}s^{-1} \times 10^{-5}\ M) \approx 1.25\text{e-}3\ s$$

$$\lambda_p = 1/(k_p\,[styrene]_{org}) \approx 1/(2936\ M^{-1}s^{-1} \times 5\ M) \approx 6.81\text{e-}5\ s$$

The ratio of characteristic times for deactivation to propagation in the particle phase is 18.4. Therefore the ratio λ_d / λ_p is ~3 times lower in the aqueous phase, meaning that dormant chains in the aqueous phase will grow relatively slowly.

The temperature used in this work (135 ^{o}C) also differs by 10 ^{o}C from that used in the modeling studies. It is possible this factor also contributes to the observed differences between model predictions and the data although the magnitudes of the effects are unlikely to be large enough to account for such pronounced changes in behavior.

The lower polymerization rate in miniemulsion compared to bulk (or presumably large droplets) is a critical issue for any emulsion-based SFRP process (macroemulsion, miniemulsion, microemulsion) in which there may cause droplets polymerization, because it implies there may be little or no thermodynamic driving force for monomer transfer from droplets to particles, since the polymer concentration may be higher in large droplets/particles. Therefore monomer droplets will not disappear in the polymerization as they do in conventional emulsion polymerizations (even when some droplet polymerization is known to occur). This may explain why repeated attempts to develop an NMP emulsion process have failed, with the exception of Charleux [25] who wisely used a semi-batch starved feed approach to eliminate droplets from the system.

The bulk system also showed unexpectedly higher livingness than the large particle size miniemulsions, despite the higher rate of polymerization in bulk which would be expected to yield higher rates of termination. Previously however, we have shown in both modeling [24, 26] and experimental [27, 28, 29] studies that alkoxyamine disproportionation may account for a significant loss of livingness at 135 ^{o}C in TEMPO-mediated styrene miniemulsions. The practical implication of this is that longer reaction

times results in greater loss of livingness due to increased disproportionation, and inversely that shorter reaction times tend to yield higher livingness provided the rates are not so high that termination becomes significant.

Our data may appear to be contradictory to the data published by El-Aasser [9], who observed no significant difference in rates for final volume average particle sizes ranging from ~60 to ~150 nm. They employed a similar approach, using DOWFAX 8390 and TTOPS, however they also used hexadecane (HD) as a costabilizer. While HD is widely used in miniemulsion polymerizations, it is not present in emulsion polymerizations. HD is not required in miniemulsions if a low molecular weight, highly water-insoluble component is present, such as TTOPS. We have run experiments using HD, and also observed that particle size effects were not as significant in the presence of HD. The reason(s) for the difference in behavior with HD is not currently known but is being investigated. It is possible that exit of monomeric and thermally generated radicals is reduced in the presence of HD, as it is effective in reducing diffusional degradation (exit) of the monomer.

Zetterlund and Okubo [30] recently published a communication on particle size effects in TEMPO-mediated miniemulsion polymerization, co-stabilized by HD. They observed that for small particles (70 nm number average diameter; 90 nm weight average diameter), control of the polymerization was lost, resulting in very fast reaction rates and broad molecular weight distributions that were independent of conversion. Decreasing rates were observed as the particle sizes were increased. This reported effect on rate is not in agreement with our results, and warrants further discussion.

Zetterlund and Okubo attributed the effect of particle size on the rate not to compartmentalization, believing the particles were too large, but rather to a significant reduction of the deactivation rate due to an interface effect in which TEMPO preferentially locates at interface. The fact that we were able to make well-controlled particles under similar conditions at ~50 nm volume average diameter suggests there may be another factor responsible for Okubo's loss of control with 70 nm particles, possibly related to the presence of SDBS. The two experiments they ran that exhibited particle size effects were at higher [SDBS] (8 wt% relative to styrene). We have shown [18, 19] that SDBS plays a major role in increasing rate in TEMPO-mediated polymerizations, possibly due to enhanced radical generation and/or consumption of TEMPO. It is conceivable that their results were at least partially attributable to the high concentration of SDBS that resulted in [TEMPO] becoming too low to effectively mediate the polymerization.

2.7 Conclusion

Particle size in TEMPO-mediated miniemulsion polymerization influences important features of the polymerization, including rate, polymer livingness and to a lesser degree the molecular weight. Smaller particles showed slower rates of polymerization in the heterogeneous system than larger particles. Furthermore the rate and livingness of bulk polymerizations have been shown to differ from miniemulsion polymerizations, with the bulk polymerization being faster than all the miniemulsions. Quantitative analysis of the livingness revealed that higher livingness was preserved in

the smaller particles. Bulk polymerization, despite having a relatively fast polymerization rate, had livingness almost identical to the 90 nm particles and higher than the 180 nm particles.

Three factors are postulated to explain the observed compartmentalization effects and influence of particle size. Geminate termination of thermally generated radicals in confined volumes will reduce rate by effectively reducing the thermal initiation rate, as well as leading to lower chain numbers (higher Mn) in smaller particles. Enhanced deactivation of propagating radicals by TEMPO in the confined volume of a small particle will result in reduced termination (increased livingness) and lower rate.

These results represent the first experimental evidence of compartmentalization effects in emulsion-based NMP, and are relevant for future development of macro-, mini- and micro-emulsion processes. The influence of particle size on the polymerization rate suggests it may not be possible to achieve nitroxide-mediated emulsion polymerization with any droplets present, because it implies loss of thermodynamic driving force for monomer transfer from droplets to particles. Because of mechanistic similarities between NMP and ATRP (both are based on reversible termination of propagating radicals), the effects reported here may also be relevant to ATRP in emulsion-based systems. We are currently investigating this phenomenon.

2.8 References

(1) Qiu, J.; Charleux, B.; Matyjaszewski, K. *Progress in Polymer Science* **2001,** 26, 2083-2134.

(2) Cunningham, M.F. *Progress in Polymer Science* **2002,** 27, 1039-1067.

(3) Cunningham, M.F. *Comptes Rendus Chimie* **2003,** 6, 1351-1374.

(4) Butte, A.; Storti, G. ; Morbidelli, M. *Macromolecules* **2001,** 34, 5885-5896.

(5) Monteiro, M.J.; Hodgson, M. ; De Brouwer, H. *J. Polym. Sci. A Polym. Chem.* **2000,** 38, 3864-3874.

(6) Prescott, S.W. *Macromolecules* **2003,** 36, 9608-9621.

(7) Butte, A. *Macromolecules* **2000,** 33, 3485.

(8) Pan, G.; Sudol, E.D.; Dimonie, V.L. ; El-Aasser, M.S. *Macromolecules* **2001,** 34, 481-488.

(9) Pan, G.; Sudol, E.D.; Dimonie, V.L. ; El-Aasser, M.S. *Macromolecules* **2002,** 35, 6915-6919.

(10) Cunningham, M.F.; Xie, M.; McAuley, K.B.; Keoshkerian, B. ; Georges, M.K. *Macromolecules* **2002,** 35, 59-66.

(11) Pan, G.; Sudol, E.D.; Dimonie, V.L.; El-Aasser, M.S. *J. Polym. Sci. A Polym. Chem.* **2004,** 42, 4921-4932.

(12) Charleux, B. *Macromolecules* **2000,** 33, 5358-5365.

(13) Butte, A.; Storti, M.; Morbidelli, M. *DECHEMA Monographs* **1998,** 134, 497-507.

(14) Zetterlund, P.B.; Okubo, M. *Macromolecules* **2006,** 39, 8959-8967.

(15) Anderson, C.D.; Sudol, E.D. ; El-Aasser, M.S. *Macromolecules* **2002,** 35, 574-576.

(16) Scott, M.E.; Parent, J.S.; Hennigar, S.L.; Whitney, R.A.; Cunningham, M.F. *Macromolecules* **2002,** 35, 7628-7633.

(17) Jones, M.J.; Moad, G.; Rizzardo, E.; Solomon, D.H. *J. Org. Chem.* **1989,** 54, 1607-1611.

(18) Cunningham, M.; Lin, M.; Smith, J.; Ma, J.; McAuley, K.; Keoshkerian, B.; Georges, M.K. *Progress in Colloid & Polymer Science* **2004,** 124, 88-93.

(19) Lin, M.; Hsu, J.C.C.; Cunningham, M.F. *J. Polym. Sci. A Polym. Chem.* **2006,** 44, 5974-5986.

(20) Gilbert, R.G. **1995,**

(21) Ma, J.W.; Cunningham, M.F.; McAuley, K.B.; Keoshkerian, B.; Georges, M.K. *J. Polym. Sci. A Polym. Chem.* **2001,** 39, 1081-1089.

(22) Ma, J.W.; Cunningham, M.F.; McAuley, K.B.; Keoshkerian, B.; Georges, M.K. *Macromolecular Theory and Simulations* **2002,** 11, 953-960.

(23) Prescott, S.W.; Ballard, M.J.; Rizzardo, E.Gilbert, R.G. *Macromolecules* **2005,** 38, 4901-4912.

(24) Ma, J.W.; Smith, J.A.; McAuley, K.B.; Cunningham, M.F.; Keoshkerian, B.Georges, M.K. *Chemical Engineering Science* **2003,** 58, 1163-1176.

(25) Nicolas, J.; Charleux, B. ; Magnet, S. *J. Polym. Sci. A Polym. Chem.* **2006,** 44, 4142-4153.

(26) Ma, J.W.; Cunningham, M.F.; McAuley, K.B.; Keoshkerian, B.; Georges, M.K. *Chemical Engineering Science* **2003,** 58, 1177-1190.

(27) Cunningham, M.; Lin, M.; Buragina, C.; Milton, S.; Ng, D.; Hsu, C.C.; Keoshkerian, B. *Polymer* **2005,** 46, 1025-1032.

(28) Lin, M.; Cunningham, M.F.; Keoshkerian, B. *Macromolecular Symposia* **2004,** 206, 263-274.

(29) Monteiro, M.J.; De Barbeyrac, J. *Macromolecular Rapid Communications* **2002,** 23, 370-374.

(30) Nakamura, T.; Zetterlund, P.B.; Okubo, M. *Macromolecular Rapid Communications* **2006,** 27, 2014-2018.

CHAPTER 3

Nitroxide Mediated Miniemulsion Polymerization: Model Development for a Compartmentalized Miniemulsion System

3.1 Chapter Overview

Compartmentalization dominates the polymerization kinetics in conventional heterogeneous systems such as miniemulsion and emulsion polymerization. In the previous chapter, we showed experimental observations of the particle size influences in SFRP miniemulsion system, and how it revealed the completely contradictory trend of the rate enhancement compared to the traditional emulsion system. That is, the smaller particles show a slower rate of polymerization in SFRP. Although some previous modelling studies have been done to understand the compartmentalization effect, none have compared the results to actual data. In addition, the current modelling studies have never explained the origins of a slower rate in miniemulsion than in bulk, which we have observed.

To provide better understanding of the actual observations in SFRP emulsion the development of a comprehensive model is presented in this chapter. The model was developed by extending the classic Smith Ewart kinetics with SFRP chemistry. It includes the phase partitioning of species and radical exit/re-entry among phases. In addition, prediction of the livingness was also discussed by incorporating alkoxyamine disproportionation as well as the termination reaction into the model.

The model developed is the first comprehensive model including chemical and physical events in SFRP emulsion systems.

3.2 Abstract

A mathematical model based on the classic Smith–Ewart equation has been developed to better understand the compartmentalization effect in SFRP miniemulsion systems. The model was designed to predict the changes of $N_{i,j}$ particles, which contain i active radicals and j free nitroxide molecules. The model also described the partitioning of the species among the phases, reactions in the aqueous phase, and the radical exit /re-entry from the particles. In addition, it also incorporated alkoxyamine disproportionation, which is believed to dominate the livingness of the chains, as well as the termination reaction.

3.3 Introduction

In SFRP homogeneous polymerization, tremendous effort has been exerted to understand the kinetic mechanisms, and control of the reaction has been progressed remarkably as a result of this improved understanding. However in heterogeneous systems such as miniemulsion and traditional emulsion system, kinetics understanding is still far behind compared to homogeneous systems[1), 2), 3), 4), 5), 6).]

In heterogeneous systems, the most important factor for understanding the kinetics is the compartmentalization effect, which causes the segregation of the chemical

species among phases. Although many studies have been done in the SFRP heterogeneous system, it is still uncertain whether or not the compartmentalization can be preserved under SFRP chemistry. The first discussions of compartmentalization effects in SFRP were made by Butte et al.[8] and Charleux et al..[9] Butte calculated that the polymerization rate (R_p) increased with increasing particle size in the heterogeneous SFRP because of the significantly small fraction of time of the radical activation period. On the other hand, Charleux who performed calculations by solving Smith-Ewart equations in miniemulsion determined that R_p increases with decreasing the particle size. The differences between Butte's and Charleux's results were a consequence of: (1) whether or not they considered the nitroxide as well as the active radicals to be compartmentalized in the particles (Butte: yes, Charleux: no); and (2) whether thermal initiation was considered in the system (Butte: yes, Charleux: no). Butte's results are in close agreement qualitatively with our observations except his predicted rate in miniemulsion was faster compared to that of the bulk system, unlike our experimental observations. Recently Zetterlund et al.[10] carried out simulations using Butte's equations. They compared miniemulsions with particle sizes less than 100 nm with a bulk system. They observed that R_p decreases in proportion to the cube of the particle size for smaller particles; they also observed and a maximum R_p at a certain particle size (~70nm). The lower R_p in the smaller particles is explained by the confined space effect, which is an enhanced deactivation reaction between a radical and a nitroxide. This confined space effect counteracts the segregation effect of the active radicals, which usually increases the rate, so that a maximum rate is observed at a certain particle size. In this case, it is worth noting that in Zetterlund's simulations the R_p in the bulk polymerization was slower than

the maximum rate in miniemulsion, unlike our results where the bulk polymerization was always fastest. In the previous chapter, we described the influence of the particle size on the polymerization rate and the livingness in SFRP miniemulsion. It showed the completely contradictory trend of rate enhancement compared to the traditional emulsion system. That is, the smaller particles showed a slower rate of polymerization, and a faster rate was observed for homogeneous bulk SFRP polymerizations (compared to all particle sizes in miniemulsion). Pan et al.[7] also observed a reduced rate in TEMPO-Mediated styrene miniemulsions compared to a bulk system. The reason for the differences between the experimental results and the simulations has not yet been clarified. As one of the possibilities, it is suspected that the previous models do not include important major events in the heterogeneous system such as radical exit/re-entry and the partitioning of species among the phases. In addition, alkoxyamine disproportionation, which causes a large impact on the final livingness of chains, is not considered in earlier studies. For further understanding of the heterogeneous system with SFRP chemistry, more comprehensive modeling studies are required.

The purpose of this chapter is to discuss the development of a comprehensive model for the SFRP emulsion system. The model considers N_i^j particles, containing i active radicals and j free nitroxide molecules, for the compartmentalization effect. In addition, the model includes radical exit /re-entry, phase partitioning of species, aqueous phase reactions and alkoxyamine disproportionation. This is the first time such a comprehensive model has been developed for a heterogeneous SFRP system (Scheme 3-1).

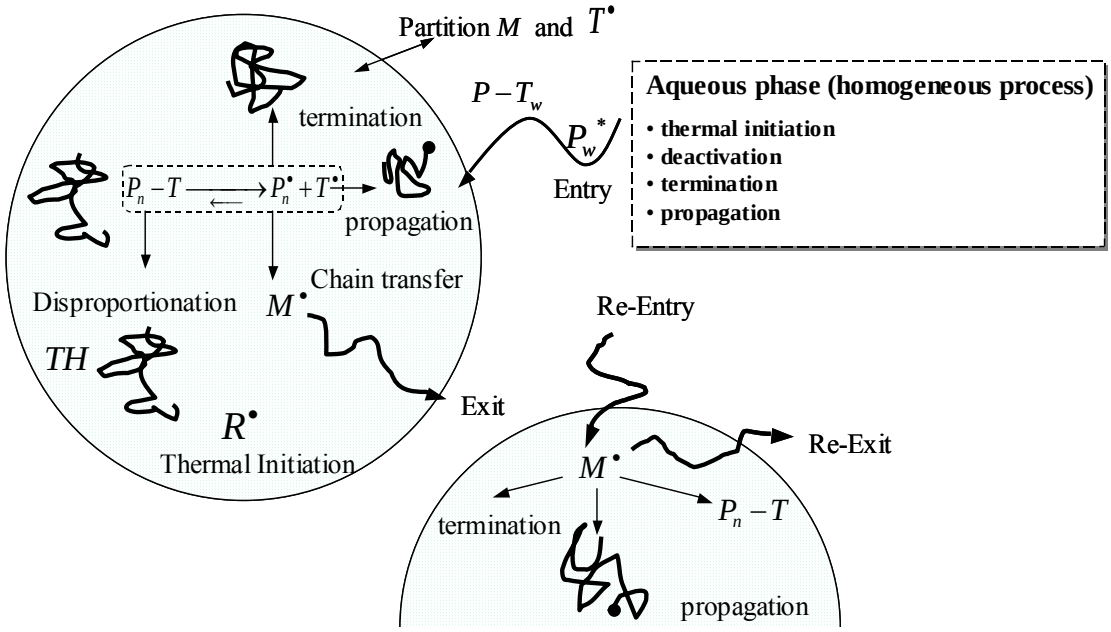

Scheme 3.1 Chemical and physical events for the process of SFRP miniemulsion

3.4 Model Development of a Compartmentalized SFRP Miniemulsion System

3.4.1 Homogeneous system

Since bulk polymerization experiments are valuable control experiments in studying SFRP miniemulsions, we also developed a homogeneous model. The system considered is based on bulk styrene polymerization. The initiation reaction for the active radicals is assumed to occur via both activation of the dormant species of alkoxyamine and thermal initiation via the Mayo mechanism[11]. The termination reaction occurs via bimolecular termination only. All reactions in SFRP bulk polymerization of styrene are summarized as follows.

(Reversible reaction and radical generation)

The reversible reaction of SFRP is represented by;

$$P_n - T \underset{k_{deact}}{\overset{k_{act}}{\longleftrightarrow}} P_n^{\bullet} + T^{\bullet} \qquad K_L = \frac{k_{act}}{k_{deact}} \tag{3-1}$$

where $P_n - T$ is the dormant species (alkoxyamine), $P_n^{\bullet}$ is an active polymer radical, and $T^{\bullet}$ is a stable nitroxide radical. K_L is an equilibrium constant in the reversible reaction (3-1). In addition, thermal initiation reaction in styrene is represented by;

$$3[M] \xrightarrow{k_{ith}} M^{\bullet} + DI^{\bullet} \tag{3-2}$$

where M denotes monomer species, $M^{\bullet}$ is the active monomer radical by the thermal initiation, and $DI^{\bullet}$ is the dimer radical by the Diels-Alder reaction.

(Propagation)

$$P_n^{\bullet} + M \xrightarrow{k_p} P_{n+1}^{\bullet} \qquad (3\text{-}3)$$

where M denotes monomer species, $P_{n+1}^{\bullet}$ is a propagating radical, and k_p is the propagation rate coefficient.

(Bimolecular Termination)

In the case of the termination reaction, bimolecular termination is only assumed.

$$P_n^{\bullet} + P_m^{\bullet} \xrightarrow{k_t} D_{n+m} \qquad (3\text{-}4)$$

where k_t is the termination rate coefficient, and D_{n+m} is dead polymer having chain length (n+m).

(Alkoxyamine disproportionation)

Alkoxyamine disproportionation in (3-5) was also considered. It is responsible for the loss of livingness (in addition to the termination reaction).

$$P_n - T \xrightarrow{k_{disp}} D_n + TH \qquad (3\text{-}5)$$

where k_{disp} is the disproportionation rate coefficient and *TH* is hydroxylamine produced by β-hydrogen abstraction from direct fragmentation of the alkoxyamine followed by a radical cage reaction[12].

Based on the above reactions, the following eq. (3-6) – eq. (3.-9) were used to calculate the mass balances for each species in the homogeneous SFRP system.

$$\frac{d[M]}{dt} = -k_p[P_n^\bullet][M] \tag{3-6}$$

$$\frac{d[P_n - T]}{dt} = k_{deact}[P_n^\bullet][T^\bullet] - k_{act}[P_{n-}T] - k_{disp}[P_n - T] \tag{3-7}$$

$$\frac{d[T^\bullet]}{dt} = k_{act}[P_n - T] - k_{deact}[P_n^\bullet][T^\bullet] \tag{3-8}$$

$$\frac{d[P_n^\bullet]}{dt} = k_{act}[P_n - T] + k_{ith}[M]^3 - k_{deact}[P_n^\bullet][T^\bullet] - 2k_t[P_n^\bullet]^2 \tag{3-9}$$

3.4.2 Heterogeneous System

For modeling compartmentalization in the dispersed system, the Smith –Ewart equations[13] extended to two dimensions (i.e. considering compartmentalization of both active radicals and nitroxide molecules), as first derived by Butte et al. were employed. In the model, the number of particles was treated as remaining constant with conversion. The aqueous phase as well as the interior of the particles was considered as the polymerization locus. Radical exit /re-entry was also incorporated into the model. In this case, the exited radicals were assumed capable of reacting with monomer, radicals, and

free nitroxide that are partitioned into the water phase. In addition, all nitroxide terminated oligomers are assumed to enter the particles. No interfacial resistance in the mass transfer of the species between the aqueous and organic phases is also assumed.

3.4.2-1 Radical Exit and Entry

(Rate coefficient for radical exit: k_f)

In terms of the radical exit from the particles**,** Nomura and Harada et al. [14), 15), 16)] theoretically derived the desorption rate coefficient from both stochastic and deterministic approaches, based on a scheme consisting of the following three consecutive steps (Scheme 3-2).

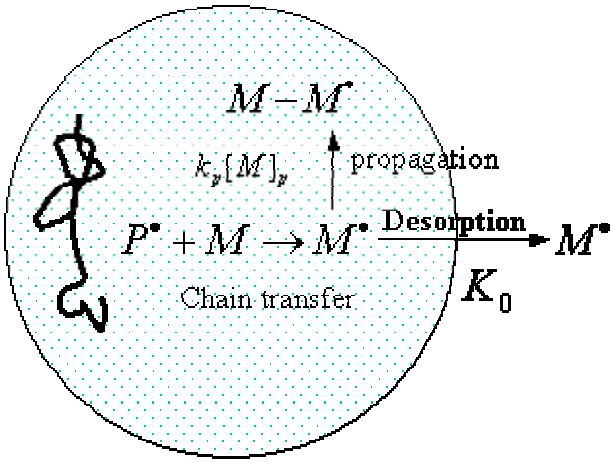

Scheme 3.2 Chemical and physical events for the process of radical exit

K_0: Overall desorption rate constant

(1) Chain transfer of a polymeric radical to a monomer in a polymer particle, followed by (2) diffusion of the resulting low molecular weight radical to the particle-water interface, and (3) successive diffusion into the water phase through a stagnant film adjacent to the surface of the particle. In styrene polymerization, when the monomer radical propagates into a dimer radical before its desorption, the diffusion of the dimer into the water phase is negligibly low due to its low solubility into water phase. They derived the rate coefficient for radical exit from a particle, k_f as;

$k_f =$ (rate of monomer radical generation) x (its desorption probability)

$$= k_{mf}[M]_p \left(\frac{K_0}{K_0 + k_p[M]_p} \right) \qquad (3\text{-}10)$$

where k_{mf} is the chain transfer rate constant to monomer, $[M]_p$ is the monomer concentration in the particles. K_0 is the overall desorption rate constant for monomer as shown in (3-11).

$$K_0 = k_0(a_p / v_p) = 12 D_w \delta / m_i d_p^2 \qquad (3\text{-}11)$$

where a_p is the surface area occupied by a unit amount of emulsifier, v_p is the volume of a particle, D_w is the diffusion coefficient for radicals in the water phase, and d_p is the particle size. k_0, δ, m_i are defined as follows:

$$1/k_0 = 1/k_L + m_i / k_w$$
$$m_i = [M]_p / [M]_w$$
$$k_L = (2D_p / d_p)$$
$$k_w = (2D_w / d_p)$$
$$\delta = [1 + (D_w / m_d D_p)]^{-1}$$

(D_p is the diffusion coefficient for radicals inside a polymer particle)

In the case of $K_0 << k_p[M]_p$, eq. (3-10) can be expressed as follows.

$$k_f = K_0\left(\frac{k_{mf}}{k_p}\right) = \left(\frac{12D_w\delta}{m_d d_p^2}\right)\left(\frac{k_{mf}}{k_p}\right) = \left(\frac{12D_w}{m_d d_p^2}\right)\left(\frac{k_{mf}}{k_p}\right)\left(1+\frac{D_w}{m_d D_p}\right)^{-1} \quad (3\text{-}12)$$

(Overall rate of radical entry: ρ_e / N_T)

In the Smith-Ewart theory, radical entry is defined as the transfer of free radical activity from the aqueous phase into the polymer particles. It is believed that the radical entry event consists of multiple steps. In order for an initiator-derived radical to enter a particle, it must first become hydrophobic by the addition of monomer units in the aqueous phase. The hydrophobic oligomer radical produced in this way arrives at the surface of a polymer particle by molecular diffusion. It can then diffuse into the polymer particle, or its radical activity can be transferred into the polymer particle via a propagation reaction with monomer in the particle surface layer. There are two major entry models widely accepted in the conventional emulsion polymerization[17]. One is the diffusion-controlled model, which assumes that the diffusion of radicals from the bulk phase to the surface of the particle is the rate-controlling step. The other is the propagation-controlled model, which assumes that since only z-mer radicals can enter the polymer particles very rapidly, the generation of z-mer radicals from (z-1)-mer radicals by a propagation reaction in the aqueous phase is the rate-controlling step. In this model development, the diffusion-controlled model was considered for the overall entry rate of the radicals.

Smith-Ewart first proposed that the transfer of free radical activity into the interior of a particle take place by the direct entry of free radicals into a polymer particle. They

pointed out that the rate of radical entry into a particle is given by the rate of diffusion of free radicals from an infinite medium with concentration $[R_w^{\bullet}]$ into a particle diameter d_p with zero radical concentration,

$$\frac{\rho_e}{N_t} = 2\pi D_w d_p [R_w^{\bullet}] = k_{ep}[R_w^{\bullet}] \tag{3-13}$$

where k_{ep} is the mass transfer coefficient for radical entry into a particle. However, Harada et al.[14] pointed out, based on their experimental observations, that the radical capture efficiency was different depending on the particle size. They predicted that the capture efficiency of a micelle, which is usually less than 10nm, is a factor of about 100 less than that of a particle. Taking this into consideration, they implicitly introduced a concept called the radical capture efficiency of a particle. Hansen et al. further elaborated the concept of the radical capture efficiency into the following expression to represent the net rate of radical absorption by a particle, introducing an absorption efficiency factor F [18),19),20).]

$$\frac{\rho_e}{N_t} = 2\pi D_w d_p [R_w^{\bullet}] F = k_{ep}[R_w^{\bullet}] \tag{3-14}$$

Therefore, F represents a factor that describes the degree to which absorption is lowered compared to irreversible diffusion, and is given by;

$$\frac{1}{F} = \left(\frac{D_w}{\lambda D_p}\right)\left(X \coth X - 1\right)^{-1} + W' \tag{3-15}$$

where $X = (d_p/2)\{(k_p[M]_p + nk_t/v_p)/D_p\}^{1/2}$, λ is the equilibrium partition coefficient between particles and water for radicals, W' is the potential energy barrier analogous to Fuchs' stability factor, n is the number of radicals in a particles whose number is 0 or 1, and v_p is the particle volume. In this case, when λ and d_p are assumed to be 1000 [21] and ≥ 50nm respectively in styrene polymerization, the predicted F is ~1.0. For simplicity, F is treated as 1.0 for styrene monomer in this model, but it could be adjusted depending on the monomer type.

The free radical concentration $[R_w^\bullet]$ was calculated by the following overall free radical balance between radical generation and the consumption in aqueous phase.

$$\frac{d[R_w^\bullet]}{dt} = \text{(thermal initiation of radicals in aqueous phase)+(exit of radicals from particles)-(termination of radicals) –(deactivation of radicals)}$$

$$= k_{ith}[M]_w^3 + k_f \bar{n} N_T - 2k_t[M^\bullet]_w^2 - k_{dea}[M^\bullet]_w[T^\bullet]_w \qquad (3\text{-}16)$$

In this case, the dormant species $[P-T]_w$ was considered to immediately enter into a particle once it was formed by deactivation of an oligomeric radical by nitroxide. Therefore no radical source from the $[P-T]_w$ exists in the aqueous phase. $[P-T]_w$ was also calculated separately by eq. 3-17 to adjust $[P_n-T]_p$ after absorption into a particle (the concentration of $[P-T]_w$ must be recalculated into $[P-T]$ per unit volume of particles).

$$-\frac{d[P-T]_w}{dt} = k_{dea}[M^\bullet]_w[T^\bullet]_w \qquad (3\text{-}17)$$

3.4.2-2 The Number Fraction of Particles: N_i^j

The modified Smith-Ewart equations derived by Butte et al [8), 10).], which contains $iP^\bullet$ and $jT^\bullet$, were extended further to incorporate the radical exit/entry mechanism as shown in eq.3-18. The population balances of all chemical and physical events are shown in scheme 3-3.

$$\begin{aligned}\frac{dN_i^j}{dt} = {} & N_A v_p k_{act}[P_n - T]_p\{N_{i-1}^{j-1} - N_i^j\} + 0.5k_{ith}[M]_p^3 N_A v_p\{N_{i-2}^j - N_i^j\} + \\ & \frac{k_t}{N_A v_p}\{(i+2)(i+1)N_{i+2}^j - (i)(i-1)N_i^j\} + \frac{k_{deact}}{N_A v_p}\{(i+1)(j+1)N_{i+1}^{j+1} + \\ & (i)(j)N_i^j\} + k_f\{(i+1)N_{i+1}^j - iN_i^j\} + \frac{\rho_e}{N_T}\{N_{i-1}^j - N_i^j\} \qquad (3-18)\end{aligned}$$

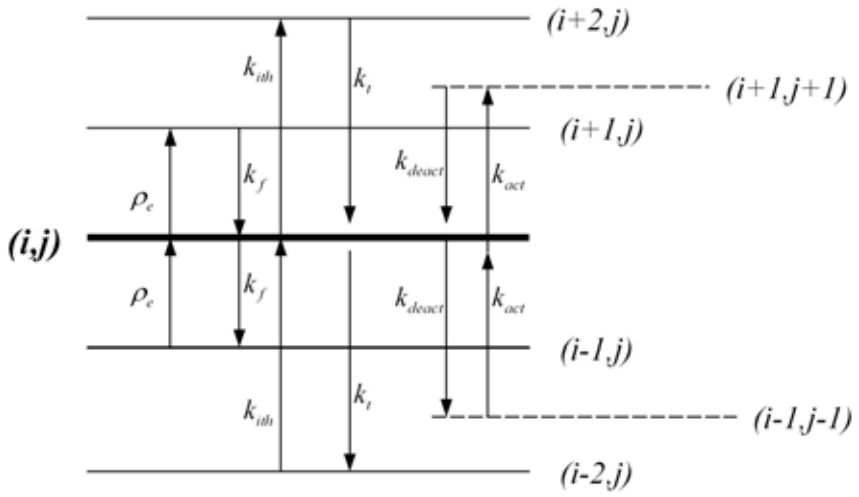

Scheme 3.3 Population balance for all chemical and physical events in N_i^j particles

In eq.3-18, $[P_n - T]_p$ and $[M]_p$ are the dormant chain concentration and monomer concentration in the particles respectively. N_A is the Avogadro number. The "2" in the termination term for the bulk system (eq.3-9) is absent, because one termination event causes the disappearance of one particle and generation of another. For the same reason, there is a factor "0.5" in the thermal initiation term in eq.3-18.[10] In addition, in the radical entry term expressed in eq.3-14 and eq.3-16, the $[R_w^\bullet]$ must be calculated on a number basis as shown in eq.3-19.

$$\frac{\rho_e}{N_T} = 2\pi D_W d_p [R_w^\bullet] F$$

F=1.0 (styrene monomer)

$$[R_w^{\bullet}] = \left[k_{ith}[M]_w^3 + \frac{k_f}{N_A} \bar{n} N_T - 2k_t[M^{\bullet}]_w^2 - k_{deact}[M^{\bullet}]_w[T^{\bullet}]_w \right] N_A \quad (3\text{-}19)$$

(N_T : the total number of particles)

The average number of the radicals ($\bar{n}$) and of nitroxides ($\bar{n}_t$) in the particles is given by;

$$\bar{n} = \sum_i \sum_j i N_i^j \quad (3\text{-}20)$$

$$\bar{n}_t = \sum_i \sum_j j N_i^j \quad (3\text{-}21)$$

The overall concentrations of $[P^{\bullet}]_p$ and $[T^{\bullet}]_p$ per unit volume organic phase are given by

$$[P^{\bullet}]_p = \frac{1}{N_A v_p} \sum_i \sum_j i N_i^j \quad (3\text{-}22)$$

$$[T^{\bullet}]_p = \frac{1}{N_A v_p} \sum_i \sum_j j N_i^j \quad (3\text{-}23)$$

3.4.2-3 Alkoxyamine Disproportionation and Livingness

Alkoxyamine disproportionation as shown in (3-24) was also considered in this model. In this case, the dormant $[P_n - T]_p$ was assumed not to partition into the water phase.

$$[P_n - T]_p \xrightarrow{k_{disp}} D_n + [TH]_p \quad (3\text{-}24)$$

Combined with eq.3-24, the concentration of $[P_n - T]_p$ per unit volume organic phase is given by

$$\frac{d[P_n - T]_p}{dt} = \frac{k_{deact}}{(N_A v_p)^2} \sum_i \sum_j ijN_i^j - k_{act}[P_n - T]_p + [P_n - T]_{w \to p} - k_{disp}[P_n - T]_p \quad (3\text{-}25)$$

where $[P_n - T]_{w \to p}$ is the dormant chain concentration entering from the aqueous phase into a particle. The original unit of $[P_n - T]_w$ is moles per 1 L of water, therefore in eq.3-25, the unit must be changed into moles per particle volume as shown in eq.3-26.

$$[P_n - T]_{w \to p} = [P_n - T]_w / \left(\frac{\pi}{6}\right) d^3 N_T \quad (3\text{-}26)$$

The compartmentalization of both $P^\bullet$ and $T^\bullet$ is considered when computing $[P_n - T]_p$.

The livingness of the polymerization was predicted by the loss of $[P_n - T]_p$, which is caused by disproportionation and the termination of radicals.

The livingness in this model was given by

$$Livingness = \frac{[P_n - T]_p}{[P_n - T]_0} \quad (3\text{-}27)$$

where $[P_n - T]_0$ is the initial concentration (t =0) of the dormant alkoxyamine.

3.4.2-4 Partitioning of Monomer and Nitroxide

The thermodynamic equilibrium for the partitioning for monomer and nitroxide was considered by the partition coefficient method, which controls chemical diffusion between phases. No interfacial resistance was considered in this model.

The partition coefficient was defined as

$$m_d = \frac{[X]_{org}}{[X]_{aq}} \qquad (3\text{-}28)$$

where m_d is the partition coefficient of species X between organic phase (or monomer swollen particles) and the water phase. Ma et al.[22] reported the partition coefficients of several nitroxides such as TEMPO and hydroxyl TEMPO in styrene monomer at 135°C. The values are 98.8 for TEMPO and 2.2 for hydroxyl TEMPO respectively. In this model, the concentration of monomer and nitroxide partitioned into water phase was re-calculated every time step before simulating the process. The concentration of species for each phase is given by

$$[X]_w = \left(\frac{1}{m_d}\right)[X]_{overall} \quad , \text{ X=monomer, nitroxide} \qquad \text{[mol/1L water]} \qquad (3\text{-}29)$$

The concentration for each species in the particles is given by

$$[X]_p = \frac{[X]_{overall} - [X]_w}{N_T v_p} , \quad \text{X=monomer, nitroxide} \qquad (3\text{-}30)$$

(mol/unit volume of particles)

3.4.2-5 Aqueous phase reactions

The aqueous phase reaction was simulated as a homogeneous process, as described in section 3.4.1.The following mass balances were calculated (based on 1L of aqueous phase).

$$\frac{d[M]_w}{dt} = -k_p[R^\bullet]_w[M]_w \tag{3-31}$$

$$\frac{d[P_n - T]_w}{dt} = k_{deact}[R^\bullet]_w[T^\bullet]_w \tag{3-32}$$

$$\frac{d[T^\bullet]_w}{dt} = -k_{deact}[R^\bullet]_w[T^\bullet]_w \tag{3-33}$$

$$\frac{d[R^\bullet]_w}{dt} = k_{ith}[M]_w^3 + k_f \frac{\bar{n} N_T}{N_A} - 2k_t[R^\bullet]_w^2 - k_{dea}[R^\bullet]_w[T^\bullet]_w \tag{3-34}$$

In this case, $[P_n - T]_w$ is quickly transferred into particles as mentioned above. In addition, the calculations of radical entry and the concentrations of $[M]_w$ and $[T^\bullet]_w$ were described in sections 3.4.2-1 and 3.4.2-4.

3.5 Computing implementation

The system of equations as shown in scheme 3.4 was solved by numerical integration using the Forward Euler integration algorithm. MATHEMATICA (ver.5.2, Wolfram Research) was used for the integration program with stepsize of 10^{-4} to 10^{-5} for

minimizing any numerical errors. The total number of particles was kept constant and the sum of the particle number fraction ($\sum_i \sum_j N_i^j$) was checked to ensure it was equal to 1.0.

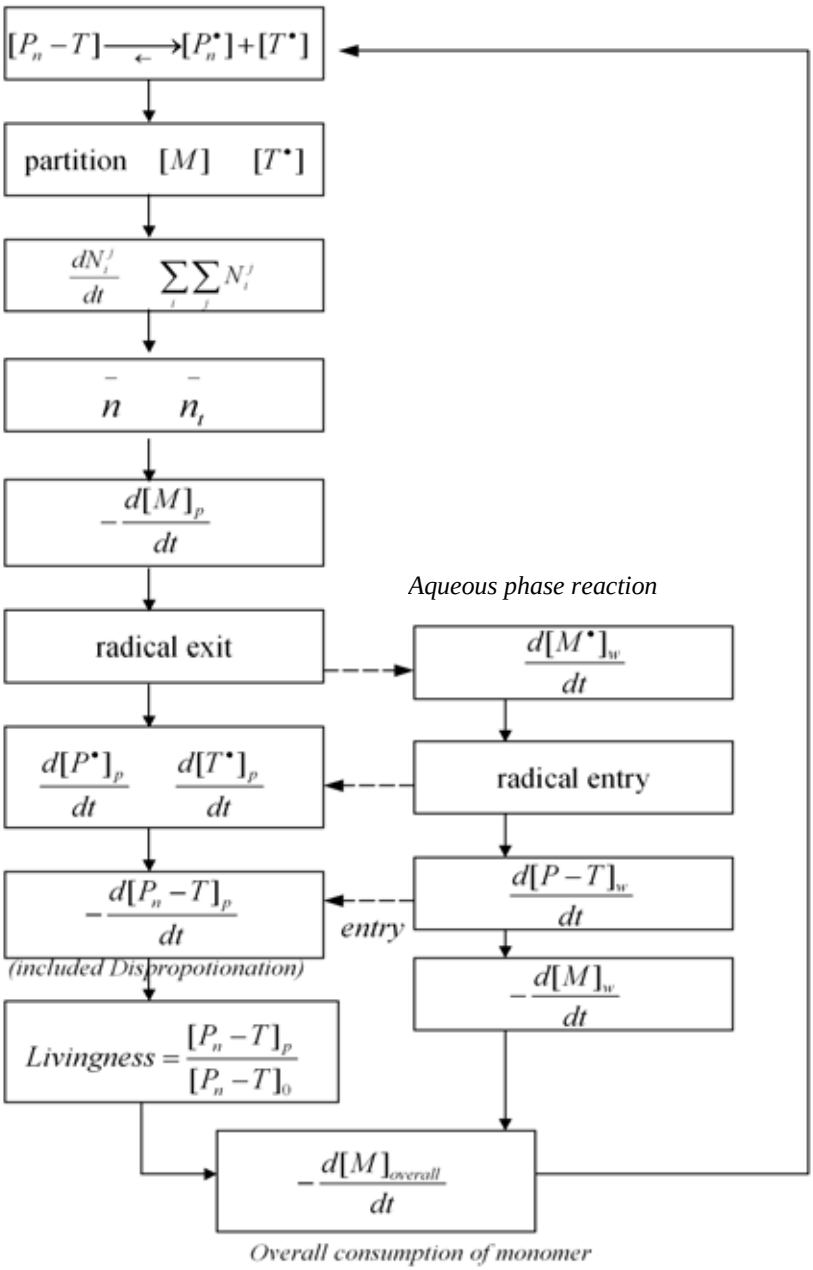

Scheme 3.4 Simulation algorithm for SFRP miniemulsion system

3.6 References

1. Kamigato, M., Ando, T., Sawamoto, M., Chem.Rev., 101, 3689, 2001
2. Matyjaszewski, K., Advances in Controlled Living Radical Polymerization, ACS, Washington D.C., 2003
3. Goto, A., Fukuda, T., Prog. Polym. Sci., 29, 329,2004
4. Cunningham, MF., Prog. Polym. Sci., 27, 1039,2002
5. Asua, JM., Prog. Polym. Sci., 27, 1283,2002
6. Cunningham, MF., C.R. Chimie, 6,1351,2003
7. Pan, G., Sudol, ED., Diomomie,VL., EL-Aasser, MS., J. Polym. Sci., Part A, 42, 4921,2004
8. Butte, A., Storti,G., Morbidelli, M., DECHEMA Monoger,134, 497,1998
9. Charleux, B., Macromolecules, 33, 5358,2000
10. Zetterlund, PB., Okubo, M., Macromolecules, 38, 8959,2006
11. Hui, AH., Hamelec, AE., J. Appl. Polym.Sci., 16,749,1972
12. Greszta, D., Matyjaszewski, K., Macromolecules, 29, 7661,1996
13. Smith, WV., Ewart, RH., J. Chem. Phys., 16,592,1948
14. Harada, M., Nomura, M., Kojima. H., Eguchi, W., Nagata, S., J.Appl. Polym. Sci., 16, 811,1972
15. Harada, M., Nomura,M., Eguchi, W., Nagata, S., J. Chem. Eng. Jpn., 4,54,1971
16. Nomura, M., Yamamoto, K., Horie, I., Fujita, K., Harada, M., J.Appl. Polym. Sci. 27,2483,1982
17. Lopez, DA.L., Barandiaran, MJ., Gugliotta, LM., Asua, JM., Polymer, 37,5907, 1996

18. Hansen, FK., Ugelsyad, J., J.Polym. Sci. Pol. Chem., 16,1953

19. Hansen, FK., ACS Sym Ser 492, 12, 1992

20. Hansen, FK., Chem Eng. Sci., 48, 437,1993

21. Gilbert, RG., Emulsion Polymerization : a mechanistic approach, Academic Press, London, 1995

22. Ma, JW., Cunningham, MF., McAuley, KB., Keoshkerian, B; Georges, MK., J. Polym.Sci.; Part A: Polym. Chem., 39, 1081,2001

CHAPTER 4

Modeling Studies of Compartmentalization in TEMPO Mediated Styrene Miniemulsion Polymerization

4.1 Chapter Overview

Simulation studies using the first comprehensive model for this system were conducted to clarify the role of the compartmentalization effect in TEMPO-mediated miniemulsion polymerization. The simulation was conducted with varying particle sizes of 50nm, 70nm, 100nm, and 120nm. Bulk polymerization was also simulated for comparison. Kinetic metrics such as the average number of radicals per particle ($\bar{n}$) and the average number of TEMPO molecules ($\bar{n}_t$) were calculated, and the results were compared with experimental results to confirm the validity of the model.
Modification of the model was further undertaken to guide our understanding and provide better agreement between predicted values and actual data. The importance of thermal initiation was discussed for both miniemulsion and bulk polymerization. I proposed introducing thermal initiation efficiency as a function of particle size. Moreover, the particle size influence on livingness was studied by employing the modified model with alkoxyamine disproportionation. Some challenges in accurately predicting livingness are also discussed.

4.2 Abstract

Compartmentalization effects in TEMPO-mediated styrene miniemulsion were examined by a newly developed model including segregation of both radicals and free nitroxide. The model also included radical exit/entry, phase partitioning, aqueous phase reactions and alkoxyamine disproportionation. The simulations were deployed for particle sizes of 50nm, 70nm, 100nm, and 120nm ($\leq 20\%$ conversion). Simulated parameters such as the average number of radical per particle ($\bar{n}$) and the average number of nitroxide molecules ($\bar{n}_t$) were verified by comparing them with experimental data. Overall radical concentration in the particles (which determines the rate of polymerization) was not strongly affected by radical exit/entry. This was a surprising result, and has been believed to be the main reason for reduced polymerization rate in smaller particles in SFRP miniemulsions.

I hypothesized that the thermal initiation efficiency (f) depended on particle size and introduced this effect into the model. Good agreement with experimental values was obtained, thus illustrating the importance of thermal initiation in heterogeneous SFRP systems. The efficiency was estimated to be proportional to particle size, with the larger particles showing a higher thermal initiation efficiency. The highest efficiency was observed in the homogeneous bulk system (f; 0.05 for 50nm, 0.15 for 70nm, 0.50 for 100nm, 1.0 for bulk, (set value)).

The modified model with the thermal initiation efficiency was also employed to predict livingness. Better livingness in miniemulsion was observed compared to that of bulk polymerization. However, the simulations for particle size effect in miniemulsion could still not completely explain the experimental observations. It was found that the

hypothesis of enhanced alkoxyamine disproportionation could provide better agreement for the particle size influence on the livingness, which was quantified by experimental analysis. More importantly, the simulation suggested that the rate of alkoxyamine disproportionation might be faster than the rate that is currently accepted. In addition, the alkoxyamine disproportionation rate may be reduced with decreasing particle size. Higher livingness is preserved with smaller particle size and faster overall rates of polymerization.

4.3 Introduction

A mathematical model that included the known important chemical and physical events in SFRP heterogeneous systems was presented in Chapter 3. Radical exit/entry, phase partitioning, aqueous phase reactions, and alkoxyamine disproportionation were considered to investigate how those factors affected polymerization kinetics and polymer livingness. In particular, how compartmentalization interacted with SFRP chemistry was of the most interest for my model studies. Some aspects of compartmentalization with SFRP were discussed in a few limited modeling studies. Charleux et al[2], in SG1-mediated styrene polymerization at 90^{o}C, simulated compartmentalization in SFRP considering only radicals (not nitroxide) and without thermal initiation, meaning rate enhancement with the smaller particles was the same as with the traditional Smith-Ewart theory. Butte et al.[1] and Zetterlund et al.[3] reported results contradictory to Charleux. They considered compartmentalization of both radicals and nitroxide and did include thermal initiation. In this case, Zetterlund observed that the rate of polymerization R_p decreased in proportion to d_p^3 (d_p : particle diameter) for

smaller particles, with a maximum at a certain d_p (70nm). The rate reduction with decreasing d_p was explained by the "*Confined Space Effect*", which arises from confining active radicals and free nitroxide into a small particle, leading to an enhanced deactivation reaction rate. It counteracts the rate enhancement effect, usually observed as the effect of radical segregation which reduces the effective termination rate. Tobita et al.[4] also found similar results for compartmentalization effects through their Monte Carlo simulations. It is worth noting that their simulated R_p in the bulk polymerization was also slower than the maximum rate in miniemulsion.

The first experimental evidence of compartmentalization with SFRP was presented in Chapter 2. The results showed slower rate with decreasing d_p, which agreed with the simulation results discussed above. However those simulations discussed above do not agree with our experimental data on the relative rate of bulk polymerization compared to miniemulsion polymerization. In terms of the experimental comparison between bulk and miniemulsion polymerization, Smith et al. [5] and Pan et al.[6] also reported that the rate of bulk polymerization was faster than that of miniemulsion (particle size $\geq$100nm). Previous models did not consider events such as radical exit and entry. Moreover previous simulations could not simulate the particle size influence on livingness, possibly in part because no consideration was given to alkoxyamine disproportionation kinetics.

Studying compartmentalization effects and validating my simulation results with my experimental data are the objectives in this chapter. I expect the results to yield a better understanding of heterogeneous systems with SFRP chemistry, and believe this to be important for the future development of heterogeneous SFRP systems.

4.4 Model Development

TEMPO mediated styrene polymerization in miniemulsion, which was presented in Chapter 2, was simulated employing the newly developed model. The details of both homogeneous bulk and miniemulsion models were described in Chapter 3. In the miniemulsion simulations, the number of particles was kept constant throughout the polymerization process. The kinetic parameters employed in this chapter are summarized in Table 4-1. The initial concentration of styrene monomer $[M]_0$ was 8.7M, and the initial concentration of dormant species (styrene oligomer $[P_n - T]_0$) was 0.02 M (organic phase).

The simulation was typically run to 20% conversion, which is sufficiently low to neglect chain length effect on the kinetic parameters. The particle sizes simulated in miniemulsion were 50nm, 70nm, 100nm and 120nm and were chosen to correspond to those experimental results under 20% conversion in Chapter 2. Note that those are not the final particle size. The final sizes for 50nm, 70nm, and 100nm in this chapter correspond to 50nm, 90nm and 180nm respectively in Chapter 2. The maximum values of *i* and *j* for calculating the fraction of N_i^j particles were set to 3 and 20 respectively after confirming that these values were significantly higher than the simulated $\bar{n}$ and $\bar{n}_t$. The model was numerically solved by the Forward Euler algorithm[7] with stepsize 10^{-4} –10^{-5} to minimize error. In addition, summation of the particle fraction ($\sum N_i^j$) was also confirmed to be 1 at every time step.

Table 4-1 Parameter values for TEMPO mediated emulsion polymerization at 135°C

Rate Parameter	Values	
k_{act} (activation)	3.92×10^{-3}	$[s^{-1}]$[8]
k_{deact} (deactivation)	1.87×10^{8}	$[M^{-1}s^{-1}]$[9]
k_{p} (propagation)	5.73×10^{3}	$[M^{-1}s^{-1}]$[10]
k_{t} (termination)	4.0×10^{8}	$[M^{-1}s^{-1}]$[11]
k_{ith} (thermal initiaton)	4.37×10^{-10}	$[M^{-2}s^{-1}]$[12]
k_{adp} (alokoxyamine disproportionation)	1.47×10^{-5}	$[s^{-1}]$[13]
k_{mf}/k_{p} (monomer transfer)	1.2×10^{-5}	
m_{st} (partition coefficient for styrene)	1300	
m_{tempo} (partition coefficient for TEMPO)	98.8	
D_{p} (diffusion coefficient of styrene in particle)	5.0×10^{9}	$[m^{2}s^{-1}]$[16), 17]
D_{w} (diffusion coefficient of styrene in water)	5.0×10^{9}	$[m^{2}s^{-1}]$[16),17]

Termination rate $=2k_{t}[P_{n}^{\bullet}]^{2}$, Thermal initiation $=k_{ith}[M]^{3}$

4.5 Results and Discussion

4.5.1 Rate of Polymerization R_p, $\bar{n}$ and $\bar{n}_t$

The simulated time –conversion relationship at 135 ^{o}C is shown in Fig.4-1. The simulations were run for both miniemulsion (50nm to 120 nm particle size) and the corresponding bulk polymerization. The maximum polymerization rate was observed for 70nm particles. In addition, the rate of the bulk system was slower than the maximum rate in miniemulsion. These results are very similar to the results reported by Zetterlund et al.[3)], who concluded that the confined space effect was responsible. The average number of radicals per particle $\bar{n}$ and of TEMPO molecules $\bar{n}_t$ are also shown as a function of conversion in Fig.4-2 for each particle size. Both $\bar{n}$ and $\bar{n}_t$ rise with increasing the particle size, due to the segregation of both radicals and TEMPO molecules. In order to confirm how segregation contributes to the overall radical and TEMPO concentration, the overall concentration for each species was also plotted as a function of particle size in Fig.4-3 (All data were calculated at 10% conversion). It was observed that the overall radical concentration for particles $\geq$70nm was larger than for bulk polymerization, which is evidence for the presence of a compartmentalization effect. The propagating radical concentration $[P_n^{\bullet}]$ increased up to 70nm, and then reached a higher value than in bulk. After leveling off at larger particle sizes, it decreased again at even larger particle sizes, eventually reaching that of bulk polymerization.

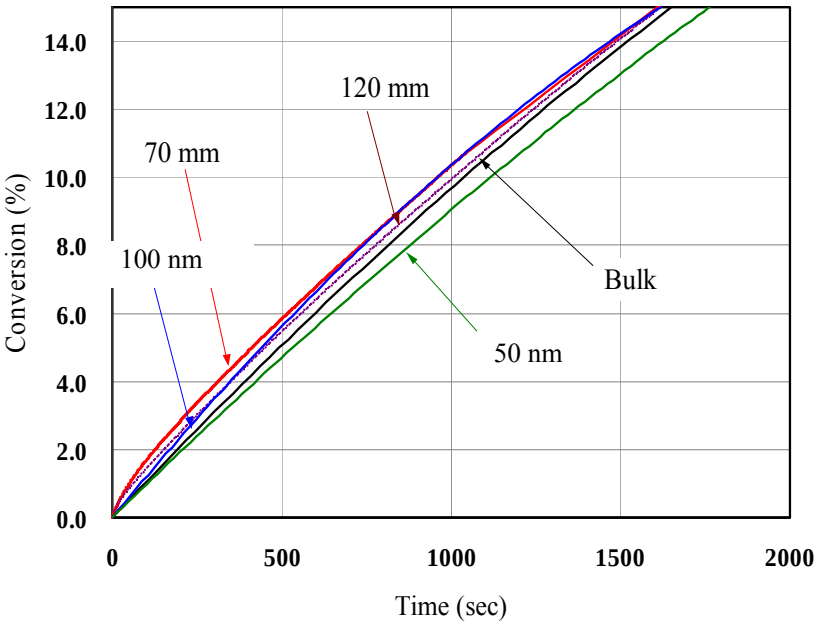

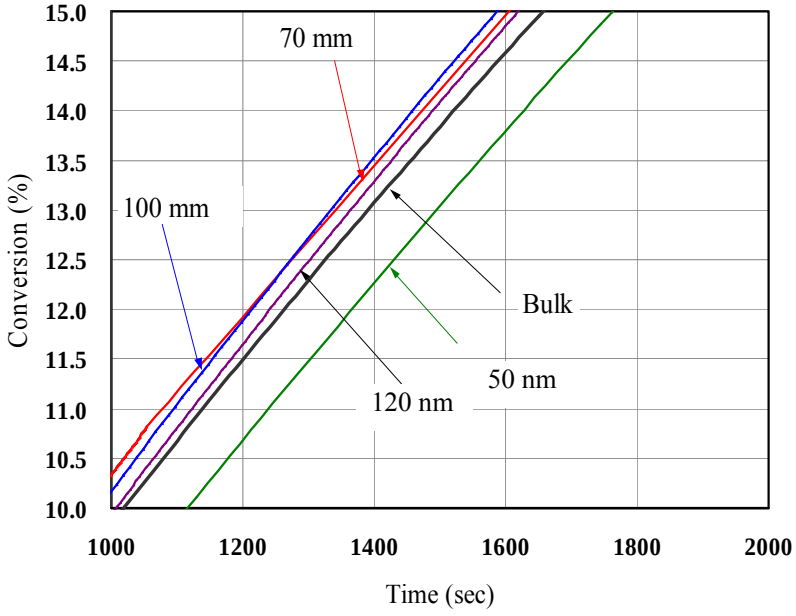

Fig. 4-1 Simulated time vs. conversion for different particle sizes in TEMPO mediated styrene miniemulsion at 135 ^{o}C

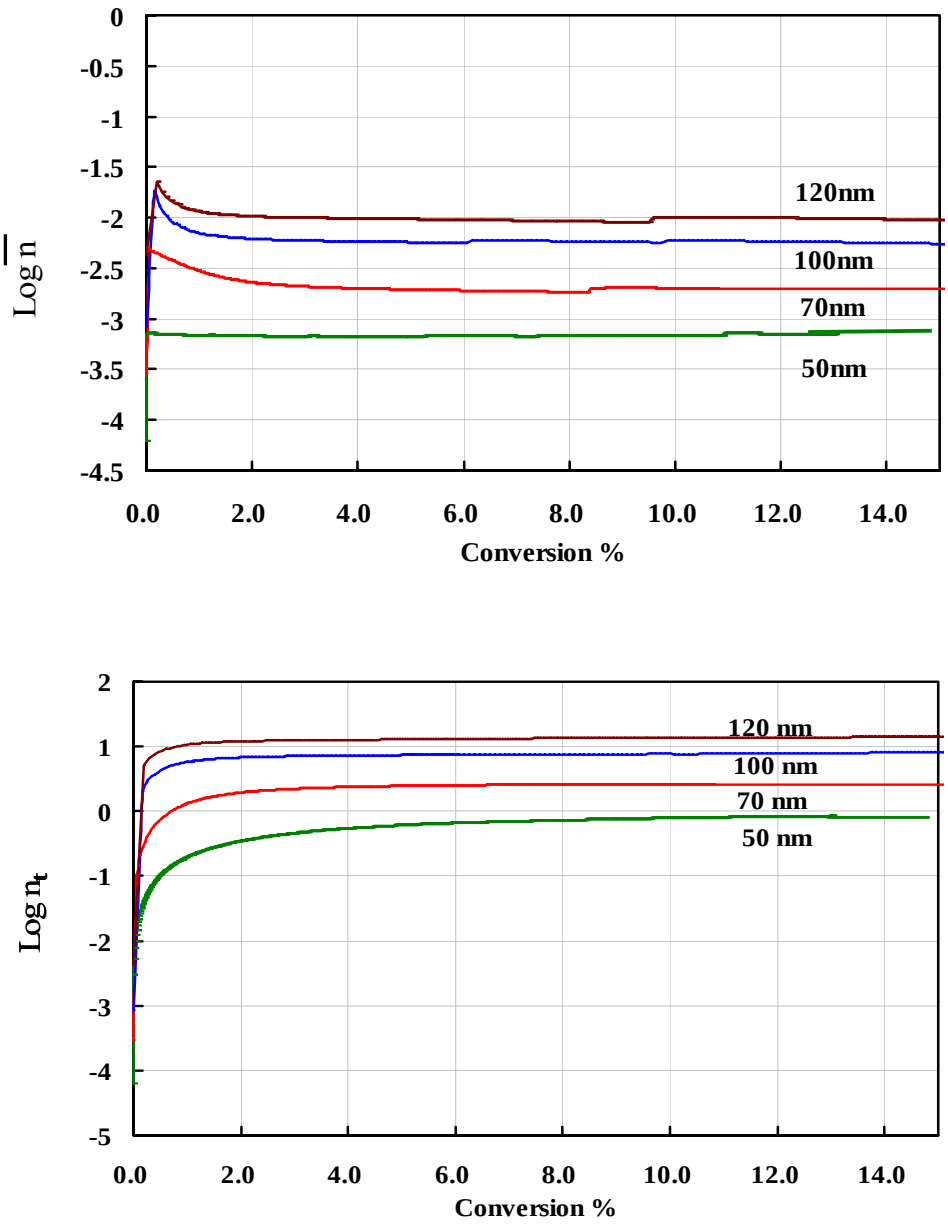

Fig. 4-2 Simulated $\bar{n}$ and $\bar{n}_t$ for different particle sizes in TEMPO mediated styrene miniemulsion at 135 ^{o}C

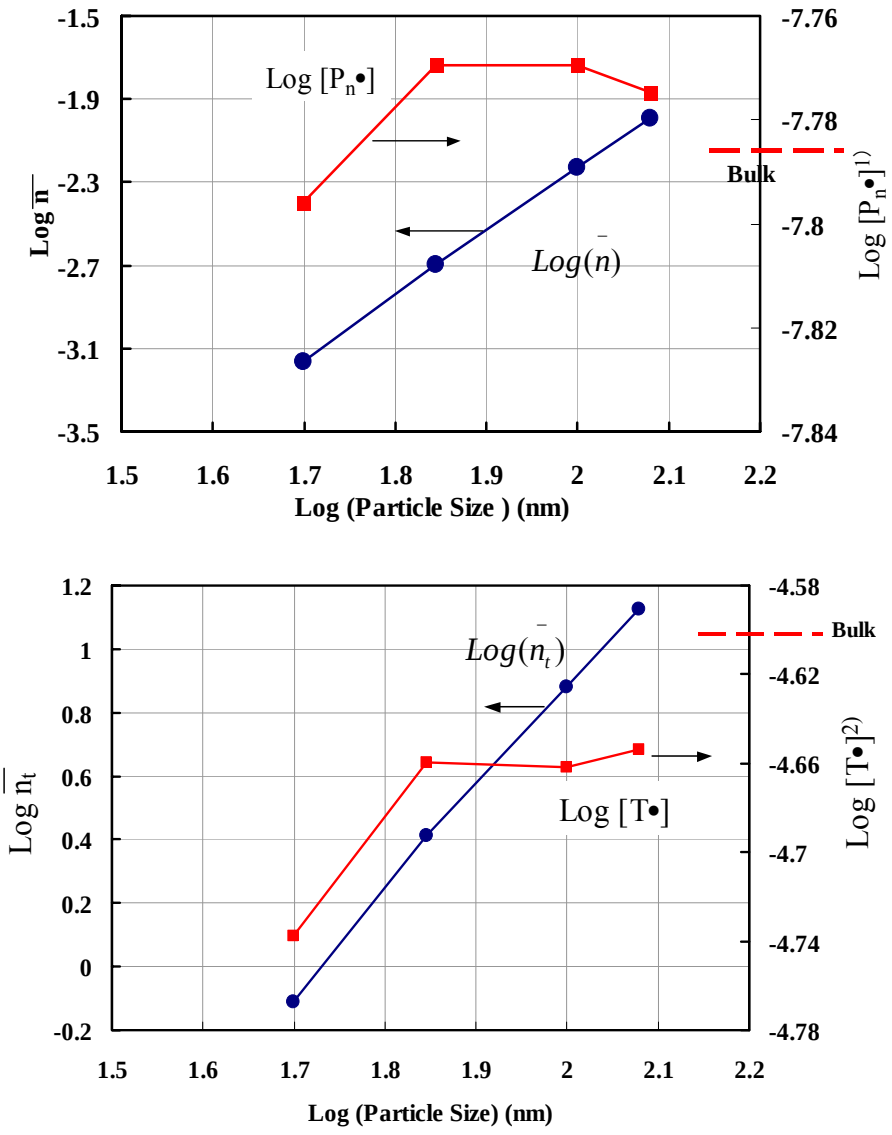

1) *[P_n•]: propagating radical concentration per unit volume in organic phase [M]*

2) *[T•]: Free nitroxide concentration per unit volume in organic phase [M]*

Fig. 4-3 Overall radical and TEMPO concentration as function of particle size at 135 °C

On the other hand, $[T^{\bullet}]$ (Fig.4-5), was lower than in bulk polymerization for all particle sizes. Although $[P_n^{\bullet}]$ eventually decreased at larger particle sizes, $[T^{\bullet}]$ continuously increased. This is assumed to be caused by free TEMPO generation arising from a higher termination rate (i.e. less radical segregation for particles $\geq$100nm). Zetterlund et al.[3] explained this behavior by the counteracting effects of segregation and the confined space effect. The lower $[P_n^{\bullet}]$ in 50nm particles (compared to bulk polymerization) is due to enhanced deactivation. After reaching 70 nm, radical segregation overwhelms the deactivation rate enhancement, thus effectively giving a higher $[P_n^{\bullet}]$ by reducing the termination rate. For even larger particles the effect of segregation is reduced, thereby resulting in a reduction in the polymerization rate. The simulated results I obtained were quite similar to those reported by Zetterlund et al.. The influence of events such as radical exit/entry and alkoxyamine disproportionation were seemingly insignificant in affecting the overall kinetics. Simulation results accounting for exit /entry of radicals at different particle sizes are shown in Fig.4-6. In terms of the overall radical concentration in the particles, the exiting radical fraction was 0.00045% for 50nm particles, 0.00038% for 70nm particles, and 0.000185 % for 100nm particles. Although the exit radical concentration slightly increased with decreasing particle size, the effect on the overall radical concentration in the particles was negligible. Furthermore, most of the radicals could likely re-enter into the particles. The presence of a large excess TEMPO ensures deactivation of a monomeric radical is rapid, so that the probability of radicals desorbing is reduced.

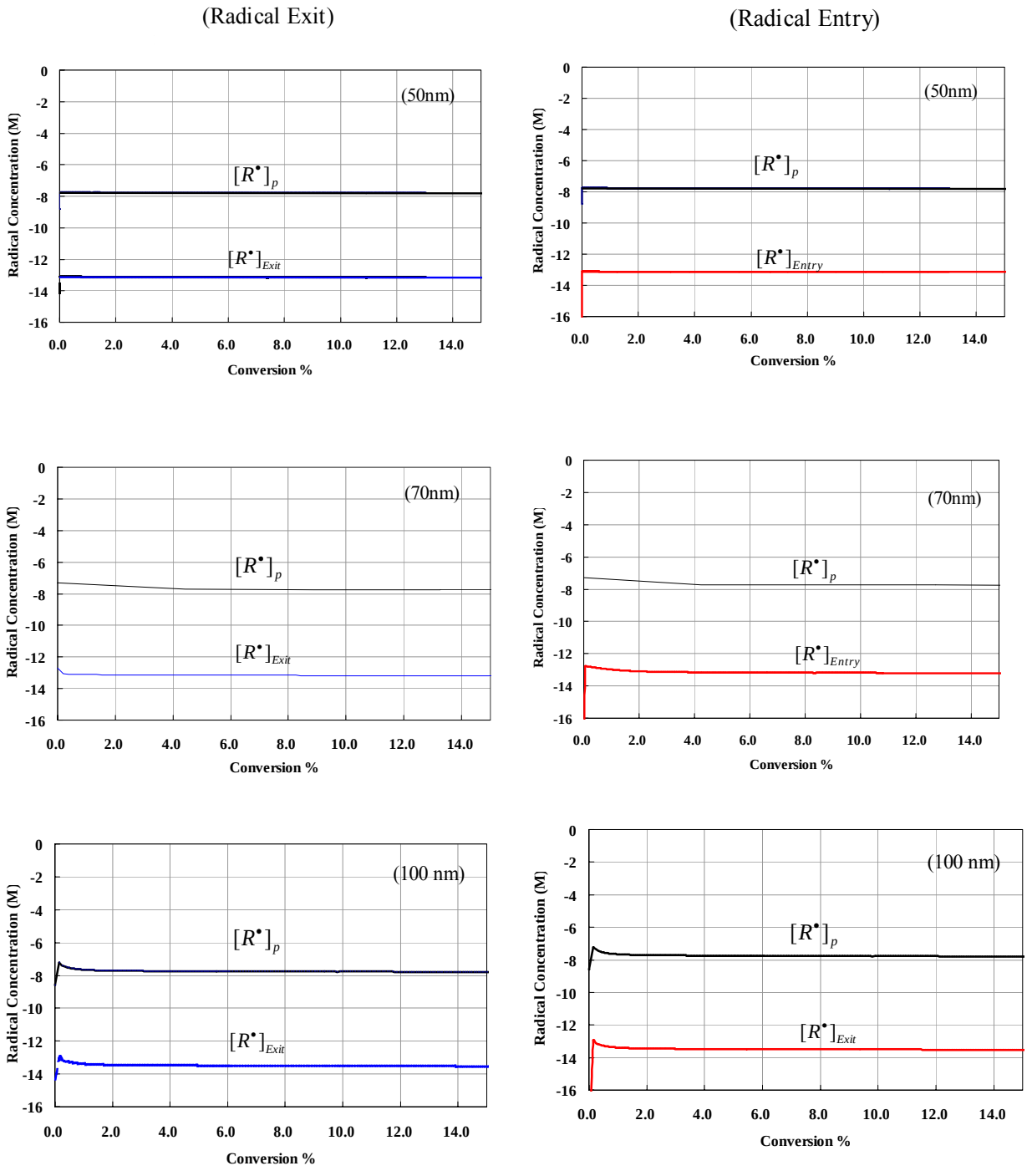

Fig. 4-4 Radical exit and entry in various particle sizes

In terms of alkoxyamine disproportionation (Scheme 4-1), the kinetic effects on R_p, $\bar{n}$, and $\bar{n}_t$ were examined, and compared with the case of no alkoxyamine disproportionation. The results in 100nm particles are shown in Fig.4-5. Unexpectedly no significant influence was observed in both cases. Their simulated livingness with conversion is shown in Fig. 4-6. In this case, the livingness was defined as $\frac{[P_n - T]}{[P_n - T]_0}$, where $[P_n - T]$ is the dormant concentration at a given conversion, and $[P_n - T]_0$ is the initial concentration of dormant species. More dead chains made by the alkoxyamine disproportionation were observed over 10% conversion, but there was not a significant difference until 20% conversion.

The details of the livingness are further discussed in the following section.

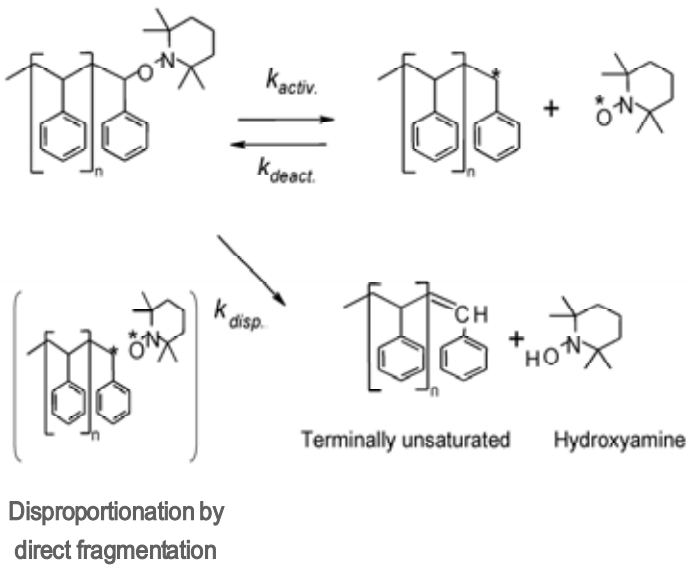

Scheme 4-1 Alkoxyamine disproportionation in TEMPO mediated styrene polymerization.

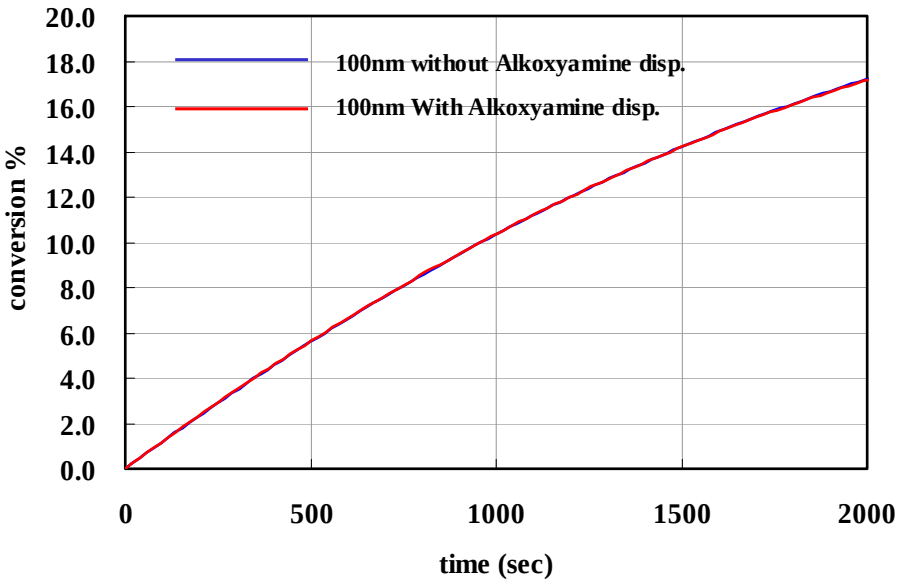

Fig 4-5 Time vs. Conversion with / without alkoxyamine disproportionation mechanism

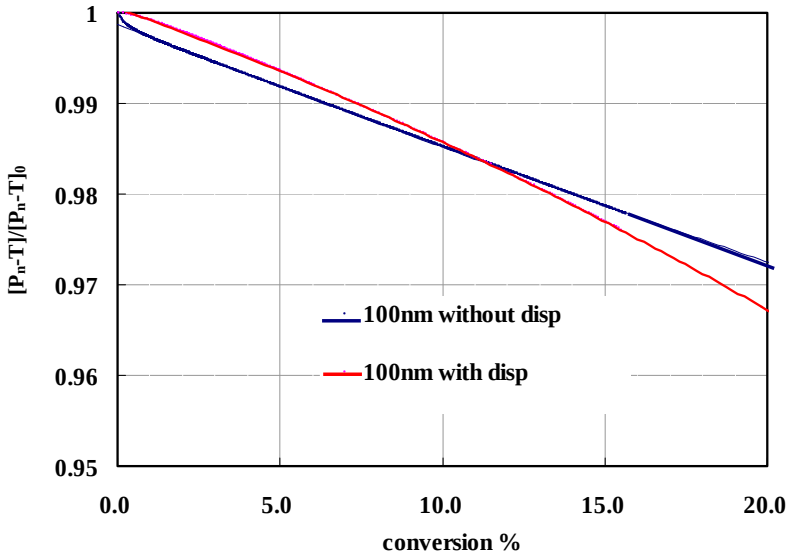

Fig.4-6 Conversion vs. livingness with / without alkoxyamine disproportionation mechanism

4.5.2 Livingness in simulation

One of the advantages expected in heterogeneous systems is better preservation of the living character compared with homogeneous bulk systems. As discussed above, the confined space effect and the segregation effect characterize polymerization kinetics in heterogeneous system, and both effects are expected to reduce the rate of the termination reaction. However, it is still an unanswered question how they impact alkoxyamine disproportionation. As the alkoxyamine disproportionation rate is affected by the total dormant chain concentration, both the segregation and confined space effects might not influence it directly. They seem to affect it only indirectly, for instance by affecting the activation –deactivation equilibrium frequency through radical and free TEMPO concentrations.

In Fig.4-7, simulated livingness with different particle sizes, and with bulk polymerization is shown as a function of conversion. The results suggest better livingness is achieved in miniemulsion, and interestingly it showed higher livingness with increasing particle size. Considering better livingness would be promoted either by the confined space effect or segregation, the difference between homogeneous bulk and miniemulsion can be understood. It does not however account for the differences among particles, where we would expect to have the highest value at 50nm, due to the highest segregation of radicals. Ma et al. and Cunningham et al [22), 23), 29)] suggested both in their experimental and modeling studies that alkoxyamine disproportionation rather than the termination reaction may account for a significant loss of livingness at 135^{o}C in TEMPO-mediated styrene miniemulsion, and longer reaction time resulted in greater loss of livingness due to increased disproportionation.

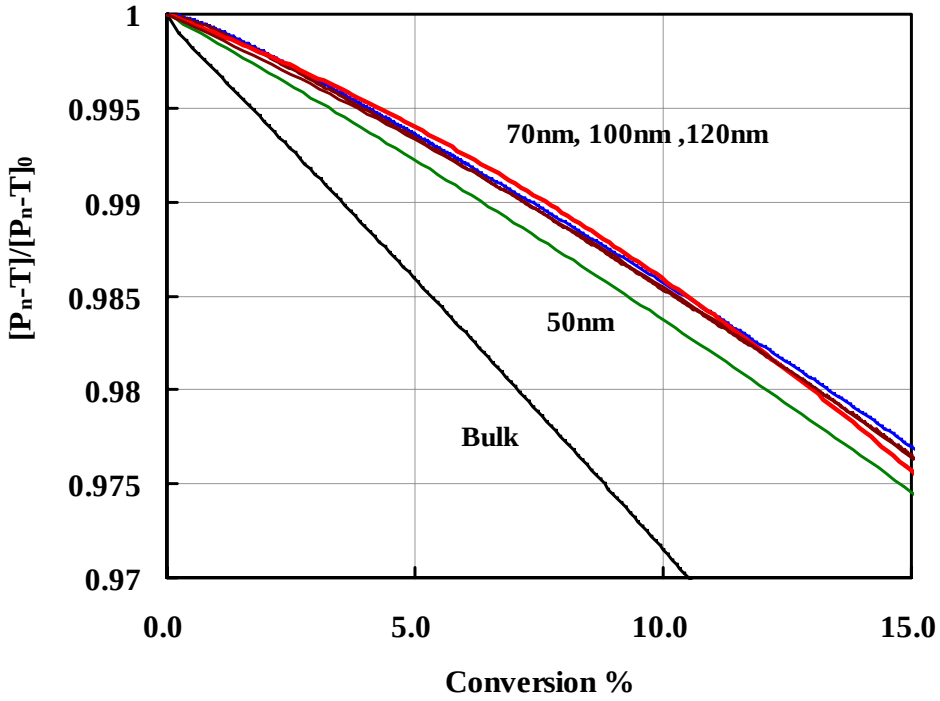

Particle Size (nm)	Experimental value [1)]
50	0.95
70	0.92
100	0.88
120	—
Bulk	0.91

1) 10% conversion

Fig. 4-7 Conversion versus livingness in various particle sizes and the experimental values at 10% conversion

Conversely shorter reaction times tended to yield higher livingness.

The relation between reaction time –livingness is plotted in Figure 4-8. It clearly shows that the relation in miniemulsion systems was almost identical for all particle sizes, and it also shows that livingness is strongly influenced by polymerization time. However in comparison with bulk polymerization, higher livingness in miniemulsion is still observed, suggesting the role of either segregation or the confined space effect or possibly both. In conclusion, the model predicts advantages in preserving livingness in heterogeneous systems compared to homogeneous systems. For the heterogeneous systems, the difference among particle sizes was relatively small among the particles over 50nm. In this case, the loss of livingness mainly seems to arise from disproportionation, thus it was not significantly influenced by segregation and the confined space effect. Rather it was more time dependent. In bulk polymerization, lower livingness is due to termination reactions as well as alkoxyamine disproportionation. In heterogeneous systems, the termination reaction rate seems to be much reduced due to either segregation or the confined space effect, thus resulting in higher livingness.

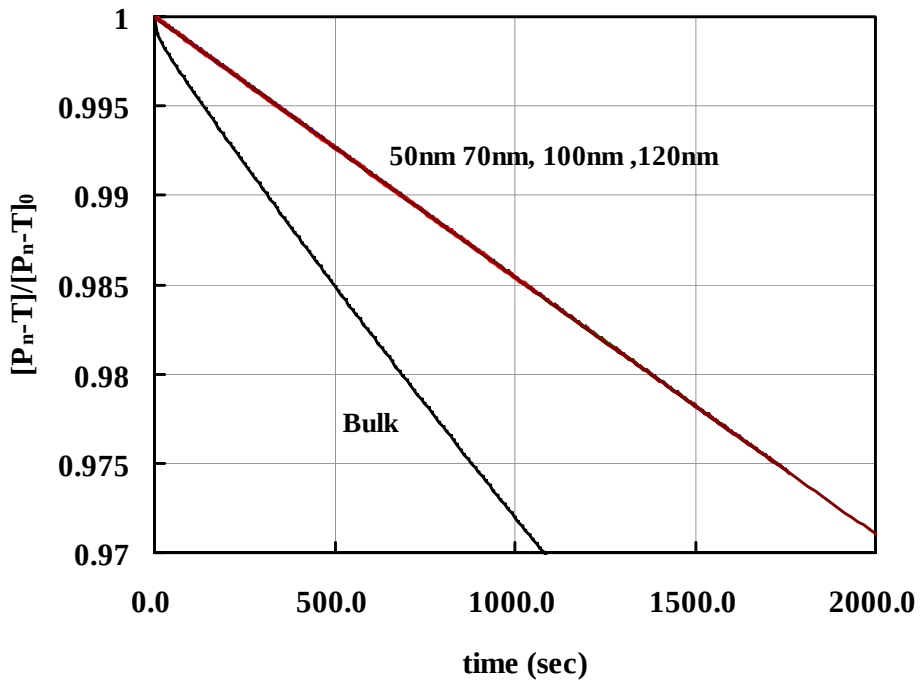

Fig. 4-8 Time versus livingness in miniemulsion and bulk polymerization

4.5.3 Validity of the Simulation – Comparison with Experimental Results

Simulation studies, employing a new model that included radical exit/entry, phase partitioning, water phase reactions, and alkoxyamine disproportionation were presented in the previous section. Similar results were obtained compared with the results reported by Butte et al.[1)] and Zetterlund et al.[3)], although their models did not incorporate the events described above. In particular, the rate of polymerization with different particle sizes showed a maximum rate under 100nm, and that the rate of bulk polymerization was relatively slow. The effects of radical exit/entry and alkoxyamine disproportionation were also observed in the simulations.

However those results still have discrepancies compared with our experimental results presented in Chapter 2, which showed the bulk polymerization rate was consistently faster than the miniemulsion systems, even in particle sizes of 100nm. Moreover, reasons for the higher livingness with smaller particles are still not clear.

Table 4-2 summarizes the simulated results for both miniemulsion and bulk polymerization at 10% conversion, compared with experimental data. Significant difference was observed in the TEMPO concentration in the particles. In addition, the simulated radical concentration tends to diminish less in smaller particles compared to the experimental observations. For example, the radical concentration in 50nm particles was 94% of that of 100nm particles in the simulations, but 57% in the experimental data.

Table 4-2 Comparison between simulated and experimental results at 10 % conversion.

	Simulation (Conversion 10%)					Experimental Value				
Particle Size (nm)	$[R^{\bullet}]$ (M)	$[TEMPO^{\bullet}]$ (M)	$\bar{n}$	$\bar{n}_t$	$\bar{n}_t/\bar{n}$	$[R^{\bullet}]$ (M)	$[TEMPO^{\bullet}]$ (M)	$\bar{n}$	$\bar{n}_t$	$\bar{n}_t/\bar{n}$
50	1.60×10^{-8}	1.83×10^{-5}	6.82×10^{-4}	0.78	1139	1.32×10^{-8}	7.32×10^{-5}	5.30×10^{-4}	2.94	5547
70	1.70×10^{-8}	2.18×10^{-5}	2.00×10^{-3}	2.59	1291	1.60×10^{-8}	6.01×10^{-5}	1.73×10^{-3}	6.49	3751
100	1.70×10^{-8}	2.19×10^{-5}	4.76×10^{-3}	8.85	1860	2.28×10^{-8}	4.24×10^{-5}	7.20×10^{-3}	13.3	1847
120	1.68×10^{-8}	2.22×10^{-5}	1.01×10^{-2}	13.4	1324	-	-	-	-	-
Bulk	1.63×10^{8}	2.50×10^{-5}	N/A	N/A	N/A	4.63×10^{-8}	7.32×10^{-5}	N/A	N/A	N/A

$[R^{\bullet}]$; Average radical concentration in particle $[TEMPO]$; Average TEMPO concentration in particle

$\bar{n}$; Average number of propagating radicals pre particle $\bar{n}_t$; Average number of TEMPO pre particle

Fig.4-9 shows the relationship between particle size and the ratio of ($\bar{n}_t / \bar{n}$) both for simulated and experimental values. Significant difference was observed with decreasing particle sizes.

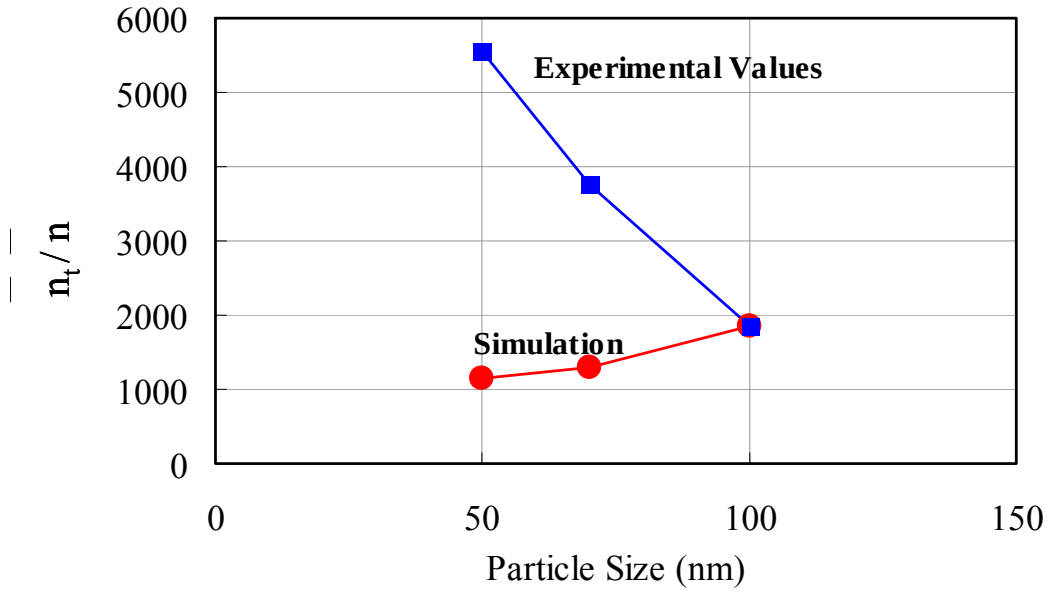

Fig. 4-9 Particle size versus $\bar{n}_t / \bar{n}$ in simulation compared with experimental values

The simulated value was almost consistently under 2000, however the actual values rose with decreasing particle sizes to 5500 at 50nm. In this case, the larger value of $(\bar{n}_t / \bar{n})$ indicates more free nitroxide with fewer propagating radicals in the particles, which reduces the polymerization rate. In connection with this, Butte et al. pointed out that with thermal initiation in small particles, which generates two radicals at the same time, some geminate recombination will occur. It could be more frequent in smaller particles, thereby reducing the polymerization rate. In the model, thermal initiation kinetics were incorporated as proportional to $[M]_p^3$. The loss of propagating radicals was accounted for only by bimolecular termination. In conventional radical polymerization, not all radicals arising from initiator decomposition initiate chains. The behavior is usually treated using an initiation efficiency "f".

Although the importance of thermal initiation in styrene SFRP is well known, the efficiency "f" for the thermal initiation step has never been considered in any existing models. TEMPO consumption by thermally initiated radicals is known to play an important role in nitroxide mediated styrene polymerization[19]. In miniemulsion, it is possible that decreased initiation efficiency in smaller particles would lead to a lower radical concentration and more free TEMPO in the particles.

4.5.4 Model Modification to Incorporate Thermal Initiation Efficiency f

The rate of thermal radical generation, which was presented in Chapter 3, was modified by introducing the efficiency f as shown in eq.4-1.

$$\frac{d[P_{ith}^{\bullet}]}{dt} = k_{ith} f [M]_p^3 \qquad (4\text{-}1)$$

where $[P_{ith}^{\bullet}]$ is the radical concentration from thermal initiation, and f is an initiation efficiency. Using the modified model, simulations with varying f were run in 50nm, 70nm, and 100nm particles (135^{o}C). The time-conversion results for each particle size are summarized in Fig.4-10. In these figures, the simulated results are compared with experimental data with an estimation of f for each particle size.

For all particle sizes, a remarkable influence on the polymerization rate is suggested. The contribution of thermal initiation was more enhanced with increased reaction time, and significant increase of free TEMPO was also observed.

From the comparison with experimental data, the efficiency f was estimated for each particle size. Table 4-3 summarizes the simulated $\bar{n}$, $\bar{n}_t$ and $\bar{n}_t / \bar{n}$ with varying initiation efficiency f at 10% conversion. Decreasing thermal efficiency f led to a considerable increase of $\bar{n}_t / \bar{n}$. In comparison with the experimental values, thermal efficiency was estimated as 0.1 in 50nm particles, 0.3 in 70nm particles, and 1.0 in 100nm particles.

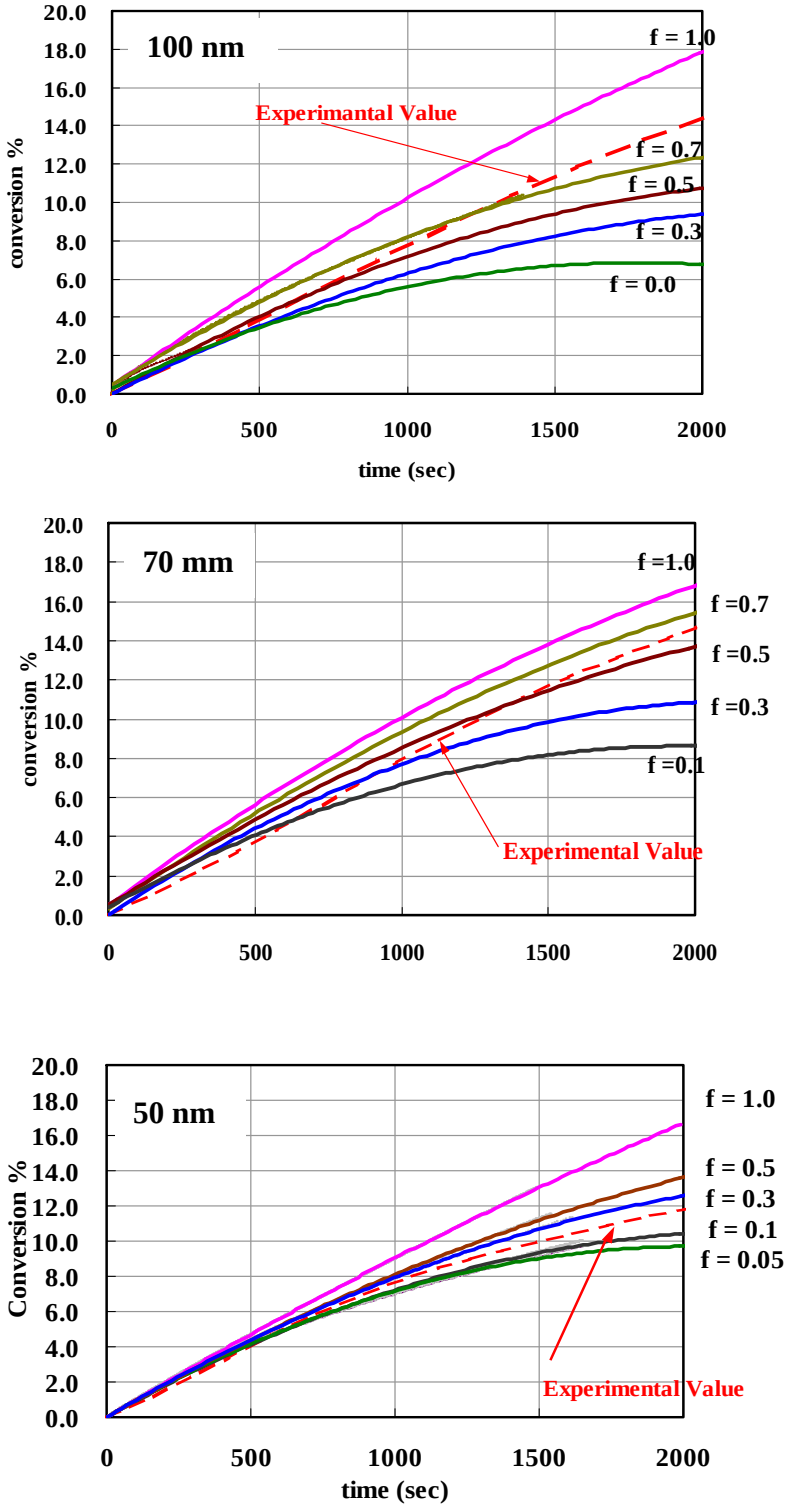

Fig. 4-10 Time versus conversion with thermal initiation efficiency f in various particles

Table 4-3 Summary of simulated $\bar{n}_t/\bar{n}$ with thermal initiation efficiency f (10% conversion)

Particle Size (nm)	f	$\bar{n}$	$\bar{n}_t$	$\bar{n}_t/\bar{n}$
50	0.1	3.32×10^{-4}	1.83	5506
	0.3	4.61×10^{-4}	1.25	2719
	0.5	5.32×10^{-4}	1.07	2013
	1.0	6.82×10^{-4}	0.78	1139
	Experiment	5.30×10^{-4}	2.94	5547
70	0.1	8.32×10^{-4}	5.70	6853
	0.3	1.03×10^{-3}	4.44	4306
	0.5	1.43×10^{-3}	3.60	2524
	0.7	1.69×10^{-2}	3.13	1851
	1.0	2.00×10^{-3}	2.59	1295
	Experiment	1.73×10^{-3}	6.49	3751
100	0.0	2.29×10^{-4}	17.59	76812
	0.3	2.72×10^{-3}	15.45	5688
	0.5	3.16×10^{-3}	13.91	4406
	0.7	3.48×10^{-3}	12.20	3505
	1.0	4.76×10^{-3}	8.86	1860
	Experiment	$7.20. \times 10^{-3}$	13.30	1847

Fig.4-11 shows the estimated $\bar{n}_t/\bar{n}$ as a function of particle size, compared with experimental values. The predicted $\bar{n}_t/\bar{n}$ values agree well with the experimental values, which suggest the importance of the thermal initiation efficiency in accurately predicting the ratio of radical to free nitroxide in the particles.

More specifically, Fig 4-12 shows the predicted N_i^j (the number fraction of particles containing $iP_n^{\bullet}$ and $jT^{\bullet}$) at 50nm with f = 1.0 and f = 0.1. In the case of f=1.0, most of the particles were N_0^0 particles (0 radical, 0 free nitroxide), but when the efficiency was reduced to 0.1, N_0^2 particle containing two excess nitroxides became the majority species, so that the activation –deactivation equilibrium was shifted toward dormant chains. The fraction of N_1^0 and N_1^1 particles also significantly decreased for f=0.1.

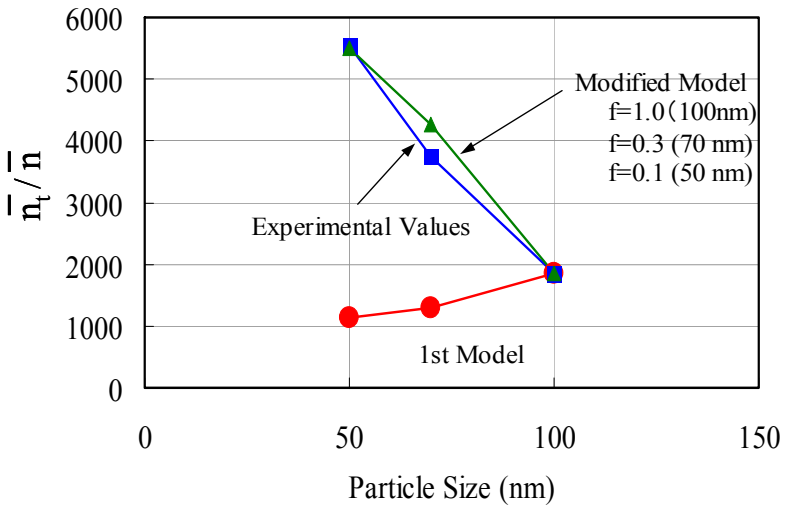

Fig. 4-11 Particle size versus $\bar{n}_t/\bar{n}$ for modified simulation compared with experimental values

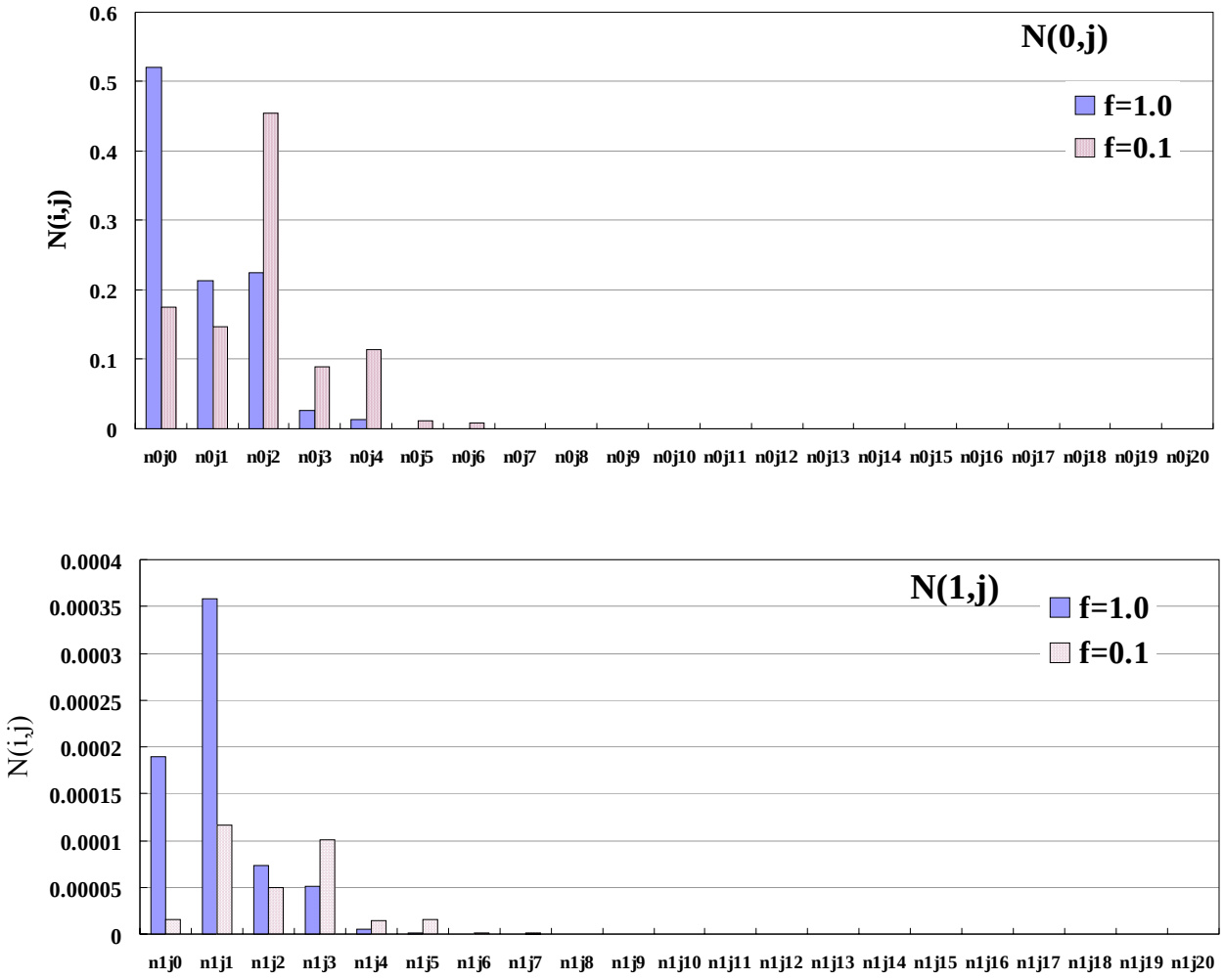

Fig. 4-12 Number fraction of N (i,j) with thermal initiation efficiency f in 50nm particles (10% conversion)

Fig.4-13 shows simulated time –conversion curves with thermal efficiency f at various particle sizes. The rate of polymerization increased with larger particle size, and bulk polymerization was faster than the miniemulsion consistent with our experimental results. However, the absolute rate in bulk polymerization is still lower than our experimental results.

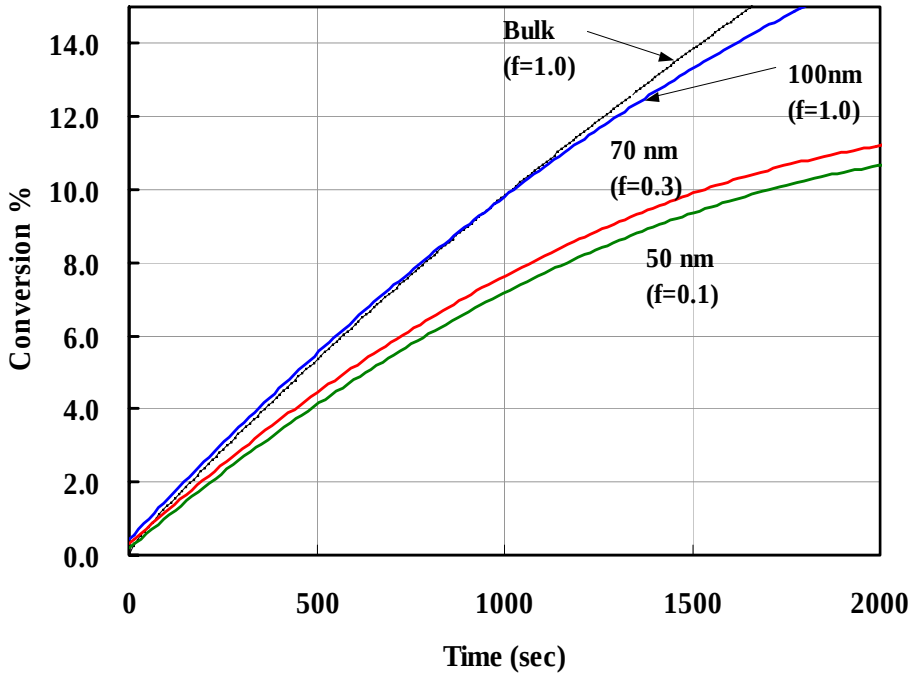

Fig. 4-13 Time versus conversion with optimized thermal initiation efficiency f in various particle sizes

In connection with this, Pan et al. [6] suggested there may be an increased thermal radical generation rate in styrene with SFRP. While this is still a hypothetical assumption, bulk polymerization with a varying rate coefficient was investigated in a homogeneous SFRP system. The results are shown in Fig.4-14. In our current model, the rate coefficient k_{ith} was 4.37×10^{-10} (L^2 mol^{-2} s^{-1}) at 135 °C, which has been widely used in conventional styrene systems (no nitroxide). When the rate coefficient was changed to 8.74×10^{-10} (L^2 mol^{-2} s^{-1}), which was two times faster than the current value, a better fit between simulation and data was observed.

Although the value was still a hypothetical coefficient as mentioned above, the

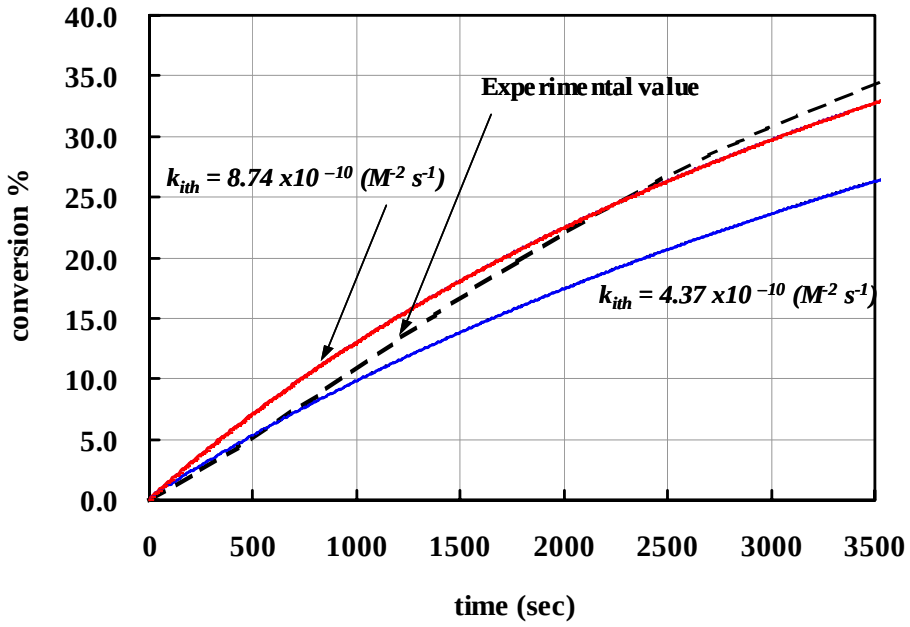

Fig. 4-14 Time versus conversion with thermal initiation coefficient 8.7×10^{-10} $M^{-2}s^{-1}$ and 4.37×10^{-10} M^{-2} s^{-1}

simulations in Fig.4-14 were re-run based on the result, as shown in Fig.4-15. In this case, the f value for each particle size was recalculated to 0.5 for 100nm particles, 0.15 for 70nm particles, and 0.05 for 50nm particles, and those were plotted as a function of particle size in Fig.4-16. Assuming an approximate linear relationship between thermal efficiency and particle size, particles with 160nm diameter would have an efficiency of about 1.0, which is comparable to bulk polymerization. Moreover, for the time-conversion relationship, these conditions agree much better with our experimental observations, and these results also support the idea, that there may be more thermal radicals generated with SFRP chemistry than in conventional free radical polymerization.

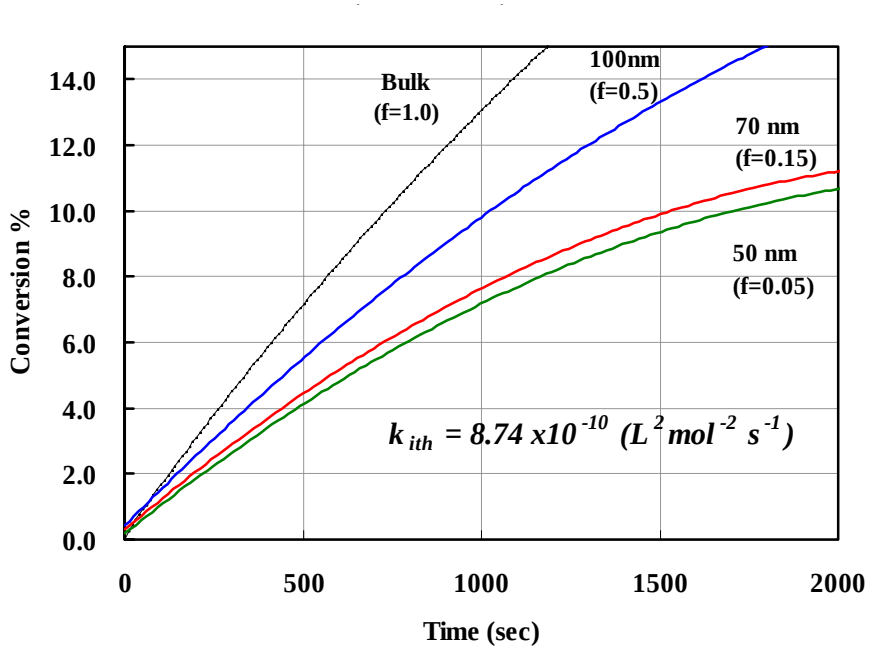

Fig. 4-15 Time versus conversion with thermal initiation coefficient 8.74 x 10-10 M^{-2} s^{-1} in various particle sizes

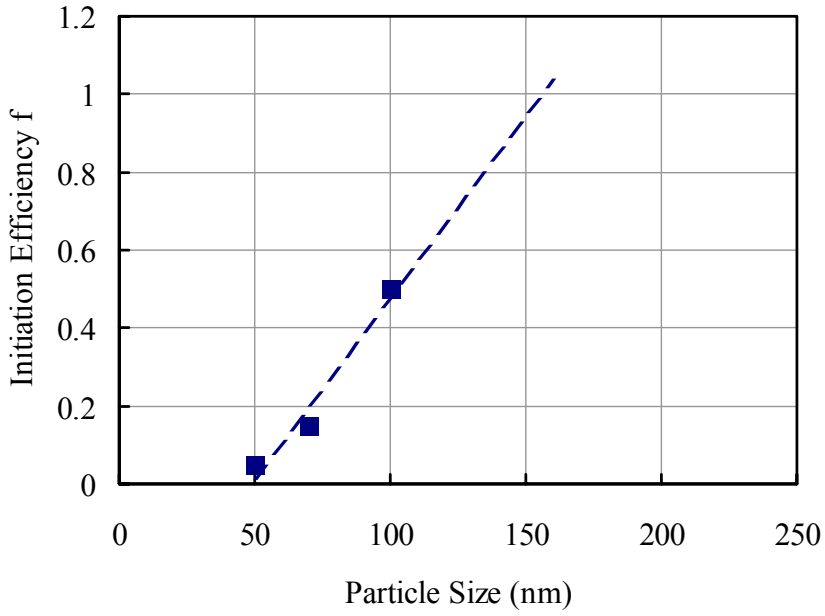

Fig. 4-16 Particle size versus thermal initiation efficiency in miniemulsion polymerization at 135 ^{o}C

Finally, the livingness with various f values is summarized in Fig.4-17. In this simulation, a thermal coefficient of 8.74 x10^{-10} (L^2 mol^{-2} s^{-1}) was adopted. In the comparison of livingness with bulk polymerization, the advantage in miniemulsion was still preserved. As mentioned before, the livingness depended much on polymerization time due to dead polymer generation from alkoxyamine disproportionation. A reduced rate with lower thermal efficiency caused longer polymerization times, and thus more dead chains were generated with the smaller particles.

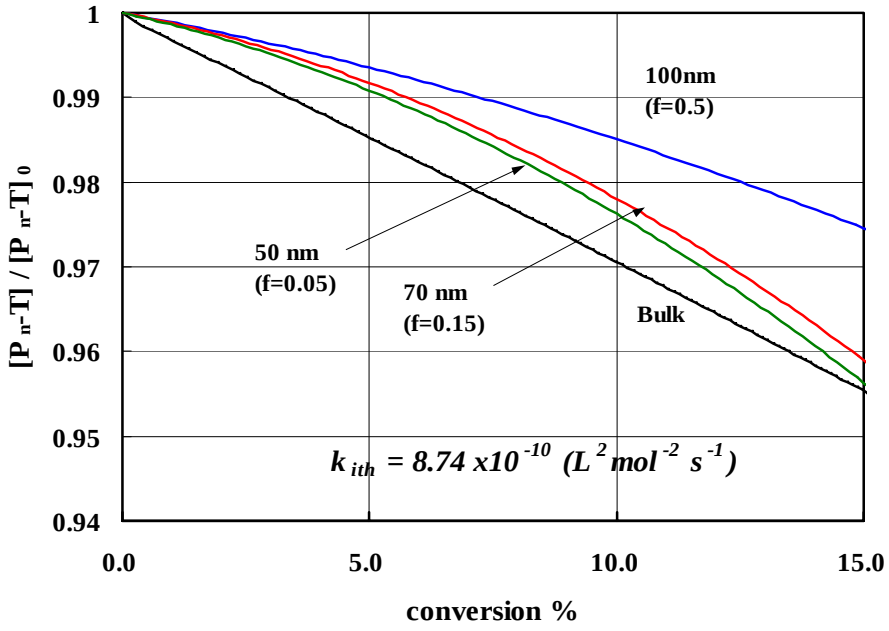

Figure 4-17 Conversion versus livingness with thermal initiation efficiency in miniemulsion polymerization, compared with bulk

There was still discrepancy in the livingness between simulation and experimental observations. The reason is not yet clear, but an unknown mechanism involving alkoxyamine disproportionation is suspected to be important. In connection with this, several possibilities to understand the discrepancy between our simulated predictions and the data have been investigated. One possibility is a larger rate coefficient in alkoxyamine disproportionation. In homogeneous bulk polymerization, the livingness between simulation and experimental data at 10% conversion was 0.97 and 0.91 respectively. For this reason, the livingness with a varying rate coefficient for bulk polymerization was further simulated. The result is shown in Fig. 4-18.

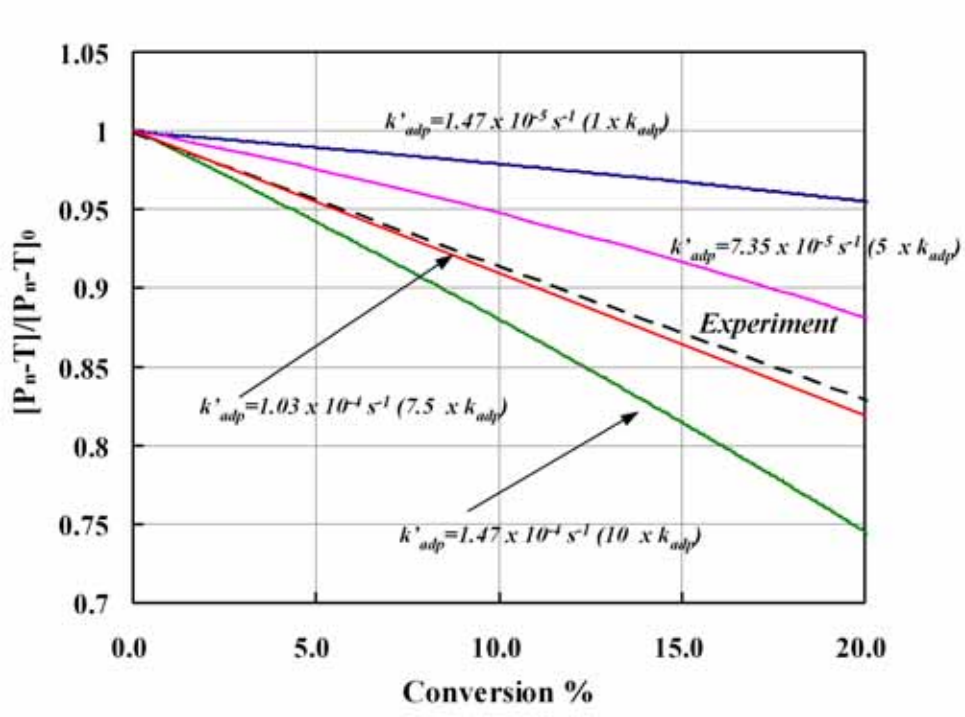

Fig. 4-18 Conversion versus livingness prediction with adjusting alkoxyamine disproportionation rate in bulk polymerization

(full line: simulation, dotted line :experimental value)

The rate coefficient, whose value is $k_{adp}=1.47 \times 10^{-5}\ s^{-1}$ in our current model, is accelerated up to $1.47 \times 10^{-4}\ s^{-1}(k_{adp} \times 10)$ When the rate coefficient was changed to $7.35 \times 10^{-5}\ s^{-1}\ (k_{adp} \times 7.5)$, a better fit between simulation and experimental data was observed. Moreover, the simulations for each particle size in miniemulsion polymerization were also examined in the same manner. The results are shown in Fig. 4-19. The ratio of the adjusted rate coefficient k'_{adp} to the original k_{adp} is also shown with the thermal initiation efficiency f for these simulations. The discrepancy between simulation and experimental values is minimized when the ratio k'_{adp} / k_{adp} is 3.0 for 50nm particles (f=0.05), 5.0 for 70nm particles (f=0.15), and 7.5 for 100nm particle (f=0.5). Interestingly, better livingness for bulk polymerization was observed than for 100nm particle size, even though the rate coefficient for the disproportionation for both systems was the same. For this reason, the time-livingness relationship was plotted in Fig.4-20. The livingness for both bulk polymerization and 100nm particle size are almost identical, and higher livingness in 50nm and 70nm particles was observed.

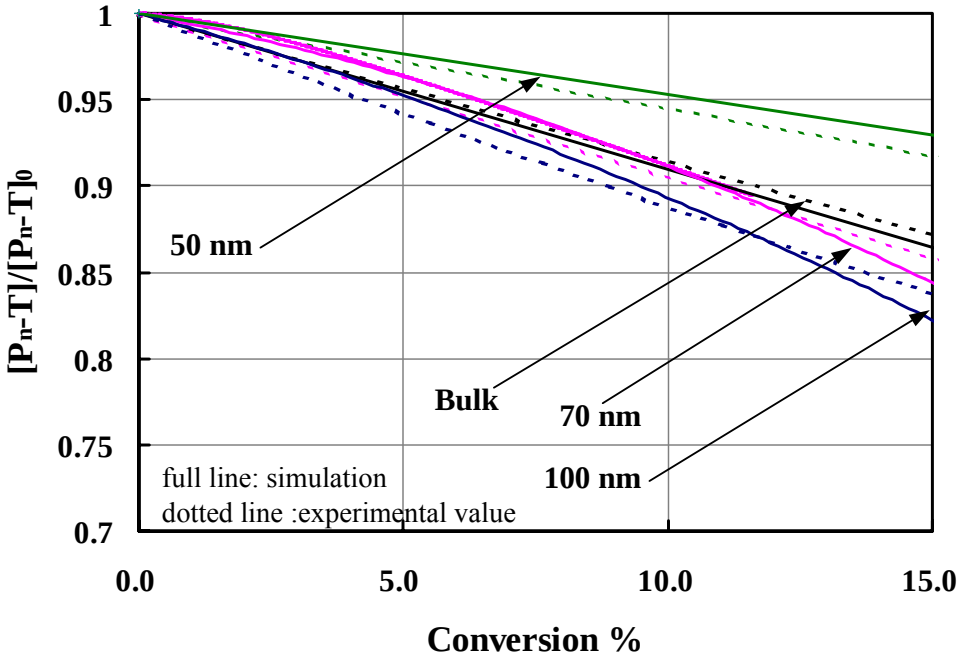

Thermal initiation efficiency f and rate coefficient of disproportionation for simulation

systems	f	k_{adp}'/k_{adp}
50 nm	0.05	3.0
70 nm	0.15	5.0
100 nm	0.5	7.5
Bulk	1.0	7.5

Fig. 4-19 Conversion versus livingness prediction with adjusting alkoxyamine disproportionation rate.

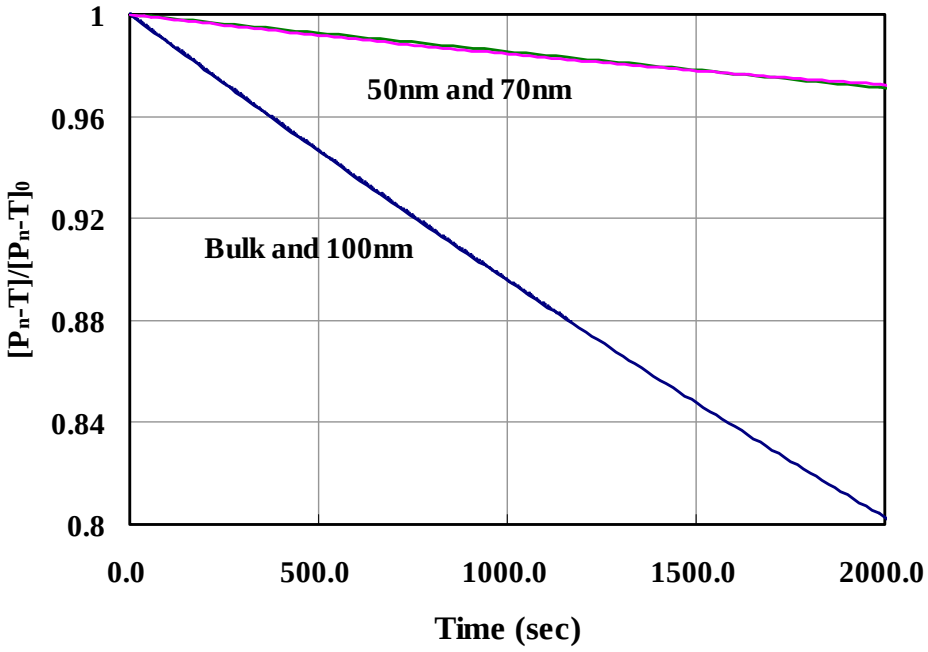

Fig. 4-20 Time versus livingness prediction with adjusting alkoxyamine disproportionation rate.

The above assumption for the rate increase of alkoxyamine disproportionation has never been confirmed experimentally, but the simulation results show improved agreement with our experimental observations. A possible mechanism for the rate reduction of alkoxyamine disproportionation in smaller particles could be the reversible nature of the disproportionation step. In the current view of alkoxyamine disproportionation, the disproportionation occurs via β hydrogen abstraction involving a transition state between the propagating radical and nitroxide. When the transition state involves a

reversible mechanism, rate reduction might be possible due to the confined space effect, which is observed in the deactivation reaction. Moreover, the disproportionation mechanism between dissociated radicals [21], which was not considered in the current model, is another possibility. Although that mechanism has not yet been clarified, it seems to be more directly influenced by compartmentalization in miniemulsion and therefore less disproportionation could be expected with smaller particles (Scheme 4-2). Further study of the reaction mechanism regarding alkoxyamine disproportionation is important for a more thorough understanding of livingness.

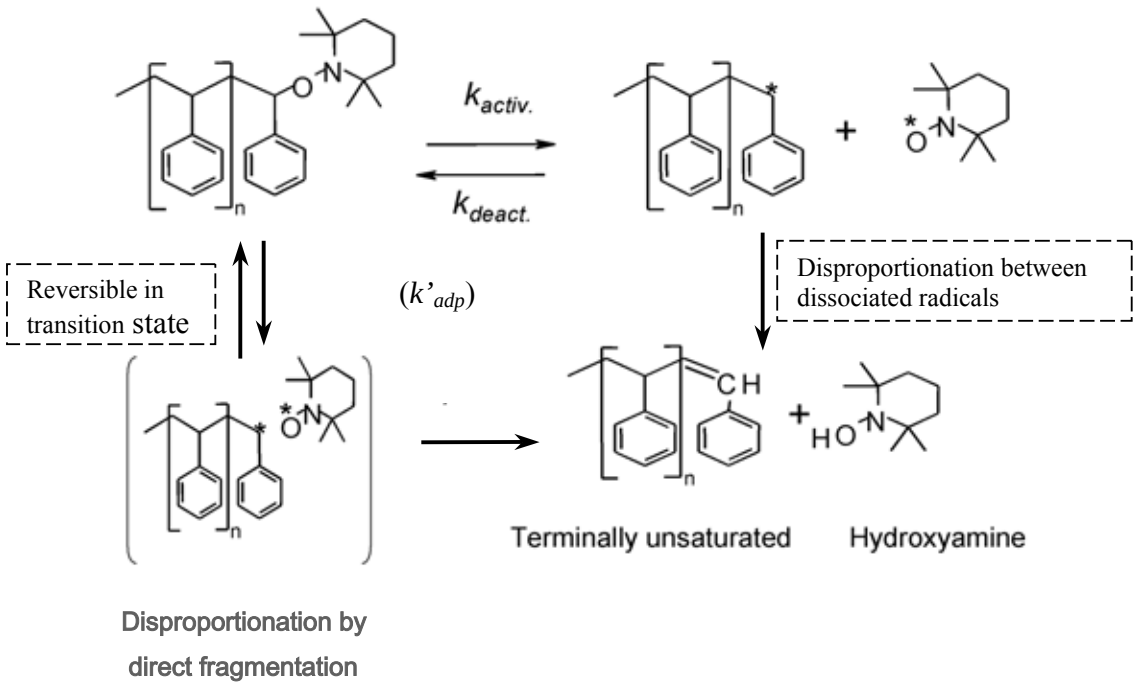

Scheme 4.2 Proposed alkoxyamine disproportionation in TEMPO mediated styrene polymerization.

4.6 Conclusion

The effects of particle size were simulated in SFRP miniemulsions. The first model developed included radical exit/entry, phase partitioning, water phase reactions, and alkoxyamine disproportionation. It was found that radical exit/entry was insignificant in determining the overall radical concentration in the particles. Introduction of thermal initiation efficiency was proposed. The new model including thermal initiation efficiency was confirmed to better agree with experimental results. In model, rate enhancement by compartmentalization effects was not observed for particle sizes under 100nm, contrary to what has been reported in SFRP miniemulsion.

In the livingness analysis, better livingness in miniemulsion was observed than for bulk polymerization in the simulations. However, the simulations for particle size effects on the livingness still did not completely explain the experimental observations.

The simulations suggested that the rate of alkoxyamine disproportionation might be faster than the rate that is currently believed. In addition, it may decrease with decreasing particle size in miniemulsion. Further studies on the mechanism of alkoxyamine disproportion are important for better understanding of livingness in heterogeneous systems.

4.7 References

1. Butte, A., Storti, G., Morbidelli, M., DECHEMA Monoger, 134, 497,1998
2. Charleux, B., Macromolecules, 33, 5358, 2000
3. Zetterlund, PB., Okubo, M., Macromolecules, 38, 8959,2006
4. Tobita, H. Macromol. Theroy Simul., 16,810, 2007
5. Smith, J., Ms. Dissertation, Queen's University Kingston, Canada, 2001
6. Pan, G., Sudol, ED., Diomomie, VL., EL-Aasser, MS., J. Polym. Sci., Part A, 42, 4921, 2004
7. Heath. MT., Scientific Computing, An introductory Survey, 2nd ed; McGraw-Hill; New York, 2002
8. Goto. A, Fukuda. T., Macromolecules, 30,4272,1997
9. Grezsta. D., Matyjaszewski, K., Macromolecules, 29,7661, 1996
10. Buback. M., Gilbert, RG., Hutchinson, RA., Klumperman, B., Kuchta, FD., Manders, BG., O'Driscoll, KF., Russell, GT., Schweer, J., Macromol. Chem. Phys., 196, 3267, 1995
11. Buback, M., Kowollik, C., Kurz, C., Wahl, A., Macromol. Chem. Phys., 201, 464, 2000
12. Hui, A., Hamielec, AE., J. Appl. Polym.Sci., 16,749, 1972
13. Ohno, K., Tsuji, Y., Fukuda, T., Macromolecules, 30, 2503, 1997
14. Sakai, H., Kihara, Y., Fujita, K., Kodani, T., Nomura, M., Polym. Sci. Pol. Chem., 39,1005, 2001
15. Nomura, M., Harada, M., Nakagawa, K., Eguchi, W., Nagata, S., J. Chem. Eng. Jpn., 4,160, 1971

16. Ma, JW., Cunningham, MF., McAuley, KB., Keoshkerian, B., Georges, MK., J. Polym. Sci. ;Part A: Polym. Chem., 39, 1081, 2001
17. Nomura, M., Yamamoto, K., Horie, I., Fujita, K., J. Appl. Polym. Sci., 27, 2483, 1982
18. Li, I., Howell, BA., Matyjaszewski, K., Shigemoto, T., Smith, PB., Priddy, DB, Macromolecules, 28, 6692, 1995
19. Veregin, RPN., Georges, MK., Hamer, GK., Kazmaier, PM., Macromolecules, 28, 4391, 1995
20. Fu, Y., Cunningham, MF., Hutchinson, R A., Macromol. React. Eng., 1, 243, 2007
21. Moffat, K., Hamer, GK., Georges, MK., Macromolecules, 32, 1004, 1999

CHAPTER 5

TEMPO-Mediated Emulsion Polymerization

5.1 Chapter Overview

Compartmentalization effects in emulsion-based nitroxide mediated polymerization was presented in both our experimental and modeling studies as discussed in Chapters 2 and 3. The influence of particle size on the polymerization rate suggests it may not be possible to achieve nitroxide mediated emulsion polymerization with any droplets present, since the faster rate in the micron size droplet causes loss of thermodynamic driving force for monomer transfer from droplet to particles, which is essential for conventional ab initio emulsion polymerization.

In order to overcome the above challenge, an idea for selectively inhibiting polymerization in the monomer droplets is demonstrated in this chapter. A new approach by using the combination of TEMPO with a highly hydrophobic TEMPO-derivative (two nitroxide combination approach) is proposed to implement SFRP in ab initio emulsion polymerization.

The material presented in this chapter has been published in Macromol. Rapid Commun. 2008, 29, 479, and appears in manuscript form.

5.2 Abstract

While miniemulsion polymerization has proven to be well-suited for conducting living / controlled radical polymerizations, emulsion polymerizations have proven to be far more challenging. ab initio emulsion polymerization, in which monomer droplets are present during polymerization, have thus far not been successful with TEMPO-mediated polymerizations, as a result of colloidal instability and coagulum formation. By selectively inhibiting polymerization in the monomer droplets, it is demonstrated that droplet polymerization is responsible for the formation of large particles (> 1 μm) that can lead to coagulum formation. Furthermore, we show that coagulum-free latexes can be produced using TEMPO-mediated ab initio emulsion polymerization by suppressing droplet polymerization.

5.3 Introduction

Dispersed phase radical polymerizations, in which the reaction loci are submicron segregated particles dispersed in an aqueous medium, represent a scientifically and technologically important class of polymerization processes. The best known of these, emulsion polymerization, yields a relatively low viscosity aqueous dispersion of particles in the ~50-500 nm range. Conventional (non-living) emulsion polymerization allows high reaction rates and high molecular weights to be achieved because of radical compartmentalization effects, although in a nitroxide-mediated living system the effects of compartmentalization are much less pronounced [1-3]. Because no volatile organic solvents are required, emulsion polymerization is also environmentally attractive, and is

increasingly being used to replace solvent-based polymerizations. The advent of living/controlled radical polymerization (L/CRP), which offers previously unattainable control of polymer chain microstructure in a radical process, has spurred interest in developing emulsion-based L/CRP processes. While considerable success has been achieved in using miniemulsion polymerization (a variant of emulsion polymerization in which submicron droplets are nucleated and act as the loci of polymerization) for L/CRP, true emulsion polymerization L/CRP processes have proven to be challenging. Because miniemulsions require use of a hydrophobe (e.g. hexadecane) and a high shear mixer (e.g. Microfluidizer), they are commercially less viable than emulsions. This is a primary factor delaying the industrial adoption of nitroxide-mediated polymerizations. Development of an emulsion polymerization process would greatly facilitate commercial adoption of TEMPO-mediated polymerization.

Early efforts to conduct SFRP in emulsion met with failure due to severe problems with colloidal stability that resulted in formation of coagulum [4-7]. Interestingly the polymerizations remained well-controlled even in the coagulated polymer, however the presence of coagulum makes a process commercially unfeasible. Subsequently, miniemulsion polymerization proved to be quite robust for SFRP (Stable Free Radical Polymerization), providing excellent colloidal stability and well-controlled polymerizations over a range of conditions and temperatures using different monomers and nitroxides [5-8]. The reasons for the failure of emulsion SFRP were never clearly established but were generally believed to be attributable to the particle nucleation step and or droplet polymerization (SFRP often requires temperatures >~115 ^{o}C, where thermal polymerization of styrene is significant). Recently, creative strategies based on

seeded polymerization have been developed to avoid using miniemulsion. Miniemulsions require high-shear mixers and the use of a costabilizer such as hexadecane, which are disincentives for industry.) Georges demonstrated a nanoprecipitation technique in which small seed particles are created by precipitation and then swollen with monomer prior to polymerization [9]. The implementation of nitroxide-mediated polymerization for styrene and n-butyl acrylate in batch ab initio emulsion polymerization using the nitroxide SG1has been demonstrated by Charleux [10;11]. In these studies, monomer droplets were present and stable latex particles without coagulum were produced. The use of SG1, which allows a lower polymerization temperature than TEMPO (SG1 can be used effectively ~110-120 ^{o}C), ensures that droplet polymerization arising from thermal polymerization of styrene is less likely to occur (n-butyl acrylate has negligible thermal initiation). Charleux also developed a semi-batch approach for polymerizations mediated by the nitroxide SG1 that also begins with small seed particles. [12-14].

Simms et al. recently reported a surfactant-free SFRP emulsion process that uses only KPS, monomer, and nitroxide (SG1) [15]. While these advances represent important contributions, the development of an ab initio TEMPO-mediated SFRP emulsion process (in which monomer droplets are present) remains elusive, as does the fundamental question of the nature of colloidal instability in emulsion SFRP. The objectives of this manuscript are to identify the specific nature of the colloidal stability problem (particle nucleation or droplet polymerization) and to demonstrate the feasibility of a TEMPO-mediated ab initio emulsion SFRP process in which droplet polymerization is suppressed.

5.4 Experimental

5.4.1 Materials

Styrene (Aldrich, 99%) was washed three times with an equal volume of 2 wt% NaOH (Aldrich, 99+%) solution to remove inhibitor. This step was repeated using distilled water, followed by drying over $CaCl_2$ (Aldrich, 96+%) and vacuum distillation. TEMPO (2,2,6,6-tetramethylpiperidine-1-oxyl]) (Aldrich, 98%), 4-hydroxy-TEMPO (4-hydroxy-2,2,6,6-tetramethylpiperidine-1-oxyl]) (Aldrich, 97%), stearoyl chloride (Aldrich, 99%), potassium persulfate (KPS) (Aldrich, 99+%), sodium dodecyl benzene sulfonate (SDBS) (Aldrich, technical), pyridine (99+%), diethyl ether 99.9%) and Vazo 88 (1,1-azobis(cyclohexane carbonitrile)) (DuPont) were used as received.

Synthesis of 4-Stearoyl-TEMPO - Diethyl ether (20 ml), 4-hydroxy-TEMPO (2.0 g) and pyridine (2.0 g) were mixed at 38 ^{o}C. Stearoyl chloride (5.3 g) dissolved in ethyl ether (20 ml) was added dropwise over ten minutes, and mixing was continued for one hour. The resulting suspension was filtered and washed three times with 3 wt% hydrochloric acid and then three times with deionized water prior to drying under vacuum.

5.4.2 Polymerizations

Emulsion polymerizations - The aqueous phase was prepared by dissolving SDBS (2.50 g) and KPS (0.33 g; 1.22 mmoles) in deionized water (DIW, 120 g). The organic phase (styrene (50 g; 0.481 moles), Stearoyl-TEMPO, TEMPO) was mixed into the aqueous phase. The emulsion was charged into a 300 mL Parr stainless steel reactor, purged with nitrogen, and then polymerized at 135 ^{o}C under nitrogen pressure of 300 kPa. Samples

were collected over the course of reaction. The conditions for each formulation are summarized in Table 5-1.

Bulk Polymerization- Styrene (50 g, 0.481 moles), Vazo-88 (0.30 g, 1.22 mmoles), and 4-Stearoyl-TEMPO were mixed in a round-bottom flask, purged with nitrogen and then heated at 135 °C for 3 hours.

5.4-3 Characterization

All samples were analyzed for monomer conversion (gravimetry), molecular weight distribution and particle size. The particle sizes of the latexes were measured by dynamic light scattering using a Microtrac UPA 150 particle size analyzer. Molecular weight distributions were measured by gel permeation chromatography (GPC) using a Waters 2960 Separation Module with a Waters 410 Differential Refractometer (DRI) (480 nm). Four Waters Styragel columns (100, 500, 10^3, 10^4 Å) were maintained at 40^{o}C. Flow rate of the eluent (distilled tetrahydrofuran, THF) was 1.0 ml/min. Polystyrene (PS) standards were used for calibration.

Table 5-1. Summary of emulsion polymerization experiments.

Experiment ID	T:I	St-T:I	t	Conv.	Mn	PDI	dv	dn	Comments on final PSD
			h	%	g·mol-1		nm		
E1	1.5	0	5	50.1	14690	1.19	1850	530	Significant population of >1 μm
E2	0	2.0	3	82.1	32320	3.10	51	45	Narrow monomodal distribution, no coagulum
E3	0	0	3	96.0	36470	3.21	56	48	Narrow monomodal distribution, no coagulum
E4	1.5	2.0	5	50.7	13030	1.16	52	45	Narrow monomodal distribution, no coagulum
E5[a)]	1.5	2.0	5	49.0	9150	1.25	190	45	Broad monomodal distribution, no coagulum
E6[b)]	0	2.2	3	73.9	14350	1.27	N/A	N/A	N/A

T:I=TEMPO:KPS, St-T:I=4-Stearoyl-TEMPO:KPS (molar ratios). Conversion (Conv), Mn, PDI and dv, dn (volume, number average diameter respectively) are based on final values. T=135 ^{o}C.

a) T=120 ^{o}C

b) bulk polymerization; St-T:I= 4-Stearoyl-TEMPO:VAZO-88

5.5 Results and Discussion

5.5.1 Ab initio emulsion polymerization with 4-Stearoyl TEMPO

In attempting to develop an ab initio SFRP emulsion process, we first needed to clearly understand the nature of the colloidal stability problem. More specifically, the roles of droplet polymerization and particle nucleation need to be isolated. Fig. 5-1 shows an SEM photograph of the coagulum from Expt E1, an ab initio TEMPO-mediated styrene emulsion polymerization initiated by KPS. Large (>1 micron) spherical particles are present in addition to well-formed spherical submicron particles, suggesting the colloidal failure may involve concurrent droplet and particle polymerization. This SEM photograph is typical of several that were taken of the sediment (coagulum) from TEMPO-mediated emulsion polymerizations (coagulum represented ~25% of total polymer). Note however that good control over the polymerization is maintained, with a final PDI of 1.19 being achieved (Fig. 5-2, 5-3; Table 5-1). The GPC traces of the coagulum and the latex are virtually identical.

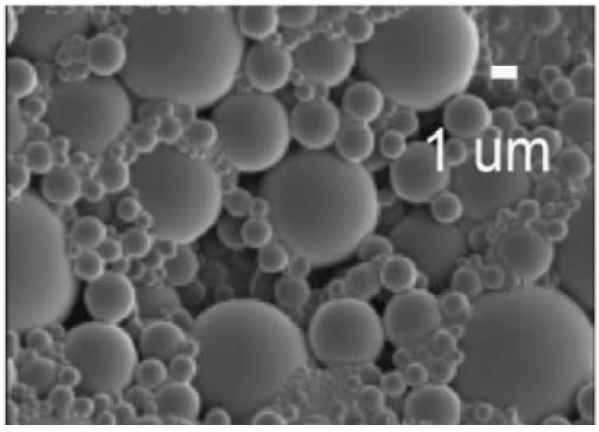

Fig.5- 1. Scanning electron microscope photograph of coagulum from Expt E1 (TEMPO-mediated emulsion polymerization), showing presence of large spherical particles.

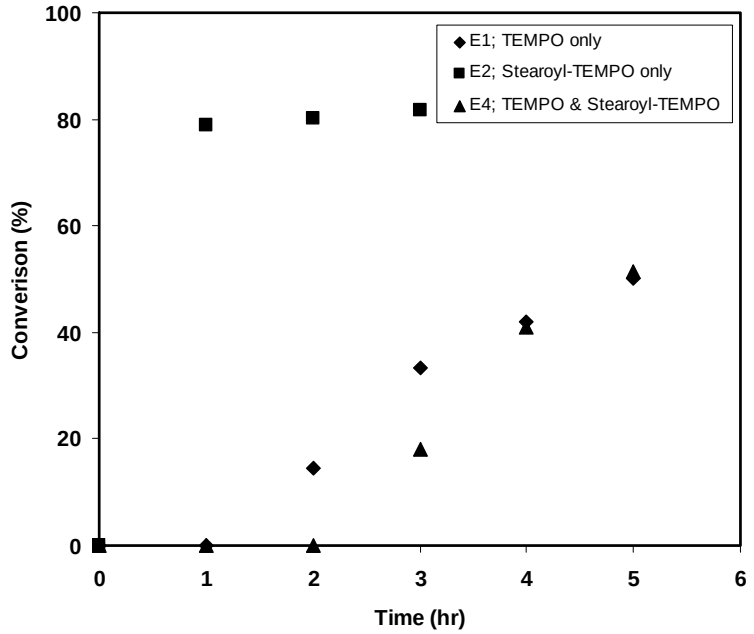

Fig.5- 2. Conversion versus time for TEMPO and 4-Stearoyl-TEMPO-mediated styrene emulsion polymerizations. E1: TEMPO:KPS=1.5:1. E2: 4-Stearoyl-TEMPO:KPS=2.0:1. E4: TEMPO:KPS;1.5:1, 4-Stearoyl-TEMPO:KPS=2.0:1. T=135 ^{o}C.

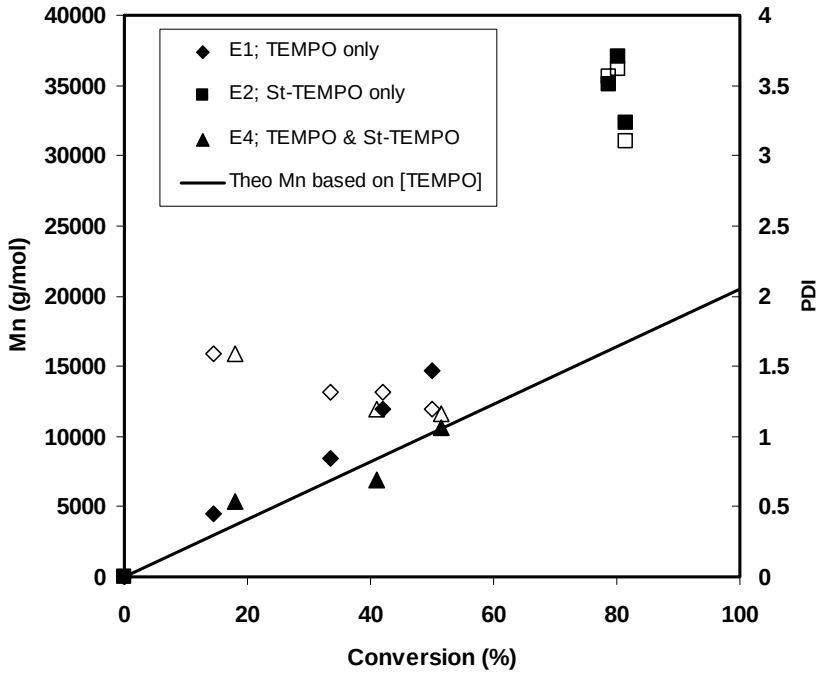

Fig.5- 3. Mn and PDI versus conversion for TEMPO and 4-Stearoyl-TEMPO-mediated styrene emulsion polymerizations. Solid points: Mn, Hollow points: PDI. E1: TEMPO:KPS=1.5:1. E2: 4-Stearoyl-TEMPO:KPS=2.0:1. E4: TEMPO:KPS;1.5:1, 4-Stearoyl-TEMPO:KPS=2.0:1. T=135 ^{o}C.

A preliminary set of experiments using conventional polystyrene seed latexes was conducted in which the volume fraction of droplets relative to particles was varied to determine how the presence of more/fewer droplets affected the polymerization. We used seeded emulsion polymerizations (seed latex made by conventional polymerization) and varied the amount of styrene added to the seed to simulate polymerizations commencing at 20, 40, and 60 % conversion. TEMPO and KPS were added to initiate nitroxide-mediated polymerizations, which were run for 5 hours at 135 ^{o}C. It can be reliably assumed from established knowledge of thermodynamics that a significant number of droplets would be present with 20% polymer initially present, fewer droplets present with 40% initial polymer, and essentially no droplets present at 60% initial polymer concentration [16]. As the initial weight percent polymer was increased from 20% to 60%, the severity of fouling decreased dramatically. Coagulum was observed in the 20% and 40% experiments, and consisted of a monomer-rich polymer layer that settled on the reactor bottom. Similar to Fig. 5-1, it consisted of well-defined large and small particles. At 60% initial polymer loading, no fouling was observed. A cautionary note is warranted here about interpreting reported results of particle size analyses: samples taken randomly from a latex may display a monomodal submicron particle size distribution that would appear to indicate a successful polymerization that was colloidally stable. Care must be taken to ensure the absence of a sediment (coagulum) layer which may not be easily detected. Attempting to conduct a process like this commercially would certainly prove to be unfeasible.

Our results contrast with those of Nicolas et al. [12], who reported the seeded emulsion polymerization of styrene at 115 ^{o}C by SG1-mediated SFRP, where the

polymer content was reduced to a very low value (4 wt% vs. monomer content). Monomer droplets were present in the second step yet whereas no macroscopic coagulum was observed. The critical difference in these results may be the higher polymerization temperature (135 ^{o}C) used in our experiments, which results in higher rates of thermal initiation within the droplets.

The results from the first set of experiments suggested that the presence of monomer droplets corresponded to increased coagulum formation. The large particles seen in Fig. 5-1 are approximately the same size as droplets, but this does not necessarily mean they are polymerized droplets. It is conceivable that the large particles arise from coalescence of smaller particles as a result of poor particle stability. One way to shed light on this problem would be to run an experiment in which droplet polymerization was prevented, and only polymerization in particles could occur. If no fouling was observed in the absence of droplet polymerization and the particles grew as expected with good colloidal stability, the presence of large particles in the coagulum seen above could be attributed to droplet polymerization and not particle nucleation. However, preventing thermal polymerization in styrene droplets at elevated temperatures is a formidable challenge.

To inhibit droplet polymerization, we first synthesized the highly hydrophobic TEMPO derivative 4-Stearoyl-TEMPO. Conceptually, the idea was as follows. We would selectively locate 4-Stearoyl-TEMPO in the monomer droplets (and not in the polymer particles), so that it acts as an inhibitor and therefore prevents droplet polymerization. (Nitroxides in excess will inhibit styrene thermal polymerization for hours in the absence of initiator [17].) As will be seen, we established that diffusion of 4-

Stearoyl-TEMPO to particles from the droplets is negligible. To conduct an ab initio emulsion SFRP, both 4-Stearoyl-TEMPO and TEMPO would be added to the monomer phase prior to dispersion in the aqueous phase. KPS would be added to initiate polymerization in the micelles. Initially, a very small fraction (<~1-2%) of each nitroxide would be present in the monomer-swollen micelles, while the droplets would contain most (>98%) of each of the two nitroxides. As the polymerization progressed, TEMPO in the monomer droplets would diffuse to the growing particles in response to a TEMPO concentration gradient between droplets and particles, thereby providing control of the polymerization according to its expected partitioning behavior [(18)]). However, the 4-Stearoyl-TEMPO would not be able to diffuse to the particles due its extremely low water solubility, but would instead inhibit polymerization in the droplets. Polymerization would thus occur only in particles, mediated by TEMPO. The reaction should then proceed in this manner until monomer droplets are all consumed.

To demonstrate the validity of this concept, we first needed to establish that 4-Stearoyl-TEMPO was sufficiently hydrophobic to remain isolated in the monomer droplets during polymerization. An ab initio emulsion polymerization was run in which only 4-Stearoyl-TEMPO was added to the styrene (Table 5-1, Expt E2). As can be see by comparison with the corresponding control experiment E3, the addition of 4-Stearoyl-TEMPO had only a slight influence on the polymerization. The molecular weight and polydispersity for the 4-Stearoyl-TEMPO containing run were comparable to the control experiment, and showed no indication of livingness nor control. (The molecular weights are lower than typically observed in conventional emulsion polymerization at lower temperatures, which is caused by higher initiation rates (autoinitiation and KPS

decomposition) at the higher temperatures used in our experiments.) The presence of the 4-Stearoyl-TEMPO resulted in a slight lowering of Mn and rate, which is probably attributable to its initial presence in the monomer-swollen micelles. If 4-Stearoyl-TEMPO had diffused to the particles, conversion, molecular weight and polydispersity would have been substantially reduced, characteristic of an L/CRP. (Incidentally, 4-Stearoyl-TEMPO is effective in yielding a living/controlled polymerization, as shown by the low PDI of Expt E6 (bulk styrene polymerization mediated by 4-Stearoyl-TEMPO), although its purpose in this study is as an inhibitor and not a control agent.)

Having established that we were able to effectively isolate 4-Stearoyl-TEMPO in the droplets, we then conducted polymerizations using both TEMPO and 4-Stearoyl-TEMPO. The quantity of 4-Stearoyl-TEMPO added is important; too little will not be effective in preventing droplet polymerization. We found that a 4-Stearoyl-TEMPO:TEMPO ratio of 1.33 was effective in eliminating coagulum formation. Results from Expt 4 are shown in Table 5-1 and Fig. 5-2 and 5- 3. In contrast to Expt E1 that contained only TEMPO and yielded a large amount of fouling and a bimodal particle size distribution, Expt E4 yielded only narrowly distributed small particles (dv=52 nm; dn=45 nm) (Fig.5-4) with no evidence of large particles nor of any fouling. The polymerization progressed to ~50% conversion in 5 hours (Fig. 5-2). The final PDI was 1.16, and a linear relationship between Mn and conversion was observed (Fig. 5-3). Comparison of the molecular weight plots for Expts E1 and E4 show that slightly lower Mn is observed when the 4-Stearoyl-TEMPO is present in addition to TEMPO, which can be attributed to higher initiation efficiency in Expt E4 (f=0.95) compared to Expt E1 (f=0.70). There is a ~~lightly~~ slightly longer induction period for E4 than E1, but the conversions are equal by

the end of the experiment. A polymerization conducted at 120 ^{o}C (E5) also yielded a coagulum-free latex and controlled polymerization. The particle size distribution was somewhat broader, which is consistent with a slower particle nucleation process resulting from the lower temperature, but the two-nitroxide approach remained effective.

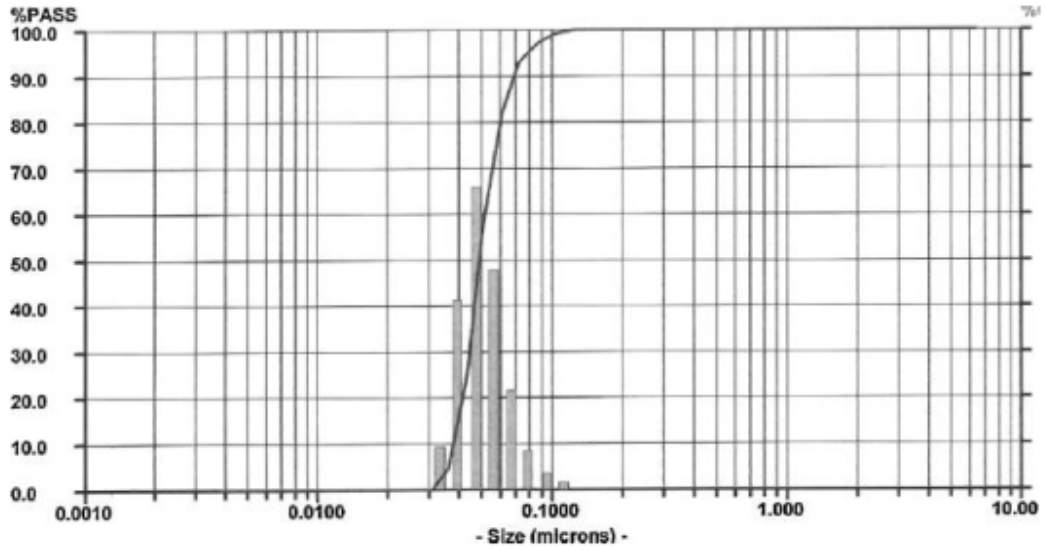

Fig. 5-4. Particle size data for Expt E4 (emulsion polymerization with both TEMPO and 4-Stearoyl-TEMPO), showing narrow monomodal distribution.

5.6 Conclusion

An excess of the highly hydrophobic TEMPO-derivative (4-Stearoyl-TEMPO) is able to suppress droplet polymerization in a styrene emulsion, and does not diffuse to polymerizing particles during polymerization. It was shown that the occurrence of droplet polymerization is responsible for the formation of large (> 1 micron) particles that can lead to coagulum formation. Using the combination of 4-Stearoyl-TEMPO in the droplets (as an inhibitor) together with TEMPO as the controlling agent (which freely partitions between the droplets and polymerizing particles), coagulum-free ab initio emulsion polymerizations were successfully conducted. The approach of suppressing monomer droplet polymerization through use of a highly hydrophobic inhibiting species is expected to be generically applicable. This study represents the first fundamental understanding of the destabilization phenomenon involved in nitroxide-mediated ab initio emulsion polymerization. The new approach proposed in this study represents the first successful strategy to implement SFRP in ab initio emulsion polymerization by using both TEMPO as nitroxide and the widely used KPS as conventional initiator.

5.7 References

1. P. B. Zetterlund, M. Okubo, *Macromolecules* **2006,** *39,* 8959.
2. H. Tobita, F. Yanase, *Macromolecular Theory and Simulations* **2007,** *16,* 476.
3. H. Maehata, C. Buragina, B. Keoshkerian, M. F. Cunningham, *Macromolecules* **2007,** 40, 7126.
4. C. Marestin, C. Noeel, A. Guyot, J. Claverie, *Macromolecules* **1998,** *31,* 4041.
5. M. F. Cunningham *Comptes Rendus Chimie* **2003,** *6,* 1351.
6. J. Qiu, B. Charleux, K. Matyjaszewski, *Progress in Polymer Science* **2001,** *26,* 2083.
7. M. F. Cunningham *Progress in Polymer Science* **2002,** *27,* 1039.
8. M. F. Cunningham *Prog Polym Sci* **2007,** in press**,** .
9. A. Szkurhan, M. K. Georges, *Macromolecules* **2004,** *37,* 4776.
10. G. Delaittre, J. Nicolas, C. Lefay, M. Save, B. Charleux, *Soft Matter* **2006,** *2,* 223.
11. G. Delaittre, J. Nicolas, C. Lefay, M. Save, B. Charleux, *Chem Commun* **2005,** 614.
12. J. Nicolas, B. Charleux, O. Guerret, S. Magnet, *Angewandte Chemie, International Edition* **2004,** *43,* 6186.
13. J. Nicolas, B. Charleux, O. Guerret, S. Magnet, *Macromolecules* **2005,** *38,* 9963.
14. J. Nicolas, B. Charleux, S. Magnet, *J Polym Sci A Polym Chem* **2006,** *44,* 4142.
15. R. W. Simms, M. D. Hoidas, M. F. Cunningham, *submitted for publication to Macromolecules,* **2007.**
16. Gilbert R, G. Emulsion Polymerization - A Mechanistic Approach. Academic Press, London 1995.
17. W. Devonport, L. Michalak, E. Malmstroem, M. Mate, B. Kurdi, C. J. Hawker, G. G.

Barclay, R. Sinta, *Macromolecules* **1997,** *30,* 1929.

18. J. W. Ma, M. F. Cunningham, K. B. McAuley, B. Keoshkerian, M. K. Georges, *J Polym Sci Part A* **2001,** *39,* 1081.

CHAPTER 6

CONCLUSIONS

The theoretical and experimental feasibility of an SFRP emulsion process was studied in this research, with particular focus on the compartmentalization effect. Particle size influence on the polymerization kinetics and the polymer livingness was found. This is the first time these effects have been experimentally demonstrated. Comparison with bulk polymerization kinetics was also done. In addition, a comprehensive mathematical model which included a comprehensive kinetic scheme (aqueous and particle phases) and physical transport events was developed. Based on a comparison of the results for the experimental and modeling studies, it was determined that rate reduction in small particles is a primary contributor to the difficulty in implementing a conventional emulsion process using SFRP chemistry (i.e. TEMPO-mediated ab initio emulsion polymerization). To overcome this difficulty, a new approach was introduced using the combination of TEMPO with highly hydrophobic 4-stearoyl TEMPO to yield a coagulum free ab initio emulsion process.

The most important conclusions in this research are summarized as follows.

1) A pronounced particle size effect in TEMPO-mediated miniemulsion polymerization was discovered. Smaller particles showed slower rates of polymerization than larger

particles. In comparison with homogeneous bulk systems, bulk polymerization was faster than miniemulsion polymerization regardless of the particle size.

2) In modeling studies, it was found that the reasons for the adverse particle size effect on polymerization kinetics were the confined space effect and low thermal initiation efficiency in smaller particles. Consequently the rate enhancement usually observed in conventional emulsion systems (compared to bulk polymerization) is not observed with SFRP chemistry. In smaller particles, the deactivation frequency by nitroxide is increased by the confined space effect (resulting in lower overall radical concentration during polymerization). In addition, lower thermal initiation efficiency in smaller particles results in the accumulation of more TEMPO. Radical exit and entry do not appear to significantly influence the overall kinetics.

3) Quantitative analysis of livingness revealed that higher livingness was preserved in the smaller particles. Bulk polymerization had livingness almost identical to 90nm particles. Simulations also predicted higher livingness in heterogeneous systems compared to bulk. However, the role of alkoxyamine disproportionation and its rate in particles of different sizes is still not well understood but is believed to be influential. Simulations suggest that the rate of alkoxyamine disproportionation might be faster than the rate that is currently believed. In addition, it may decrease with decreasing particle size in miniemulsion. More detailed studies on the mechanism of alkoxyamine disproportionation are important for better understanding livingness in heterogeneous systems.

4) Based on the above results, it was concluded that the difficulties in conducting ab initio emulsion polymerization with SFRP are caused by a diminishing segregation effect in smaller particles, which is the essential kinetic feature of rate enhancement. Consequently monomer transfer from droplets to particles is reduced, and the particles and droplets polymerize at comparable rates. The occurrence of droplet polymerization yields micron size particles that are responsible for destabilizing the latex.

5) For selectively inhibiting the droplet polymerization, use of a highly hydrophobic inhibiting species was found to be an effective approach to allow implementation of an ab initio emulsion process with SFRP. The combination of 4-stearoyl TEMPO in the droplet together with TEMPO successfully gave a coagulum-free ab initio emulsion polymerization process.

CHAPTER 7

RECOMMENDATIONS

I would like to make the following recommendations for future work based on the results from this research.

1) Mechanistic studies on alkoxyamine disproportionation are required to better understand livingness in heterogeneous systems. In particular, the influence of particle size should be further investigated to explain the experimental observations. β - hydrogen abstraction by disproportionation should be examined in the model. In connection with this, the modified Smith Ewart equations used in this research must be further modified in terms of both radical and nitroxide consumption by the occurrence of disproportionation in the particles.

2) Experimental studies are required on the rate coefficient of thermal initiation in styrene in the presence of TEMPO. The importance of the thermal initiation efficiency was presented through simulation studies in this research, but experimental confirmation should be made by employing only thermal initiated miniemulsion polymerization with TEMPO (i.e. no added initiator). The number of chains generated at varying TEMPO concentrations in different particle sizes will provide useful information to more accurately the rate of thermal initiation.

3) Simulations at higher conversion are required to know the ultimate livingness (at near complete conversions) for SFRP. The model employed in this research should be modified to account for chain length dependence of all reactions, but especially termination. Hutchinson et al. pointed out that accounting for the gel effect with diffusion controlled termination rate coefficients was important to accurately simulate experimental results in homogeneous SFRP systems. (Reference 20 in Chapter 4)

APPENDIX A – Nitroxide Mediated Emulsion Polymerization By Conventional Seeding Process

Conventional emulsion polymerization of styrene in the presence of Tempo and 4-hydroxy Tempo (OH-Tempo) was conducted for identifying potential issues in NMEP (nitroxide mediated emulsion polymerization). 60 mM (water phase) of SDBS (sodium dodecylbenzene sulfonate sodium salt) and 10.3mM (water phase) of KPS (potassium persulfate) were used as surfactant and initiator respectively at a monomer to water ratio of 1/3. Polymerization was performed at 135^{o}C in a system purged with nitrogen. Two moles of nitroxide per mole of KPS were used to control the polymerization. In addition, in order to examine influence on particle size distribution of autopolymerization, a non-nitroxide, a non-KPS system was also studied. The polymerization rate and the molecular weight development are shown in Figure A-1, and the final particle size analysis after 5 hrs polymerization is shown in Fig. A-2.

NMEP progressed up to ~60-70% conversion to give a latex consisting of a population of 50-500 nm particles, but also a population of ~ 5-20 micron particles, suggesting droplet polymerization. These larger particles tend to settle out slowly, forming a sticky layer of polymer on the reactor internals. However, in the linear relationship between conversion and Mn, these results are consistent with the findings reported in literatures even with colloidal instability.

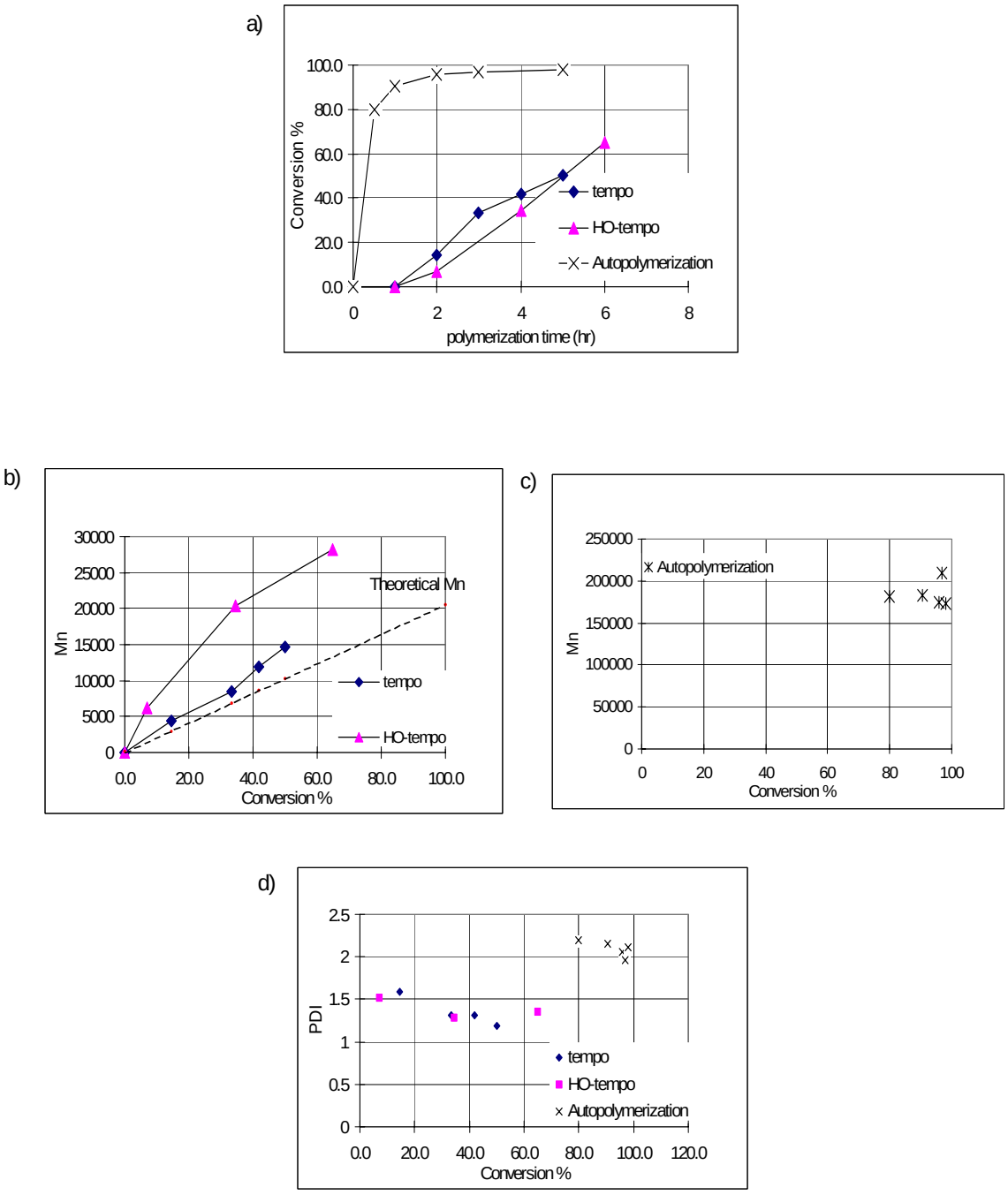

Fig. A-1 Nitroxide mediated styrene emulsion polymerization, compared with auto-polymerization at 135 ^{o}C

a) Conversion vs polymerization time with /without nitroxide
b) Mn vs Conversion with nitroxide
c) Mn vs Conversion without nitroxide
d) Polydispersity index (PDI) with /without nitroxide

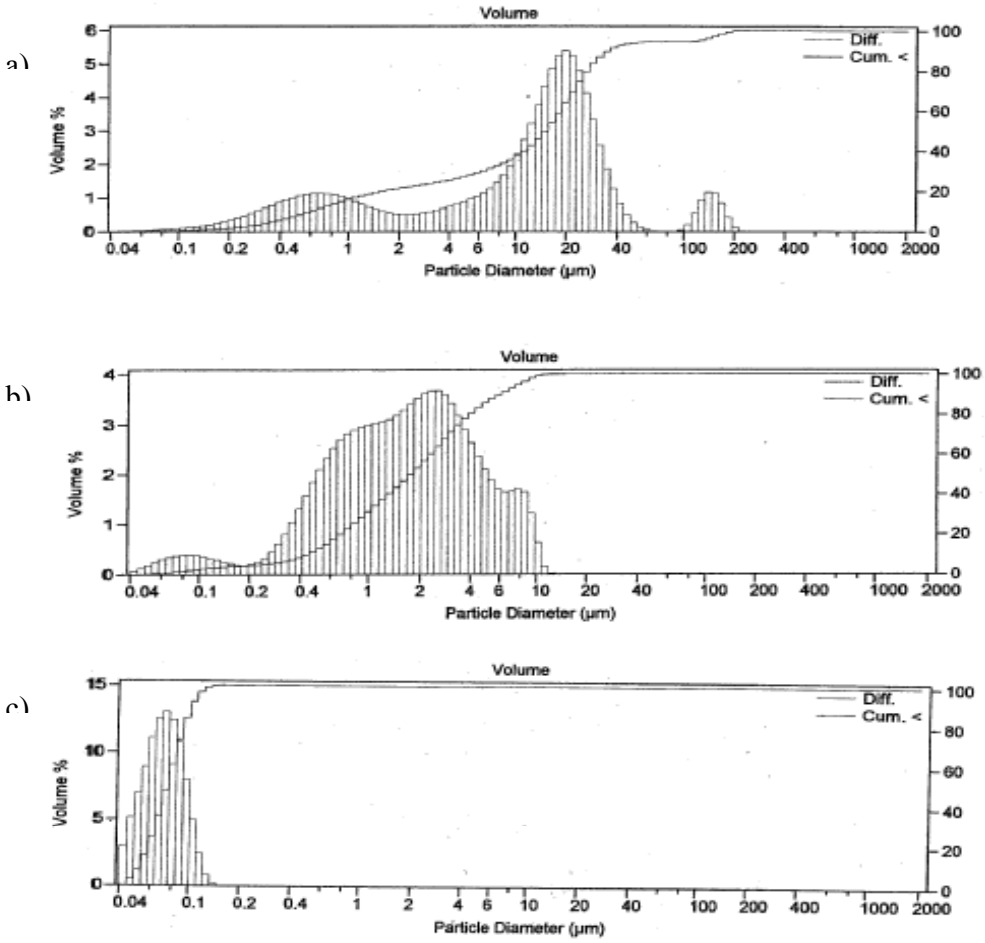

Fig.A-2 Particle size distribution of nitroxide mediated styrene emulsion polymerization and auto-polymerization at 135 ^{o}C.

a) Tempo, d_v = 21.2 μm, b) 4-hydroxy Tempo, dv = 2.4 μm,

c) auto-polymerization (non –nitroxide), dv =0.074 μm

Mn increased with conversion, which was typical of living radical polymerization. The styrene auto-polymerization experiment without nitroxide gave a very stable latex around 70 nm particle size. Colloidal instability was not observed. This result suggests that the compartmentalization effect is preserved with styrene auto-polymerization, but nitroxide impact the compartmentalization effect.

The rate of radical generation by auto-polymerization is proportional to $[M]^3$, therefore radical concentration in particles (or micelle) and droplets is theoretically equal per unit volume. However, due to the compartmentalization effect in the particles (radical segregation in particles), the termination reaction in the particles is less likely compared with that of the droplets, consequently the radical concentration can be kept higher to cause a faster rate of polymerization in the particles.

For further confirmation on the droplet polymerization in NMEP, we have also conducted seeded styrene NMEP polymerizations beginning with different initial amounts of monomer, which is 10% ~60 % seed particles to total monomer weight (i.e. different amount of seed particles with constant monomer amount). In this case, monomer droplets are usually not present in conventional emulsion polymerization. The results were shown in Fig.A-3 and Fig.A-4. With 30% of initial seed particles, for which most of monomer should be absorbed into the seed particles, the polymerization can be conducted with preservation of the original particle size distribution, showing molecular weight increase consistent with a living system. However if droplets are initially present, the existence of large particles persists.

a)

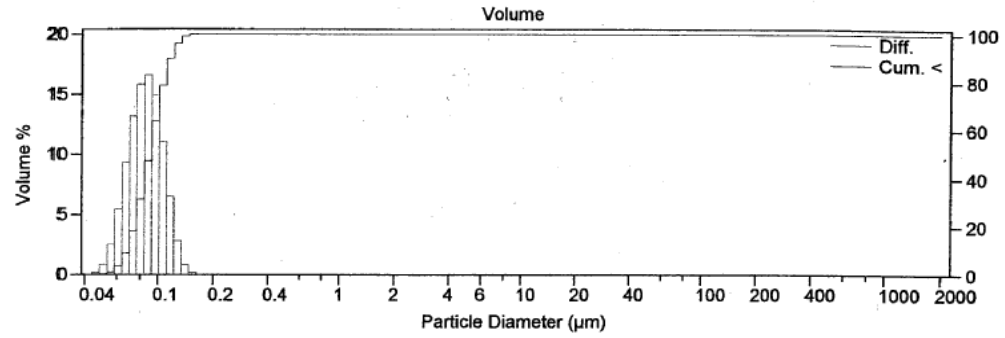

b)

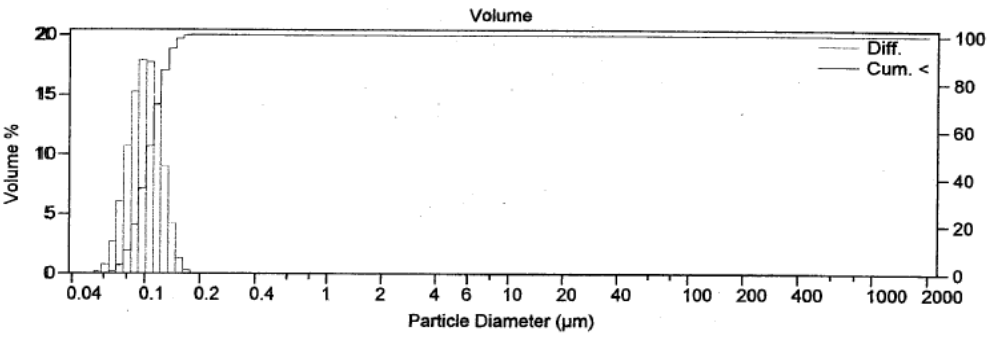

Fig.A-3 Particle size distribution of nitroxide mediated styrene seeded emulsion polymerization at 135 ^{o}C for 6 hrs.

a) Seed particles; dv = 0.087 μm,

b) Seeded polymerization (30% seed), dv =0.101 μm

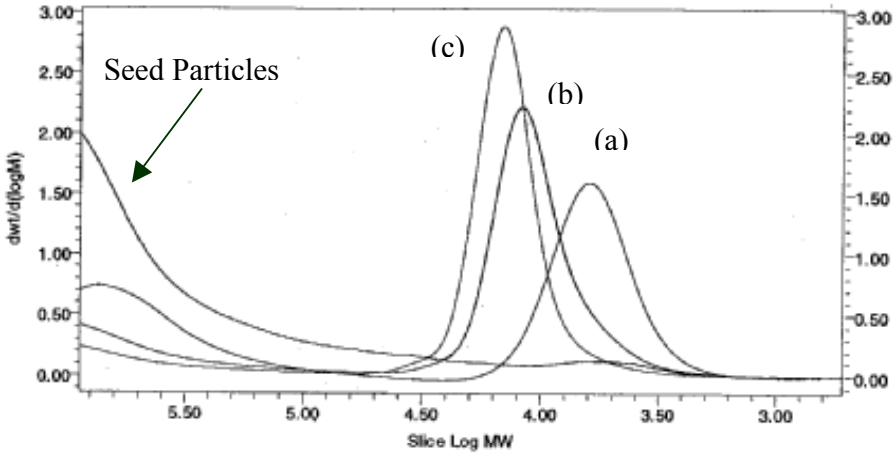

Fig.A-4 GPC trace for nitroxide mediated seeded emulsion polymerization at 135 ^{o}C.

a) 3 hrs, Mn 5559,PDI 1.30, b) 4.5 hrs, Mn 11362, PDI 1.15

c) 6 hrs Mn 13779, PDI 1.15

Of much interest is the thermal polymerization under SFRP chemistry that occurs in the monomer droplets. The issue observed in the above studies seems to be a lack of compartmentalization kinetics in heterogeneous SFRP systems, coupled with droplet polymerization. In conventional emulsion polymerization (no nitroxide), the polymerization rate in the particles is much higher than in droplet because the growing chains are segregated. However in NMEP, the impact of the compartmentalization effect seems to be largely reduced.

From the above experimental observations, it is hypothesized that the rate of polymerization in particles is equal or slower than that in the droplet. Consequently there

is no thermodynamic driving force for monomer diffusion from droplet to particles, which is essential for ab initio emulsion polymerization.

APPENDIX B – Stearoyl TEMPO Synthesis and Characterization

Synthesis of 4-Stearoyl-TEMPO - Diethyl ether (20 ml), 4-hydroxy-TEMPO (2.0 g) and pyridine (2.0 g) were mixed at 38 ^{o}C. Stearoyl chloride (5.3 g) dissolved in ethyl ether (20 ml) was added dropwise over ten minutes, and mixing was continued for one hour (Scheme B-1). The resulting filtrate was filtered and washed three times with 3 wt% hydrochloric acid and then three times with deionized water prior to drying under vacuum. The IR spectrum is shown in Fig. B-1.

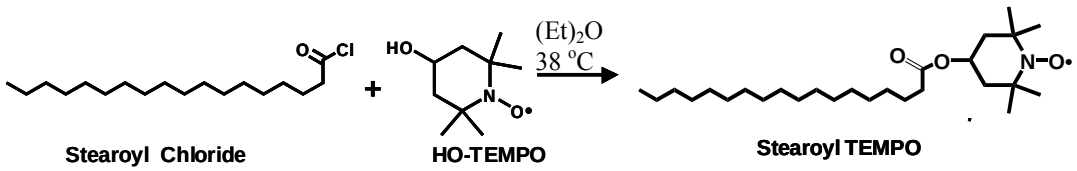

Scheme B-1 Synthesis of Stearoyl TEMPO

Fig. B-1 IR Spectrum for Stearoyl TEMPO

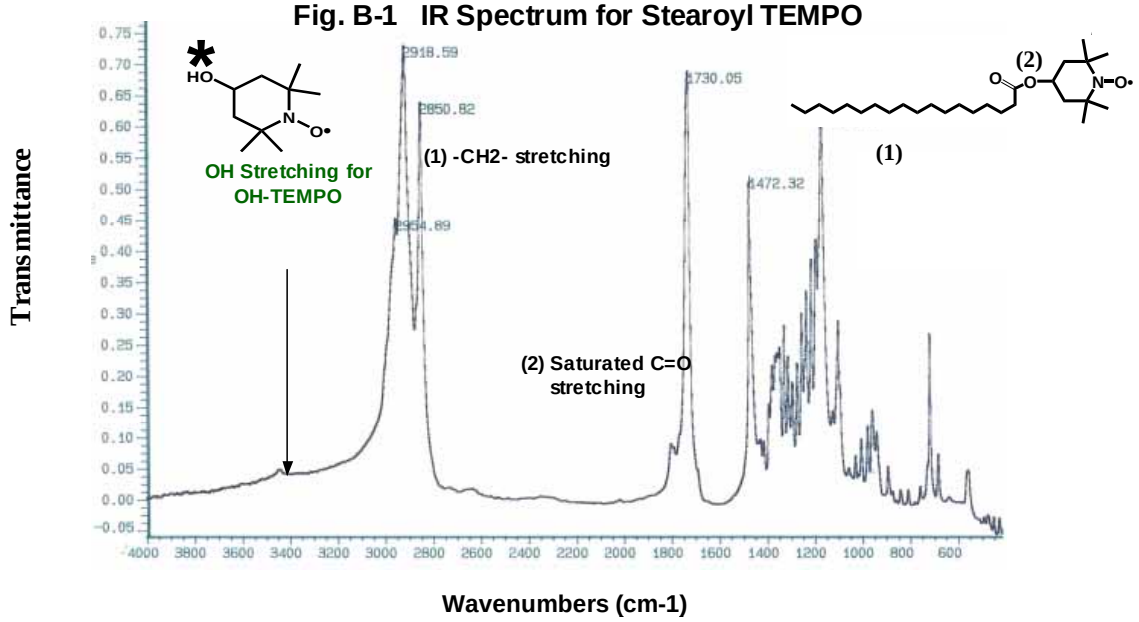

Octanol –water partition coefficient for stearoyl –TEMPO (LogP**:** partition coefficient for *n*-octanol/water)- was predicted by using atomic physicochemical parameter (Crippen M et al.,Journal of Computational Chemistry Vol.9, No.1,80,1988). The predicted Log P for stearoyl TEMPO is shown in Fig. B-2 compared with various materials including TEMPO.

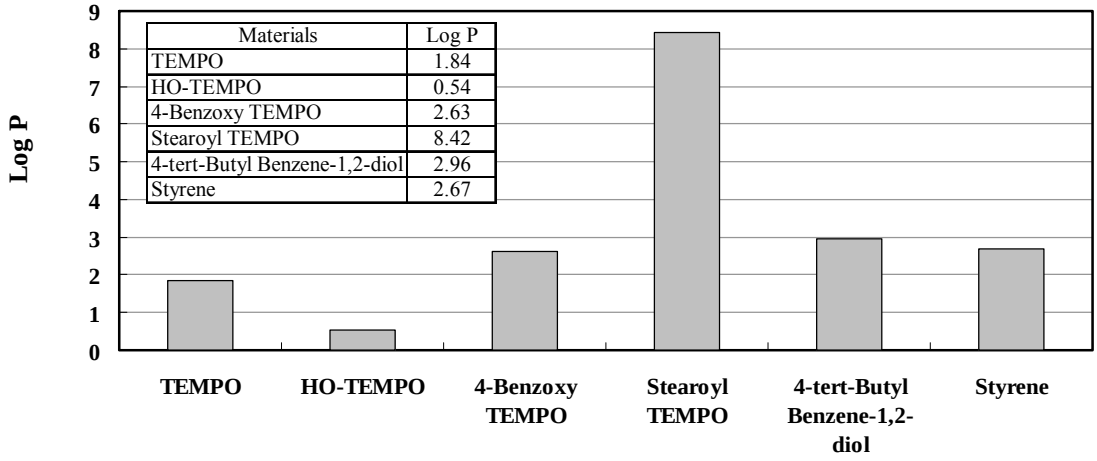

Materials	Log P
TEMPO	1.84
HO-TEMPO	0.54
4-Benzoxy TEMPO	2.63
Stearoyl TEMPO	8.42
4-tert-Butyl Benzene-1,2-diol	2.96
Styrene	2.67

Fig. B-2 Partition coefficient Log P for Stearoyl TEMPO